

Deeper insight into the protease-sensitive "covalent-assembly" fluorescent probes for practical biosensing applications

Kévin Renault,^a Sylvain Debieu,^{a†} Jean-Alexandre Richard^b and Anthony Romieu^{*a}

^a ICMUB, UMR 6302, CNRS, Univ. Bourgogne Franche-Comté, 9, Avenue Alain Savary, 21000 Dijon, France.

E-mail: anthony.romieu@u-bourgogne.fr; Lab homepage: <http://www.icmub.com>

^b Functional Molecules and Polymers, Institute of Chemical and Engineering Sciences (ICES), Agency for Science, Technology and Research (A*STAR), 8 Biomedical Grove, Neuros, #07-01, Singapore 138665.

E-mail: jean_alexandre@ices.a-star.edu.sg

[†] Present address: PSL Université Paris, Institut Curie, CNRS UMR 3666, INSERM U1143, 75005 Paris France

Supporting Information

Table of Contents

Abbreviations.....	S7
Instrument and methods.....	S7
High-performance liquid chromatography separations	S8
<i>In vitro</i> activation of fluorogenic "turn-on" probes 2-10 by PGA - experimental details	S9
Stock solutions of probes, enzyme and chemical reagents	S9
Fluorescence assays	S9
HPLC-fluorescence analyses	S10
Stability studies of fluorogenic "turn-on" probes 3, 5, 6, 8-10 in aq. solutions and/or in the presence of GSH - experimental details	S10
Analytical data	S11
ESI+ mass spectrum (high resolution) of compound 4	S11
ESI+ (left) / ESI- (right) mass spectrum (low resolution) of compound 4	S11
IR-ATR spectrum of compound 4	S12
¹H NMR spectrum of compound 5 in CDCl₃ (500 MHz)	S12
¹³C NMR spectrum of compound 5 in CDCl₃ (126 MHz)	S13
¹⁹F NMR spectrum of compound 5 in CDCl₃ (470 MHz)	S13
ESI+ mass spectrum (high resolution) of compound 5	S14
ESI+ (left) / ESI- (right) mass spectrum (low resolution) of compound 5	S14
RP-HPLC elution profile of compound 5 (system A, detection at 260 nm)	S15
RP-HPLC elution profile of compound 5 (system A, detection at 450 nm)	S15
RP-HPLC elution profile of compound 5 (system A, detection at 500 nm)	S16
RP-HPLC elution profile of compound 5 (system C, detection at 260 nm)	S16
RP-HPLC elution profile of compound 5 (system C, detection at 450 nm)	S17
RP-HPLC elution profile of compound 5 (system C, detection at 500 nm)	S17
IR-ATR spectrum of compound 5	S18
¹H NMR spectrum of compound 6 in CDCl₃ (500 MHz)	S18
¹³C NMR spectrum of compound 6 in CDCl₃ (126 MHz)	S19
¹⁹F NMR spectrum of compound 6 in CDCl₃ (470 MHz)	S19
ESI+ mass spectrum (high resolution) of compound 6	S20
ESI+ (left) / ESI- (right) mass spectrum (low resolution) of compound 6	S20
RP-HPLC elution profile of compound 6 (system A, detection at 260 nm)	S21
RP-HPLC elution profile of compound 6 (system A, detection at 450 nm)	S21
RP-HPLC elution profile of compound 6 (system A, detection at 500 nm)	S22
IR-ATR spectrum of compound 6	S22
¹H NMR spectrum of compound 7 in CDCl₃ (600 MHz)	S23
¹³C NMR spectrum of compound 7 in CDCl₃ (151 MHz)	S23
¹⁹F NMR spectrum of compound 7 in CDCl₃ (565 MHz)	S24
ESI+ mass spectrum (high resolution) of compound 7	S24
ESI+ (left) / ESI- (right) mass spectrum (low resolution) of compound 7	S25

RP-HPLC elution profile of compound 7 (system A, detection at 260 nm)	S25
RP-HPLC elution profile of compound 7 (system A, detection at 450 nm)	S26
RP-HPLC elution profile of compound 7 (system A, detection at 500 nm)	S26
IR-ATR spectrum of compound 7	S27
TFA determination by ionic chromatography - results	S27
¹H NMR spectrum of compound 8 in CDCl₃ (500 MHz)	S28
¹³C NMR spectrum of compound 8 in CDCl₃ (126 MHz)	S28
¹⁹F NMR spectrum of compound 8 in CDCl₃ (470 MHz)	S29
ESI+ mass spectrum (high resolution) of compound 8	S29
ESI+ (left) / ESI- (right) mass spectrum (low resolution) of compound 8	S30
RP-HPLC elution profile of compound 8 (system A, detection at 260 nm)	S30
RP-HPLC elution profile of compound 8 (system A, detection at 450 nm)	S31
RP-HPLC elution profile of compound 8 (system A, detection at 500 nm)	S31
IR-ATR spectrum of compound 8	S32
TFA determination by ionic chromatography - results	S32
¹H NMR spectrum of compound 9 in CDCl₃ (500 MHz)	S33
¹³C NMR spectrum of compound 9 in CDCl₃ (126 MHz)	S33
¹⁹F NMR spectrum of compound 9 in CDCl₃ (470 MHz)	S34
ESI+ mass spectrum (high resolution) of compound 9	S34
ESI+ (left) / ESI- (right) mass spectrum (low resolution) of compound 9	S35
RP-HPLC elution profile of compound 9 (system A, detection at 260 nm)	S36
RP-HPLC elution profile of compound 9 (system A, detection at 450 nm)	S36
RP-HPLC elution profile of compound 9 (system A, detection at 500 nm)	S37
IR-ATR spectrum of compound 9	S37
TFA determination by ionic chromatography - results	S38
¹H NMR spectrum of compound 10 in CDCl₃ (500 MHz)	S38
¹³C NMR spectrum of compound 10 in CDCl₃ (126 MHz)	S39
¹⁹F NMR spectrum of compound 10 in CDCl₃ (470 MHz)	S39
ESI+ mass spectrum (high resolution) of compound 10	S40
ESI+ mass spectrum (low resolution) of compound 10	S40
RP-HPLC elution profile of compound 10 (system A, detection at 260 nm)	S41
RP-HPLC elution profile of compound 10 (system A, detection at 450 nm)	S41
RP-HPLC elution profile of compound 10 (system A, detection at 500 nm)	S42
IR-ATR spectrum of compound 10	S42
Fig. S1 UV-vis absorption spectrum of dimedone-based probes 4 in PB (concentration: 9.0 μM)^a at 25 °C.	S43
Fig. S2 UV-vis absorption spectrum of barbiturate-based probes 5 in PB (concentration: 11 μM) at 25 °C.	S43
Fig. S3 UV-vis absorption spectrum of Meldrum's acid-based probes 6 in PB (concentration: 20 μM) at 25 °C.	S44
Fig. S4 UV-vis absorption spectrum of rosamine-based probes 7 in PB (concentration: 25 μM) at 25 °C.	S44

Fig. S5 UV-vis absorption spectrum of hemicyanine-based probes 8 in PB (concentration: 29 μM) at 25 $^{\circ}$C.	S45
Fig. S6 UV-vis absorption spectrum of hemicyanine-based probes 9 in PB (concentration: 25 μM) at 25 $^{\circ}$C.	S45
Fig. S7 UV-vis absorption spectrum of edaravone-based probes 10 in PB (concentration: 16 μM) at 25 $^{\circ}$C.	S46
Fig. S8 UV-vis Normalised absorption, excitation (Em. 615 nm, slit 5 nm), emission (Ex. 440 nm, slit 7 nm) spectra of Meldrum's acid-based probes 10 in PB at 25 $^{\circ}$C.	S46
Fig. S9 UV-vis Normalised absorption, excitation (Em. 400 nm, bandwidth 5 nm)^a, emission (Ex. 300 nm, bandwidth 5 nm) spectra of 4,7-dihydroxycoumarin in PB at 25 $^{\circ}$C.	S47
Fig. S10 Time-dependent changes in the green-yellow fluorescence intensity (Ex./Em. 525/545 nm, slit 5 nm) of fluorogenic probe 4 (concentration: 1.0 μM) in the presence of PGA (1 U) in PB (100 mM, pH 7.6) at 37 $^{\circ}$C.	S47
Fig. S11 Time-dependent changes in the green-yellow fluorescence intensity (Ex./Em. 525/545 nm, slit 5 nm) of fluorogenic probe 5 (concentration: 1.0 μM) in the presence of PGA (1 U) in PB (100 mM, pH 7.6) at 37 $^{\circ}$C.	S48
Fig. S12 Time-dependent changes in the green-yellow fluorescence intensity (Ex./Em. 525/545 nm, slit 5 nm) of fluorogenic probe 6 (concentration: 1.0 μM) in the presence of PGA (1 U) in PB (100 mM, pH 7.6) at 37 $^{\circ}$C.	S48
Fig. S13 Time-dependent changes in the green-yellow fluorescence intensity (Ex./Em. 525/545 nm, slit 5 nm) of fluorogenic probe 7 (concentration: 1.0 μM) in the presence of PGA (1 U) in PB (100 mM, pH 7.6) at 37 $^{\circ}$C.	S49
Fig. S14 Time-dependent changes in the green-yellow fluorescence intensity (Ex./Em. 525/545 nm, slit 5 nm) of fluorogenic probe 8 (concentration: 1.0 μM) in the presence of PGA (1 U) in PB (100 mM, pH 7.6) at 37 $^{\circ}$C.	S49
Fig. S15 Time-dependent changes in the green-yellow fluorescence intensity (Ex./Em. 525/545 nm, slit 5 nm) of fluorogenic probe 9 (concentration: 1.0 μM) in the presence of PGA (1 U) in PB (100 mM, pH 7.6) at 37 $^{\circ}$C.	S50
Fig. S16 Time-dependent changes in the green-yellow fluorescence intensity (Ex./Em. 525/545 nm, slit 5 nm) of fluorogenic probe 10 (concentration: 1.0 μM) in the presence of PGA (1 U) in PB (100 mM, pH 7.6) at 37 $^{\circ}$C.	S50
Fig. S17 Time-dependent changes in the green-yellow fluorescence intensity (Ex./Em. 525/545 nm, slit 5 nm) of fluorogenic probe 3 (concentration: 1.0 μM) in the presence of PGA (1 U) with or without GSH (50 equiv.), in PB (100 mM, pH 7.6) at 37 $^{\circ}$C.	S51
Fig. S18 Time-dependent changes in the green-yellow fluorescence intensity (Ex./Em. 525/545 nm, slit 5 nm) of fluorogenic probe 6 (concentration: 1.0 μM) in the presence of PGA (1 U) with or without GSH (50 equiv.), in PB (100 mM, pH 7.6) at 37 $^{\circ}$C.	S51
Fig. S19 Time-dependent changes in the green-yellow fluorescence intensity (Ex./Em. 525/545 nm, slit 5 nm) of fluorogenic probe 10 (concentration: 1.0 μM) in the presence of PGA (1 U) with or without GSH (50 equiv.), in PB (100 mM, pH 7.6) at 37 $^{\circ}$C.	S52
Fig. S20 Bar charts related to UV-vis absorbance changes (at λ_{max}) of fluorogenic probes 2-10 (concentration: 2.0 μM) after 30 min incubation with GSH (50 equiv.), in PB (100 mM, pH 7.6) at 25 $^{\circ}$C.	S52
Fig. S21 RP-HPLC elution profile (system J, fluorescence detection Ex./Em. 525/545 nm) of fluorogenic probe 3 before enzymatic activation	S53

Fig. S22 RP-HPLC elution profile (system J, fluorescence detection Ex./Em. 525/545 nm) of fluorogenic probe 3 after incubation with PGA (1 U, 30 min, 37 °C).....	S53
Fig. S23 RP-HPLC elution profile (system J, fluorescence detection Ex./Em. 525/545 nm) of fluorogenic probe 4 before enzymatic activation	S54
Fig. S24 RP-HPLC elution profile (system J, fluorescence detection Ex./Em. 525/545 nm) of fluorogenic probe 4 after incubation with PGA (1 U, 30 min, 37 °C).....	S54
Fig. S25 RP-HPLC elution profile (system J, fluorescence detection Ex./Em. 525/545 nm) of fluorogenic probe 5 before enzymatic activation	S55
Fig. S26 RP-HPLC elution profile (system J, fluorescence detection Ex./Em. 525/545 nm) of fluorogenic probe 5 after incubation with PGA (1 U, 30 min, 37 °C).....	S55
Fig. S27 RP-HPLC elution profile (system J, fluorescence detection Ex./Em. 525/545 nm) of fluorogenic probe 6 before enzymatic activation	S56
Fig. S28 RP-HPLC elution profile (system J, fluorescence detection Ex./Em. 525/545 nm) of fluorogenic probe 6 after incubation with PGA (1 U, 30 min, 37 °C).....	S56
Fig. S29 RP-HPLC elution profile (system J, fluorescence detection Ex./Em. 525/545 nm) of fluorogenic probe 7 before enzymatic activation	S57
Fig. S30 RP-HPLC elution profile (system J, fluorescence detection Ex./Em. 525/545 nm) of fluorogenic probe 7 after incubation with PGA (1 U, 30 min, 37 °C).....	S57
Fig. S31 RP-HPLC elution profile (system J, fluorescence detection Ex./Em. 525/545 nm) of fluorogenic probe 8 before enzymatic activation	S58
Fig. S32 RP-HPLC elution profile (system J, fluorescence detection Ex./Em. 525/545 nm) of fluorogenic probe 8 after incubation with PGA (1 U, 30 min, 37 °C).....	S58
Fig. S33 RP-HPLC elution profile (system J, fluorescence detection Ex./Em. 525/545 nm) of fluorogenic probe 9 before enzymatic activation	S59
Fig. S34 RP-HPLC elution profile (system J, fluorescence detection Ex./Em. 525/545 nm) of fluorogenic probe 9 after incubation with PGA (1 U, 30 min, 37 °C).....	S59
Fig. S35 RP-HPLC elution profile (system J, fluorescence detection Ex./Em. 525/545 nm) of fluorogenic probe 10 before enzymatic activation	S60
Fig. S36 RP-HPLC elution profile (system J, fluorescence detection Ex./Em. 525/545 nm) of fluorogenic probe 10 after incubation with PGA (1 U, 30 min, 37 °C).....	S60
Fig. S37 RP-HPLC elution profile (system J, fluorescence detection Ex./Em. 525/545 nm) of reference pyronin AR116	S61
Fig. S38 RP-HPLC elution profiles (system B) of blank (injection of PB alone). UV detection at 220 nm; UV detection at 260 nm; visible detection at 470 nm; visible detection at 525 nm; ESI+ mass detection (SIM mode at $m/z = 175.5 \pm 0.5$) (top-down)	S61
Fig. S39 RP-HPLC elution profiles (system B) of enzymatic reaction mixture of probe 10 with PGA (20 h of incubation in PB at 37 °C). UV detection at 220 nm; UV detection at 260 nm; visible detection at 470 nm; visible detection at 525 nm; ESI+ mass detection (SIM mode at $m/z = 175.5 \pm 0.5$) (top-down)	S63
Fig. S40 RP-HPLC elution profiles (system B) of co-injection (enzymatic reaction mixture of probe 10 + edaravone). UV detection at 220 nm; UV detection at 260 nm; visible detection at 470 nm; visible detection at 525 nm; ESI+ mass detection (SIM mode at $m/z = 175.5 \pm 0.5$) (top-down)	S65
Fig. S41 RP-HPLC elution profiles (system B) of pure sample of edaravone. UV detection at 220 nm; UV detection at 260 nm; visible detection at 470 nm; visible	

detection at 525 nm; ESI+ mass detection (SIM mode at $m/z = 175.5 \pm 0.5$) (top-down)
..... S67

Abbreviations

The following abbreviations are used throughout the text of the ESI file: Abs, absorption; aq., aqueous; a.m.u, atomic mass unit; ATR, attenuated total reflectance; DAD, diode array detector/detection; DMSO, dimethylsulfoxide; Em., emission; ESI, electrospray ionisation; Ex., excitation; FA, formic acid; FLD, fluorescence detector; FT, fourier transform; H₂O, water; HPLC, high-pressure liquid chromatography; IR, infrared; MeCN, acetonitrile; MeOH, methanol; min, minutes; NMR, nuclear magnetic resonance; PB, phosphate buffer; PGA, penicillin G acylase; MS, mass spectrometry; PMT, photomultiplier tube; R101, rhodamine 101; RP, reversed phase; rpm, revolution per minute; RS, rapid separation; SIM, selected ion monitoring; TFA, trifluoroacetic acid; *t_R*, retention time; UV, ultraviolet; vis, visible.

Instrument and methods

UV-vis absorption measurements (both spectra scan and kinetics modes) were conducted on a Varian Cary 50 Scan spectrophotometer (Cary WinUV software) using rectangular quartz cells (Hellma, 100-QS, 45 × 12.5 × 12.5 mm, pathlength: 10 mm, chamber volume: 3.5 mL), at 25 °C (using a temperature control system combined with water circulation). Fluorescence spectroscopic studies (scan and kinetics modes) were performed with an HORIBA Jobin Yvon Fluorolog spectrofluorimeter (software FluorEssence) at 25 °C or 37 °C (using a temperature control system combined with water circulation), with standard fluorometer cells (Labbox, LB Q, light path: 10 mm, width: 10 mm, chamber volume: 3.5 mL). Some UV-vis and fluorescence spectra were also recorded on a SAFAS Xenius XC spectrofluorimeter using quartz cells (SAFAS, Quartz Suprasil for SAFAS flx Xenius, 45 × 12.5 × 12.5 mm, pathlength: 10 mm, chamber volume: 3.5 mL), at 25 °C (using a temperature control system combined with water circulation). The absorption spectra of fluorophores (pyronin **AR116** and 4,7-dihydroxycoumarin) and PGA-sensitive probes **4-10** were recorded in PB with concentrations in the range 5-25 μM (total volume: 3.0 mL, three distinct dilutions for the accurate determination of molar extinction coefficients). Ex./Em. spectra were recorded after emission/excitation at the suitable wavelength (see Table S1, set of parameters for Fluorolog: shutter: Auto Open, excitation/emission slit = 5 nm, integration time = 0.1 s, 1 nm step, HV(S1) = 950 V; set of parameters for SAFAS: Ex./Em. bandwidth = 5 or 10 nm, integration time = 0.1 s, 1 nm step, tunable PMT voltage). All fluorescence spectra were corrected. Relative fluorescence quantum yields were measured in the corresponding buffer at 25 °C by a relative method using the suitable standard (see table S1). The following equation was used to determine the relative fluorescence quantum yield:

$$\Phi_F(x) = (A_s/A_x)(F_x/F_s)(n_x/n_s)^2\Phi_F(s)$$

where A is the absorbance (in the range of 0.01-0.1 A.U.), F is the area under the emission curve, n is the refractive index of the solvents (at 25 °C) used in measurements, and the subscripts s and x represent standard and unknown, respectively.

Table S1. Experimental conditions used for the determination of relative fluorescence quantum yields.

Cmpd ^a / Instrument	Solvent ^b	λ Ex (nm) ^c	Standard (std) ¹	$\Phi_{F(\text{std})}$ (%) / solvent	Φ_F
6 / Fluorolog	PB, pH 7.6	440	Ru(bpy) ₃ Cl ₂	4.2 / H ₂ O	1%
9 / SAFAS PMT = 290 V	PB, pH 7.6	535	R101	100 / MeOH ^d	<< 1%
4,7-dihydroxycoumarin / SAFAS PMT = 470 V	PB, pH 7.6	300	7-hydroxycoumarin	76% / PB	8.5%

^a stock solutions (1.0 mg/mL) of fluorophores were prepared either in DMSO (for **6** and **9**) or in PB (66 mM, pH 7.5, for 4,7-dihydroxycoumarin).

^b refractive index for PB was measured and found to be similar to that of water (1.333).

^c emission range for **6** = 455-800 nm, emission range for **9** = 550-800 nm, emission range for 4,7-dihydroxycoumarin = 320-600 nm.

^d refractive index = 1.331.

High-performance liquid chromatography separations

Several chromatographic systems were used for the analytical experiments (HPLC-MS or HPLC-fluorescence) and the purification steps: System A: RP-HPLC-MS (Phenomenex Kinetex C₁₈ column, 2.6 μ m, 2.1 \times 50 mm) with MeCN (+ 0.1% FA) and 0.1% aq. formic acid (aq. FA, pH 2.7) as eluents [5% MeCN (0.1 min) followed by linear gradient from 5% to 100% (5 min) of MeCN] at a flow rate of 0.5 mL min⁻¹. UV-visible detection was achieved at 220, 260, 450 and 500 nm (+ DAD in the range 220-700 nm). Low resolution ESI-MS detection in the positive/negative mode (full scan, 100-1000 a.m.u., data type: centroid, needle voltage: 3.0 kV, probe temperature: 350 °C, cone voltage: 75 V and scan time: 1 s). System B: system A with UV-visible detection at 220, 260, 470 and 525 nm (+ DAD in the range 220-800 nm). Low resolution ESI-MS detection in the positive/negative mode (full scan, 100-1000 a.m.u. and SIM mode with the following mass range (m/z 175.5 \pm 0.5)). System C: system A with ultrapure H₂O and MeCN (without FA additive) as eluents. System D: semi-preparative RP-HPLC (SiliCycle SiliaChrom C₁₈ column, 10 μ m, 20 \times 250 mm) with MeCN and ultrapure H₂O as eluents [25% MeCN (5 min), followed by a gradient of 25% to 55% MeCN (10 min), then 55% to 100% MeCN (45 min)] at a flow rate of 20.0 mL min⁻¹. Quadruple UV-vis detection was achieved at 220, 260, 460 and 550 nm. System E: system D with UV-visible detection at 220, 260, 470 and 530 nm. System F: system D with UV-visible detection at 220, 260, 280 and 475 nm. System G: system D with the following gradient [30% MeCN (5 min), followed by a gradient of 30% to 60% MeCN (10 min), then 60% to 100%

¹(a) A. M. Brouwer, *Pure Appl. Chem.*, 2011, **83**, 2213; (b) K.-I. Setsukinai, Y. Urano, K. Kikuchi, T. Higuchi and T. Nagano, *J. Chem. Soc., Perkin Trans. 2*, 2000, 2453.

MeCN (40 min)] at a flow rate of 20.0 mL min⁻¹. Quadruple UV-vis detection was achieved at 220, 260, 350 and 470 nm. *System H*: semi-preparative RP-HPLC (SiliCycle SiliaChrom C₁₈ column, 10 µm, 20 × 250 mm) with MeCN and aq. 0.1% TFA (pH 2.0) as eluents [10% MeCN (5 min), followed by a gradient of 10% to 30% MeCN (10 min), then 30% to 100% MeCN (95 min)] at a flow rate of 20.0 mL min⁻¹. Quadruple UV-vis detection was achieved at 220, 260, 500 and 550 nm. *System I*: system H with the following gradient [25% MeCN (5 min), followed by a gradient of 25% to 45% MeCN (10 min), then 45% to 100% MeCN (75 min)] at a flow rate of 20.0 mL min⁻¹. Quadruple UV-vis detection was achieved at 220, 260, 350 and 550 nm. *System J*: RP-HPLC-fluorescence (Phenomenex Kinetex C₁₈ column, 2.6 µm, 2.1 × 50 mm) with same eluents and gradient as system A. Fluorescence detection was achieved at 45 °C at the following Ex./Em. channels: 525/545 nm, 510/530 nm and 440/600 nm (sensitivity: 1, PMT 1, filter wheel: auto).

***In vitro* activation of fluorogenic "turn-on" probes 2-10 by PGA - experimental details**

Stock solutions of probes, enzyme and chemical reagents

- Solutions Ax (x = 2-10): a stock solution (1.0 mg/mL) of PGA fluorogenic probe in DMSO (for molecular biology, Sigma - Life Science, #D8418) except for **2** (stock solution prepared in HPLC-grade MeCN), *please note: some probes were found to be poorly stable after prolonged storage in DMSO (duration > 1 month, purity checking by HPLC analysis before using). Thus, it was sometimes necessary to use freshly prepared solutions for some experiments.*

- Solution B: Commercial PGA from *Escherichia coli* (Iris Biotech GmbH, #EZ50150, 841 U / mL) directly used without dilution,

- Solution C: a stock solution (1.0 mg/mL, 3.25 mM) of GSH in DMSO (for molecular biology, Sigma - Life Science, #D8418),

- Solution D: a stock solution (1.0 mg/mL, 5.75 mM) of edaravone in DMSO (for molecular biology, Sigma - Life Science, #D8418),

- Solution E: a stock solution (1.0 mg/mL, 8.0 mM) of NEM in DMSO (for molecular biology, Sigma - Life Science, #D8418).

Fluorescence assays

All assays were performed at 37 °C (using a temperature control system combined with water circulation and conducted with magnetic stirring). For all probes **2-10** (final concentration in 3.5 mL fluorescence quartz cell: 1 µM, volume: 3.0 mL), the fluorescence emission of the released pyronin **AR116** was monitored at λ = 525/545 nm (slit = 5 nm) over time with measurements recorded every 5 s. 1 U of PGA (1.2 µL of solution B) was added after 5 min of incubation of the probe in buffer. Blank experiments to assess the stability of the probes in PB, were achieved in the same way but without adding the enzyme.

For rosamine-based probe **7**, a second fluorescence based PGA assay was performed under the same conditions with the following detection parameters Ex./Em. = 535/560 nm (slit = 5 nm) optimised for the released of free rosamine.

For the kinetics performed in the presence of GSH (50 equiv.) with or without PGA, 46 µL of solution C was added after 5 min of incubation of the probe in PB.

HPLC-fluorescence analyses

Enzymatic reaction mixtures from fluorescence-based *in vitro* assays were directly analysed by RP-HPLC-fluorescence after an incubation time of 30 min (injected volume: 20 μ L, system J).

HPLC-MS analyses of PGA activation of probe 10 (enzymatic incubation and sample treatment) to confirm the release of edaravone

Fluorogenic PGA-sensitive probe **10** (12 μ L of solution A10, final concentration: 10 μ M) was dissolved in PB (3.0 mL) containing 12 μ L of PGA solution (solution B, 10 U). The resulting enzymatic reaction mixture was incubated at 37 °C for 20 h. Thereafter, the enzymatic reaction mixture (soft pink colour) was freeze-dried. The resulting white-off amorphous powder was dissolved in a 3:1 (v/v) mixture of ultrapure H₂O and MeCN (total volume = 400 μ L). The solution was vortexed followed by centrifugation (9 000 rpm, 1 min). 20 μ L of supernatant was injected into the HPLC-MS apparatus (system B).

Please note: injection of PB also was also achieved before this analysis, especially to confirm the lack of residual contaminants within the C₁₈ column or ESI probe at $m/z = 175.5 \pm 0.5$ and then avoid misinterpretations in SIM detection mode.

For HPLC analysis of pure edaravone sample, 5 μ L of solution D was added to 1.0 mL of PB (100 mM, pH 7.6) and 20 μ L was injected into the HPLC-MS apparatus (system B).

For "co-injection" analysis, 100 μ L of sample from enzymatic activation (*vide supra*) combined to 100 μ L of PB containing 0.5 μ L of solution D. 20 μ L was injected into the HPLC-MS apparatus (system B).

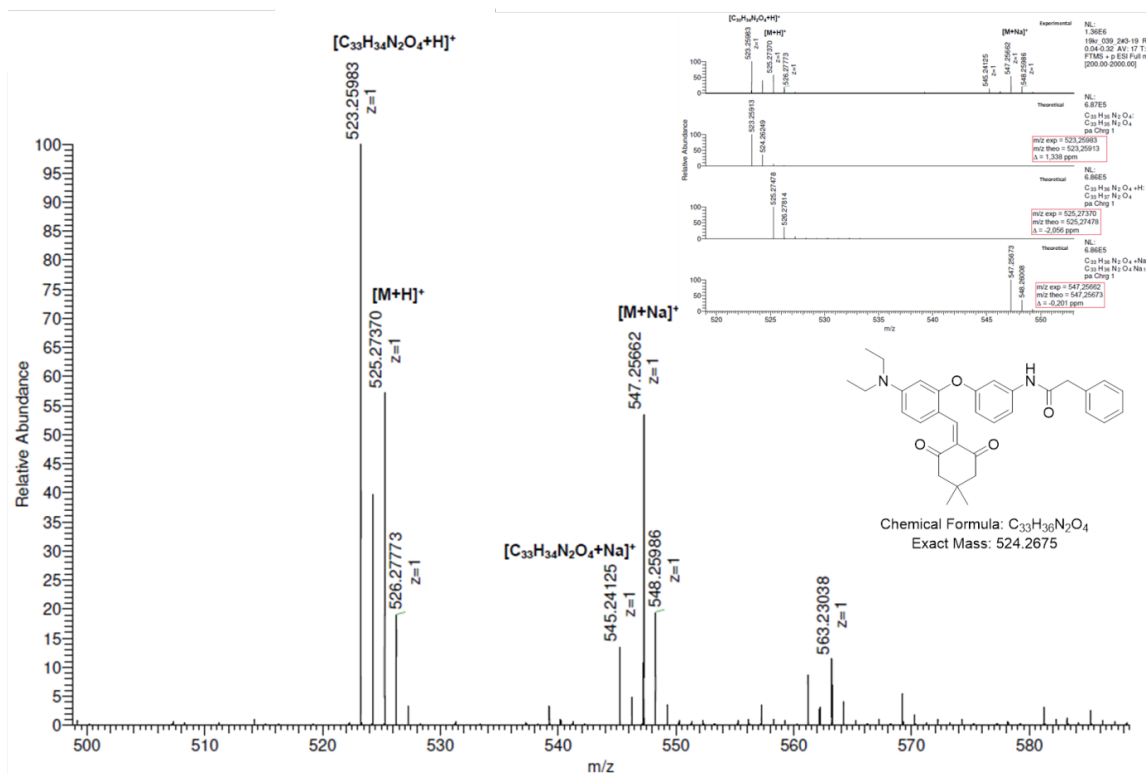
Stability studies of fluorogenic "turn-on" probes 3, 5, 6, 8-10 in aq. solutions and/or in the presence of GSH - experimental details

For each probe, a 2.0 μ M solution was prepared in the corresponding aq. buffer (PB, 100 mM, pH 7.6 or borate buffer, 100 mM, pH 8.6 and 9.5, volume: 3.0 mL). A UV-vis absorption spectrum was recorded (200-800 nm) at 25 °C. Thereafter, the solution was incubated at 25 °C for 30 min and a second UV-vis absorption spectrum was finally recorded under the same conditions. Ratio of absorbance (A_{t30min}/A_{t0}) at λ_{max} was calculated.

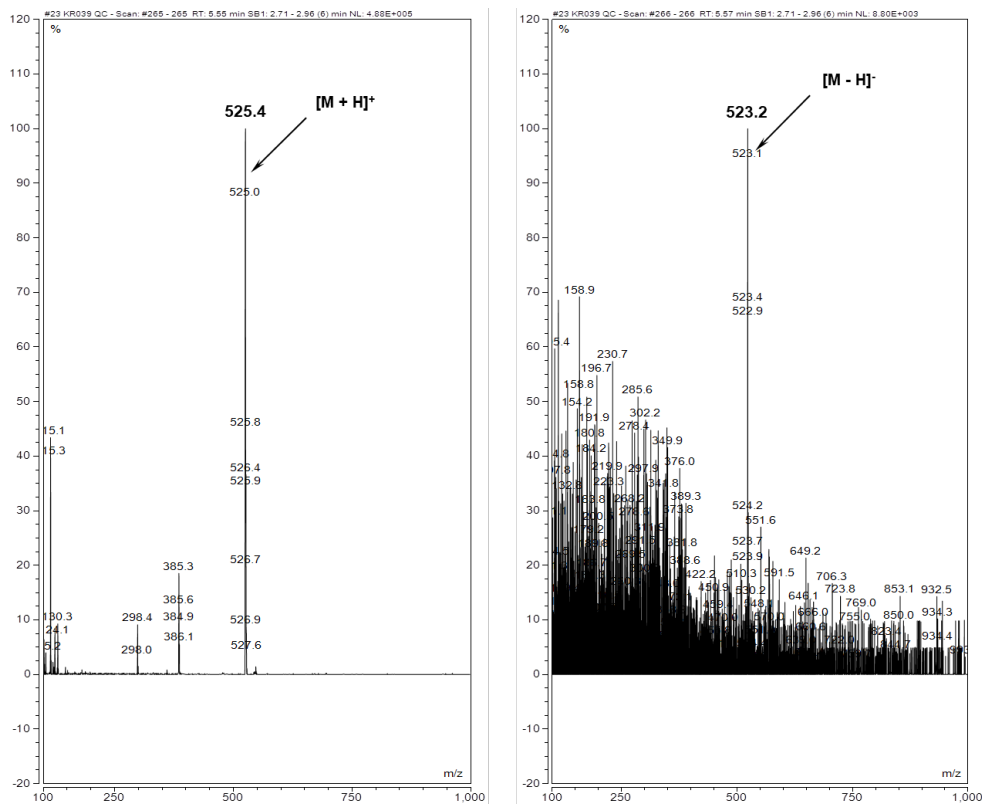
The same procedure was used to assess thiol reactivity of probes **3, 5, 6, 10**, by adding excess of GSH (50 equiv., 92 μ L of solution C) in PB. For barbiturate-based probe **5**, reversibility of thiol addition was demonstrated by further addition of NEM (50 equiv., 37.5 μ L of solution E) in the same reaction mixture after 30 min of incubation at 25 °C.

Analytical data

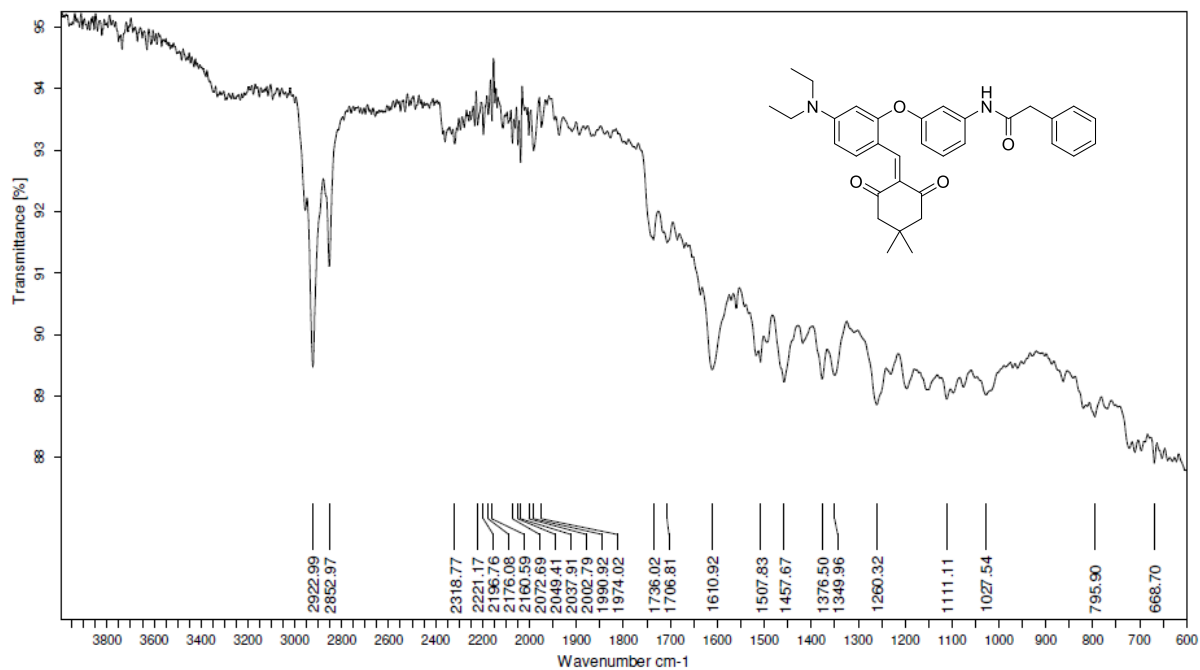
ESI+ mass spectrum (high resolution) of compound 4



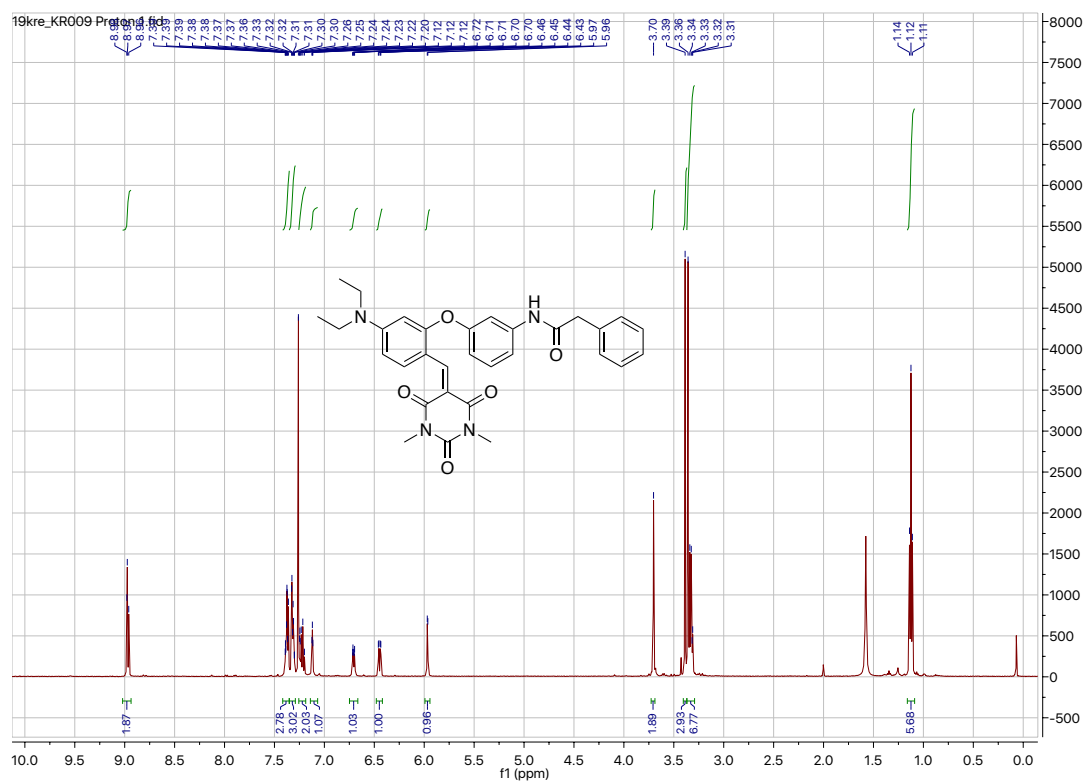
ESI+ (left) / ESI- (right) mass spectrum (low resolution) of compound 4



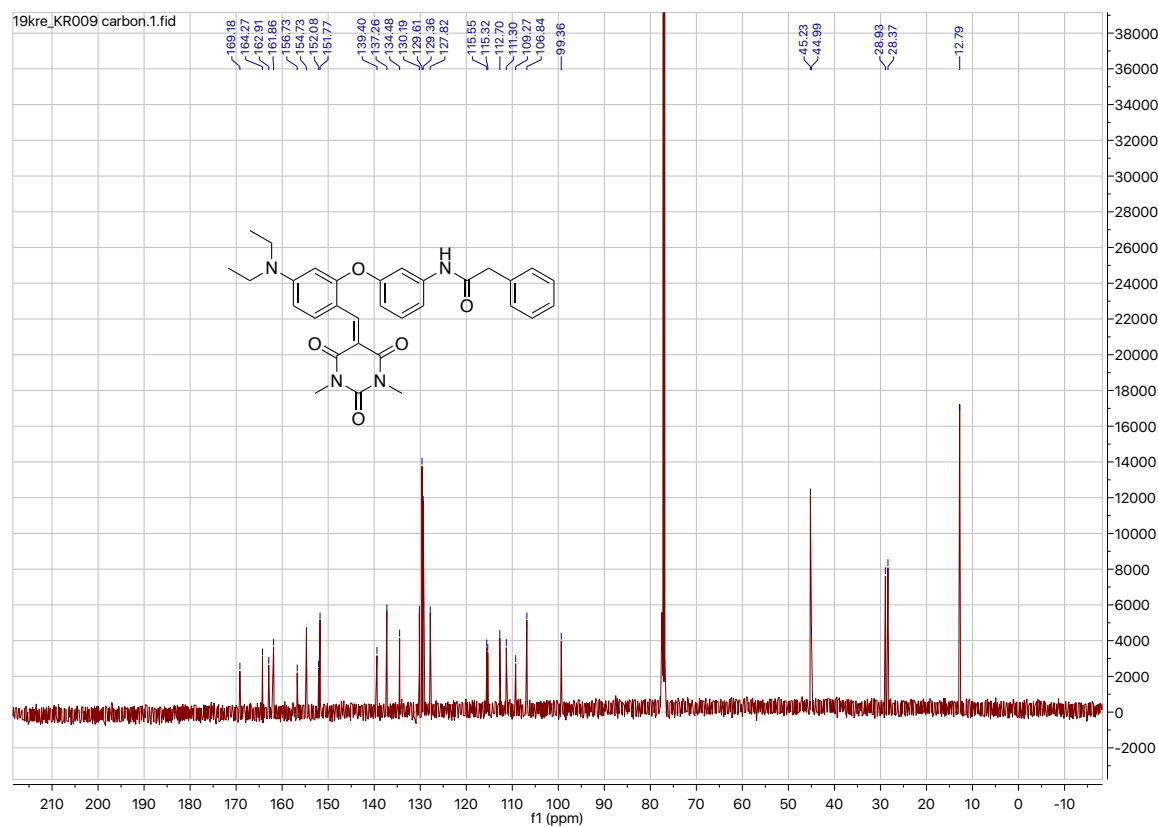
IR-ATR spectrum of compound 4



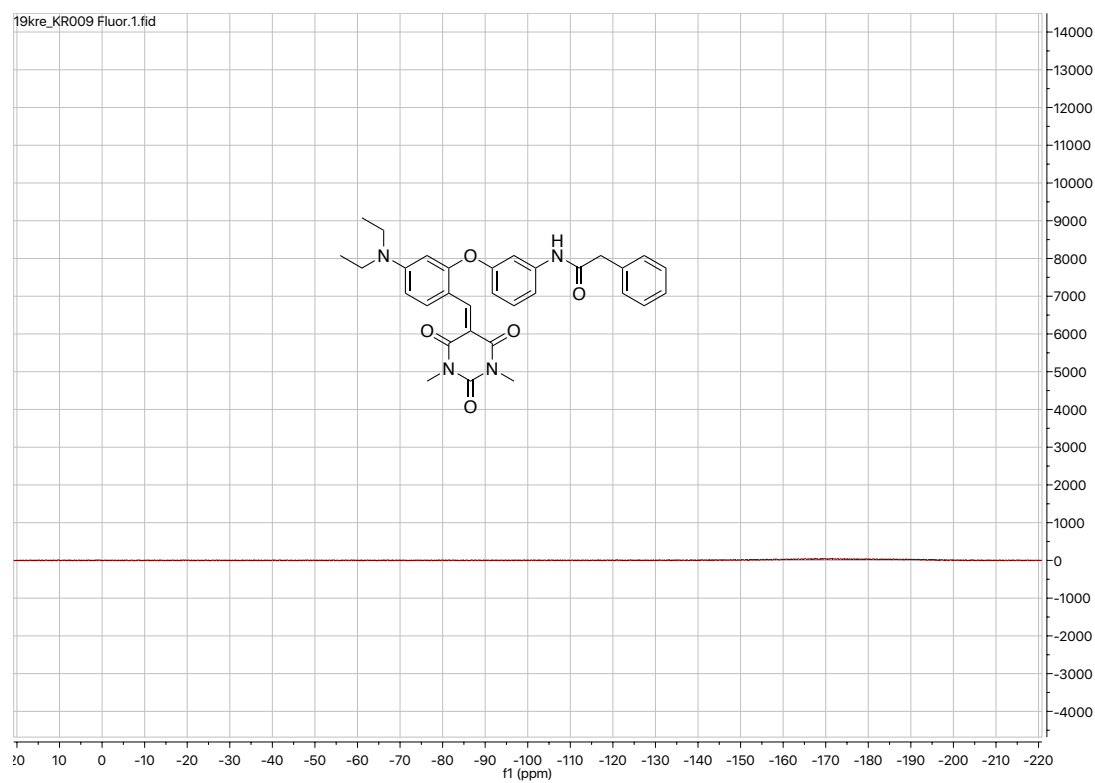
¹H NMR spectrum of compound 5 in CDCl₃ (500 MHz)



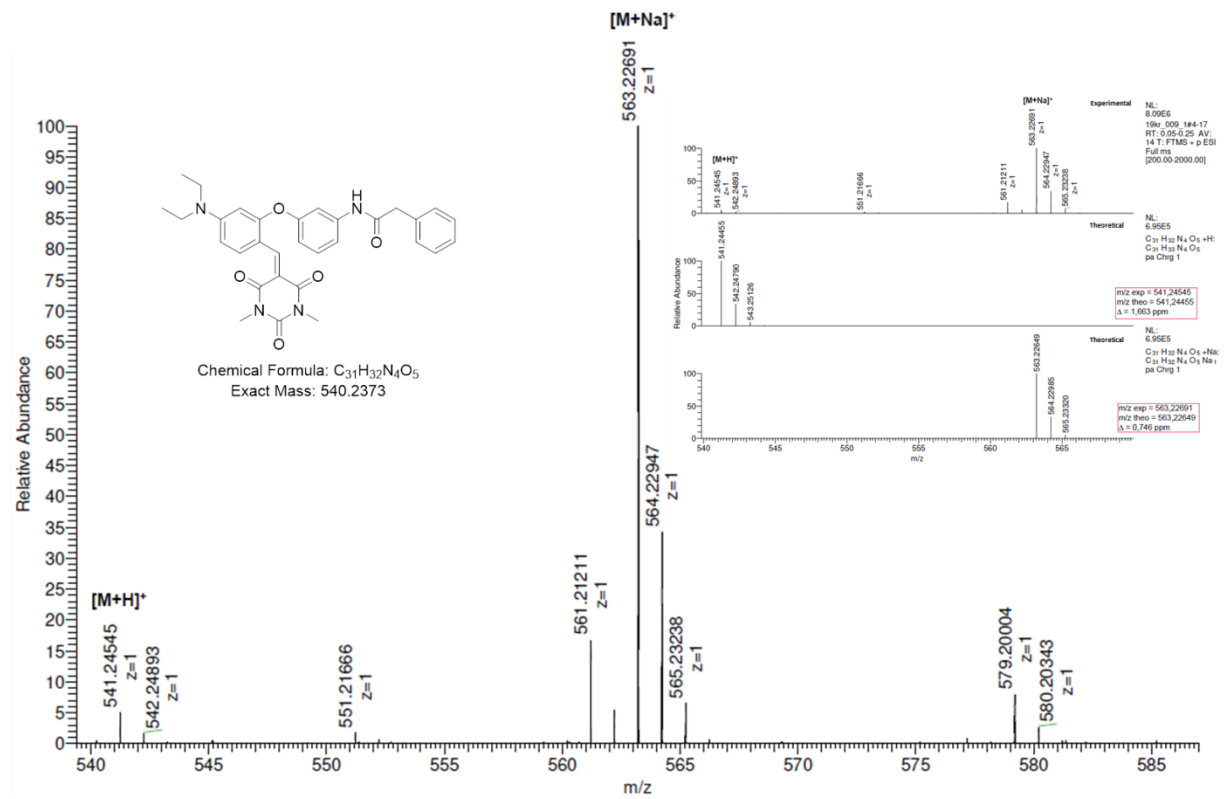
¹³C NMR spectrum of compound 5 in CDCl₃ (126 MHz)



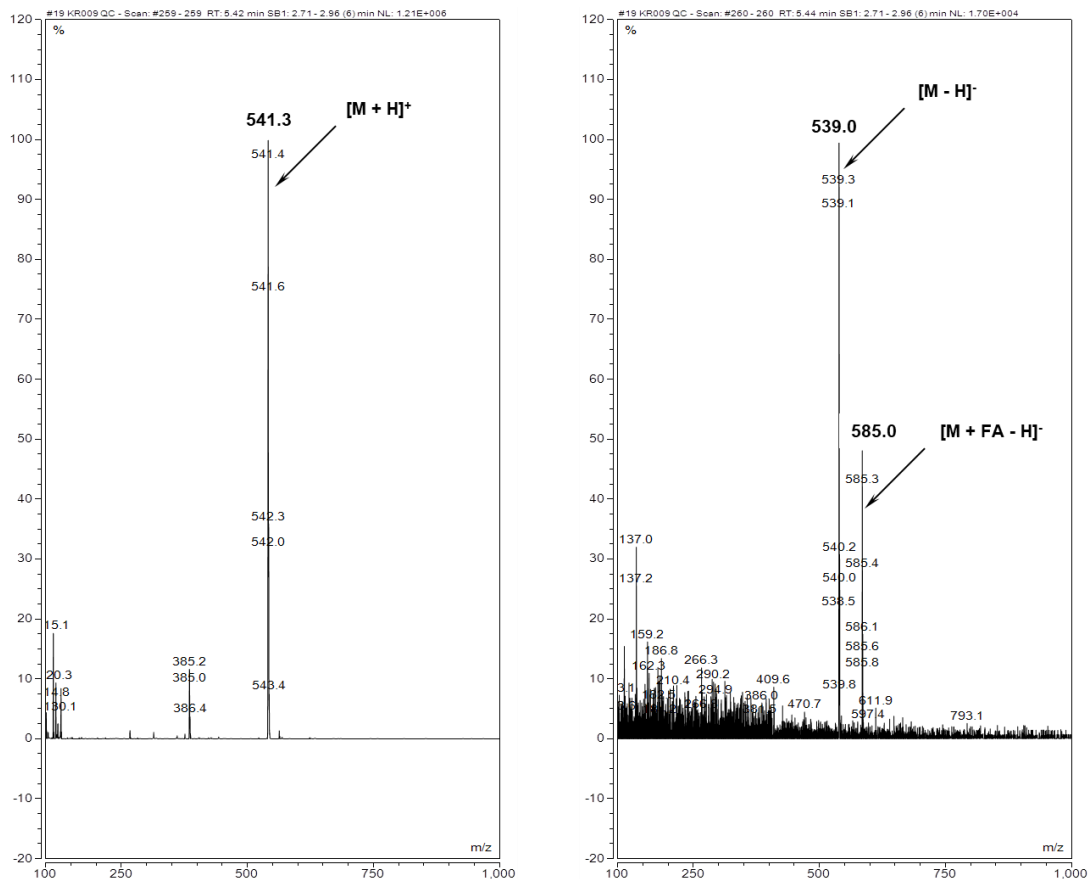
¹⁹F NMR spectrum of compound 5 in CDCl₃ (470 MHz)



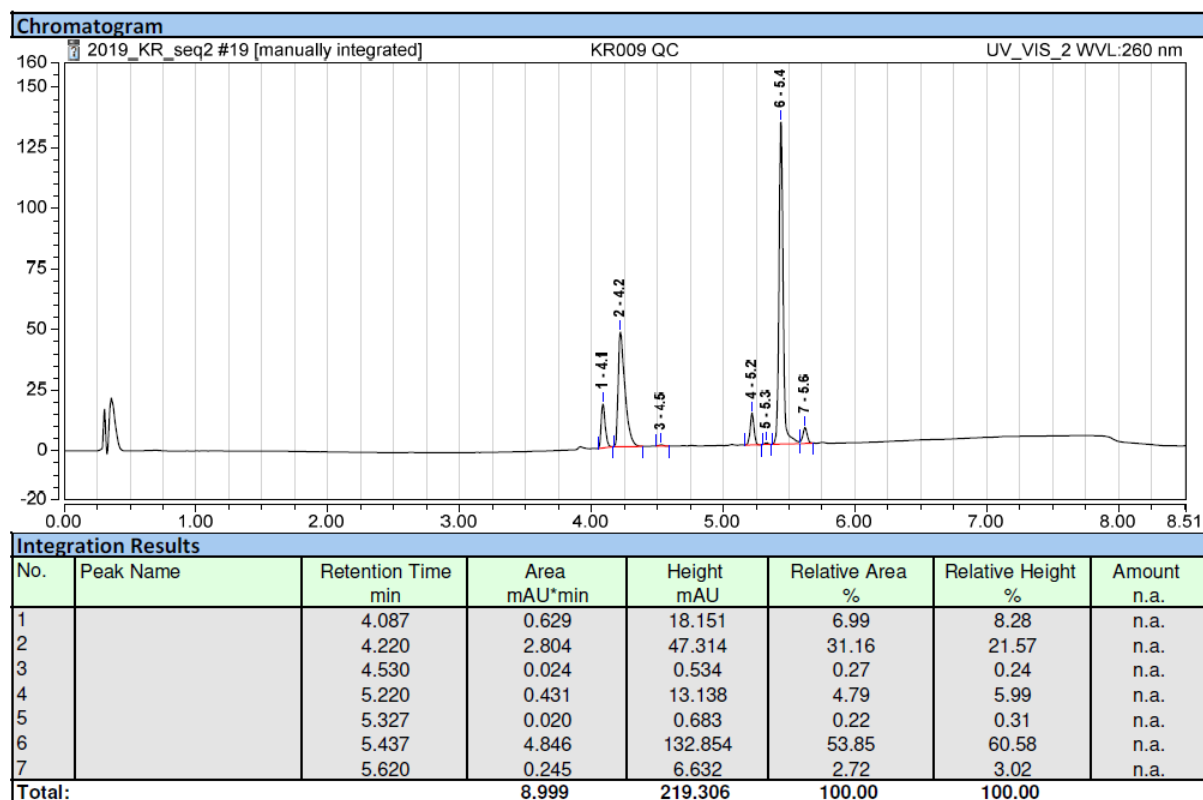
ESI+ mass spectrum (high resolution) of compound 5



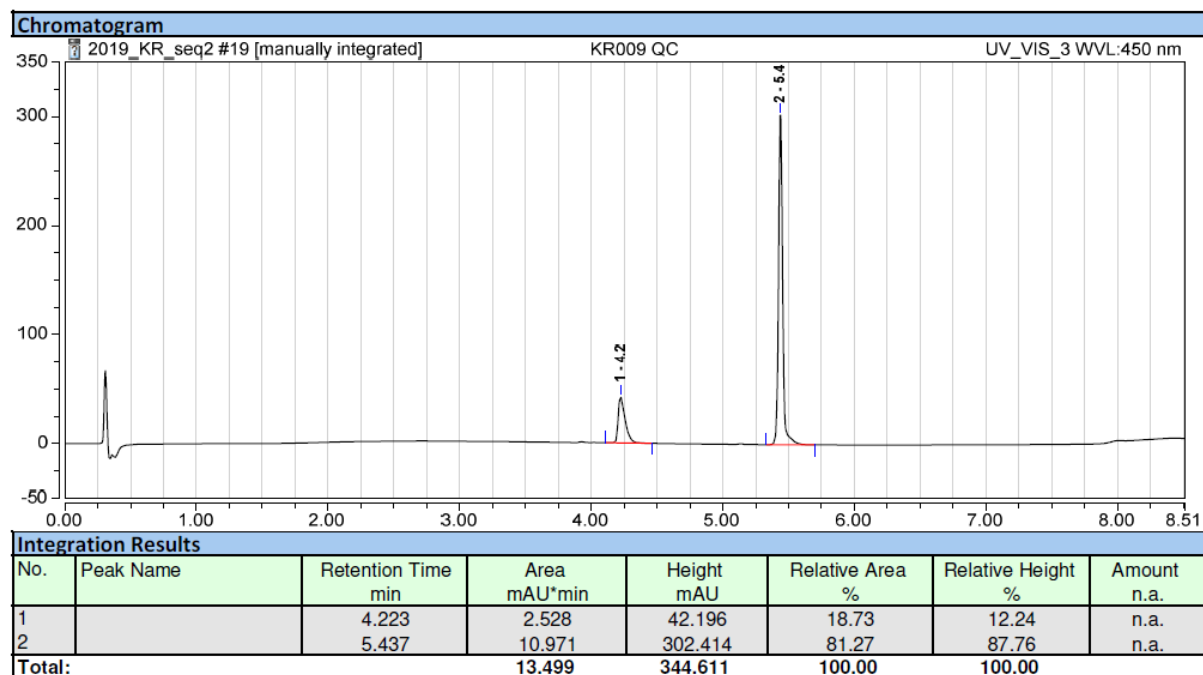
ESI+ (left) / ESI- (right) mass spectrum (low resolution) of compound 5



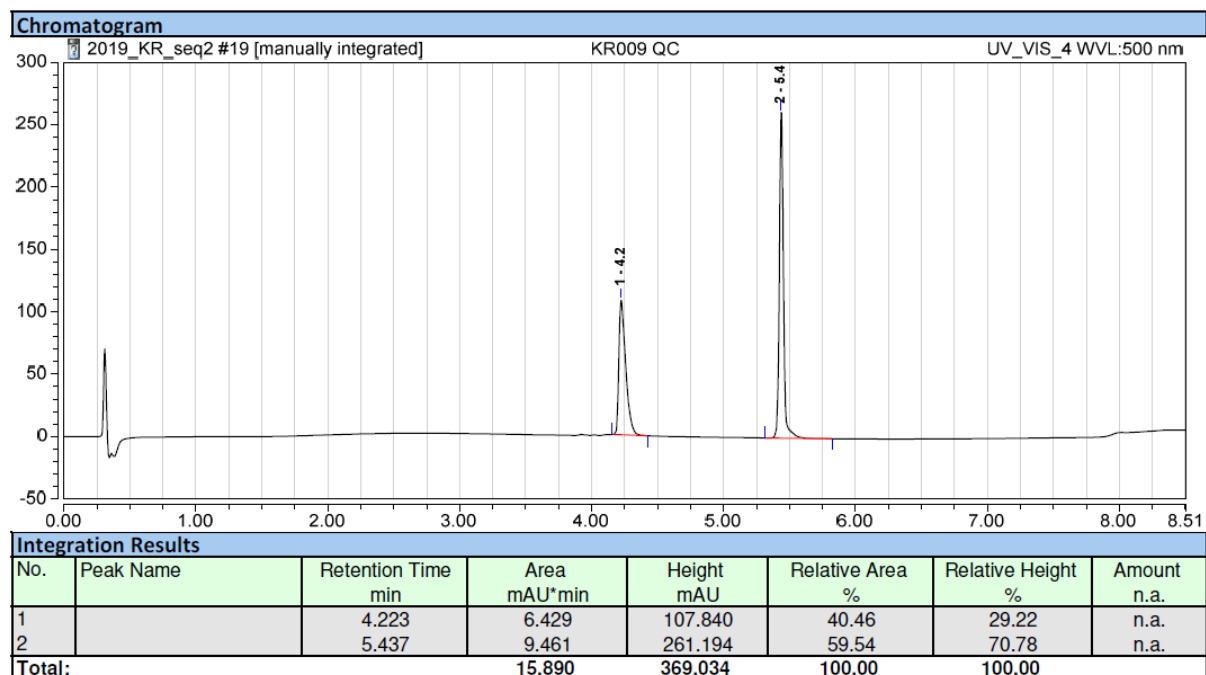
RP-HPLC elution profile of compound 5 (system A, detection at 260 nm)



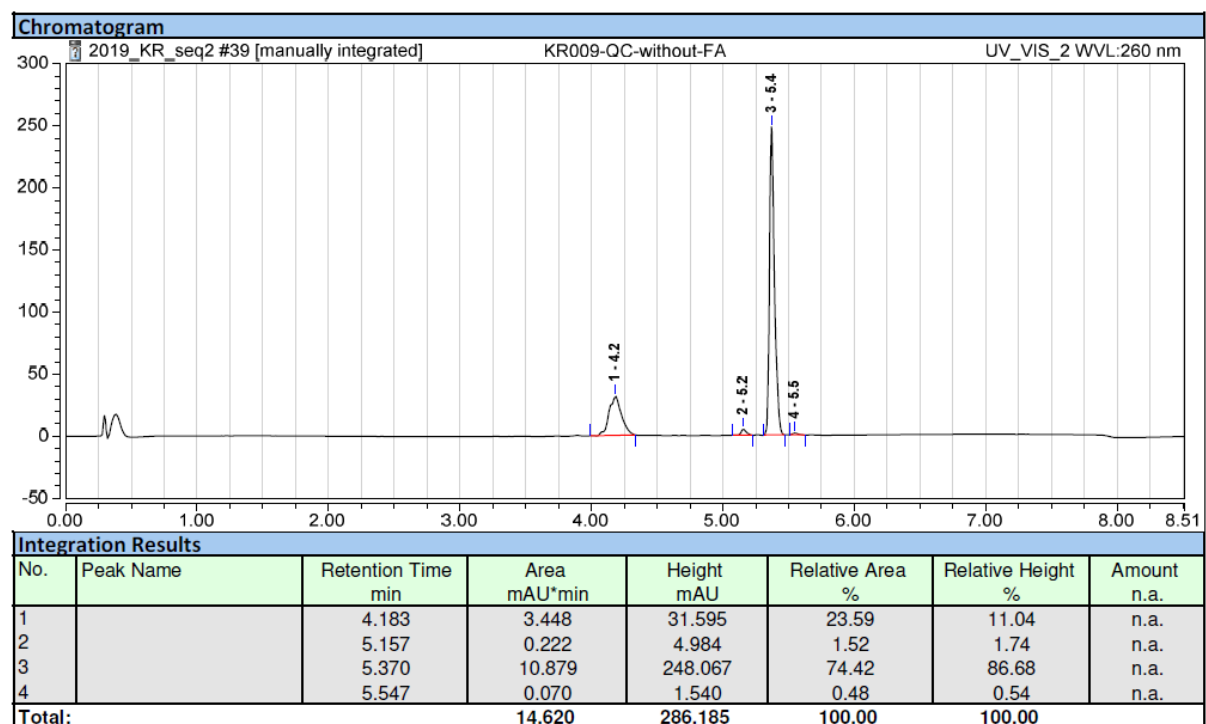
RP-HPLC elution profile of compound 5 (system A, detection at 450 nm)



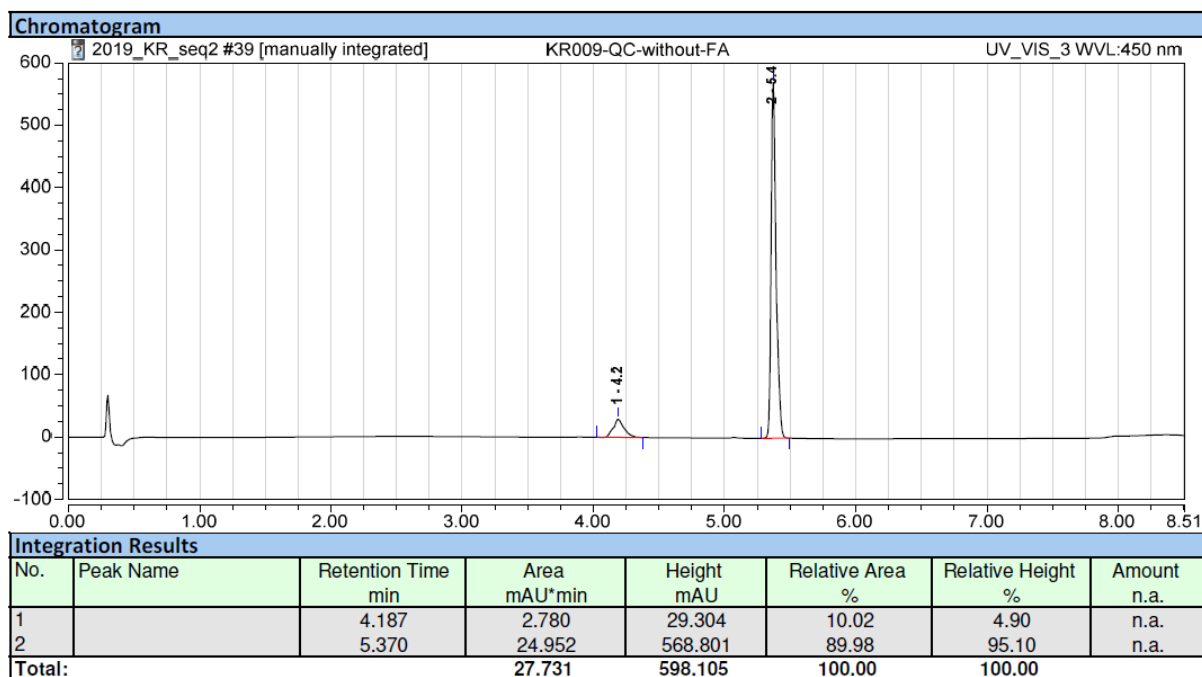
RP-HPLC elution profile of compound 5 (system A, detection at 500 nm)



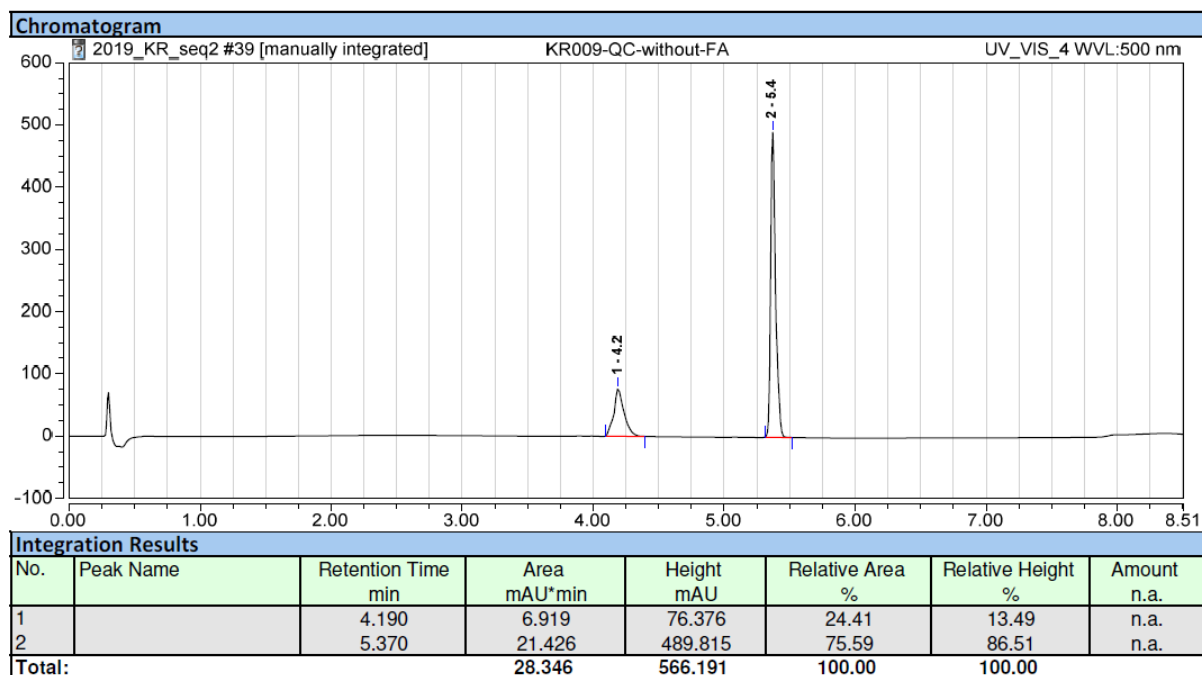
RP-HPLC elution profile of compound 5 (system C, detection at 260 nm)



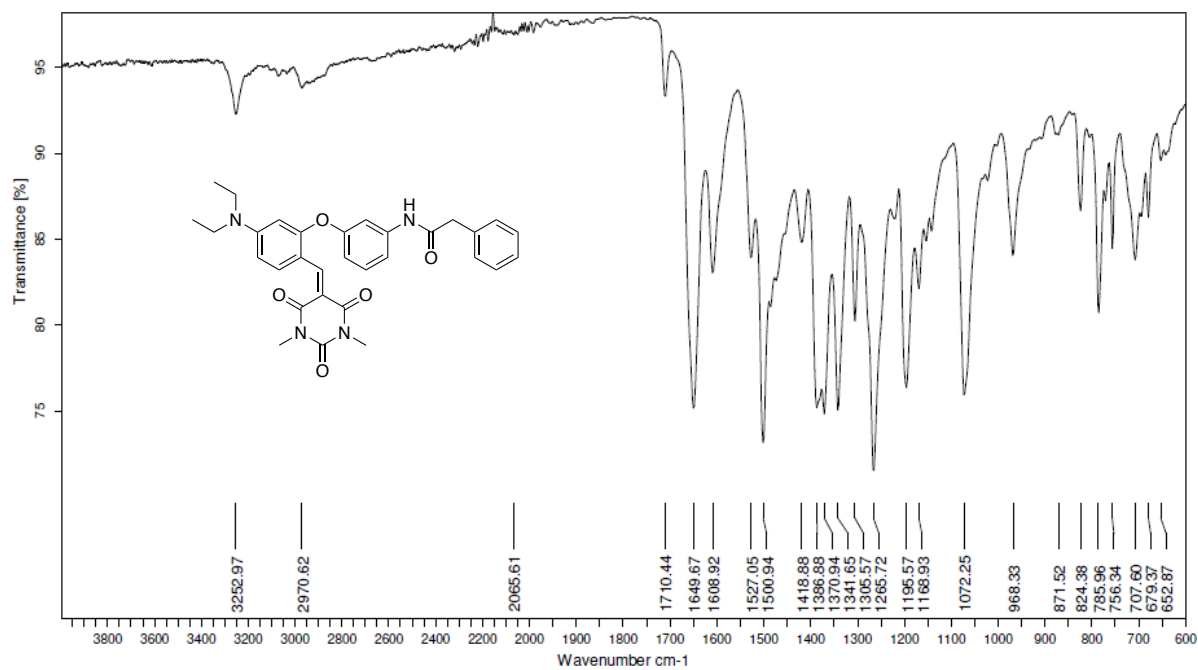
RP-HPLC elution profile of compound 5 (system C, detection at 450 nm)



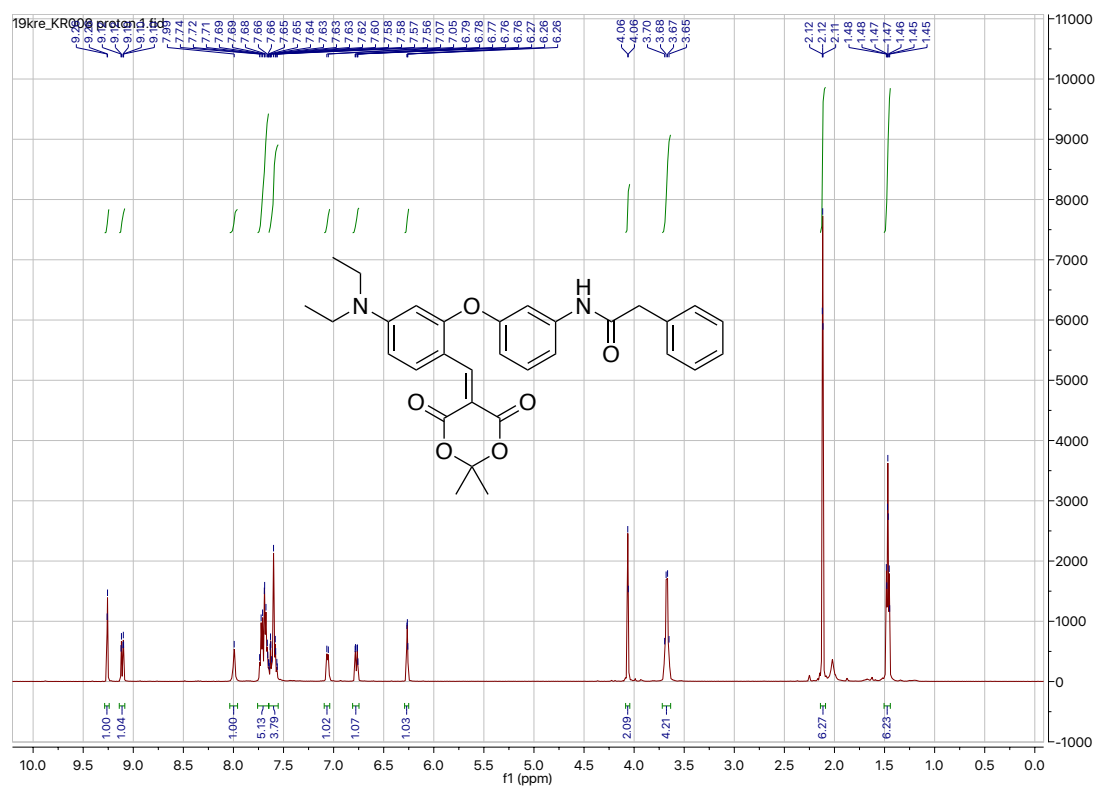
RP-HPLC elution profile of compound 5 (system C, detection at 500 nm)



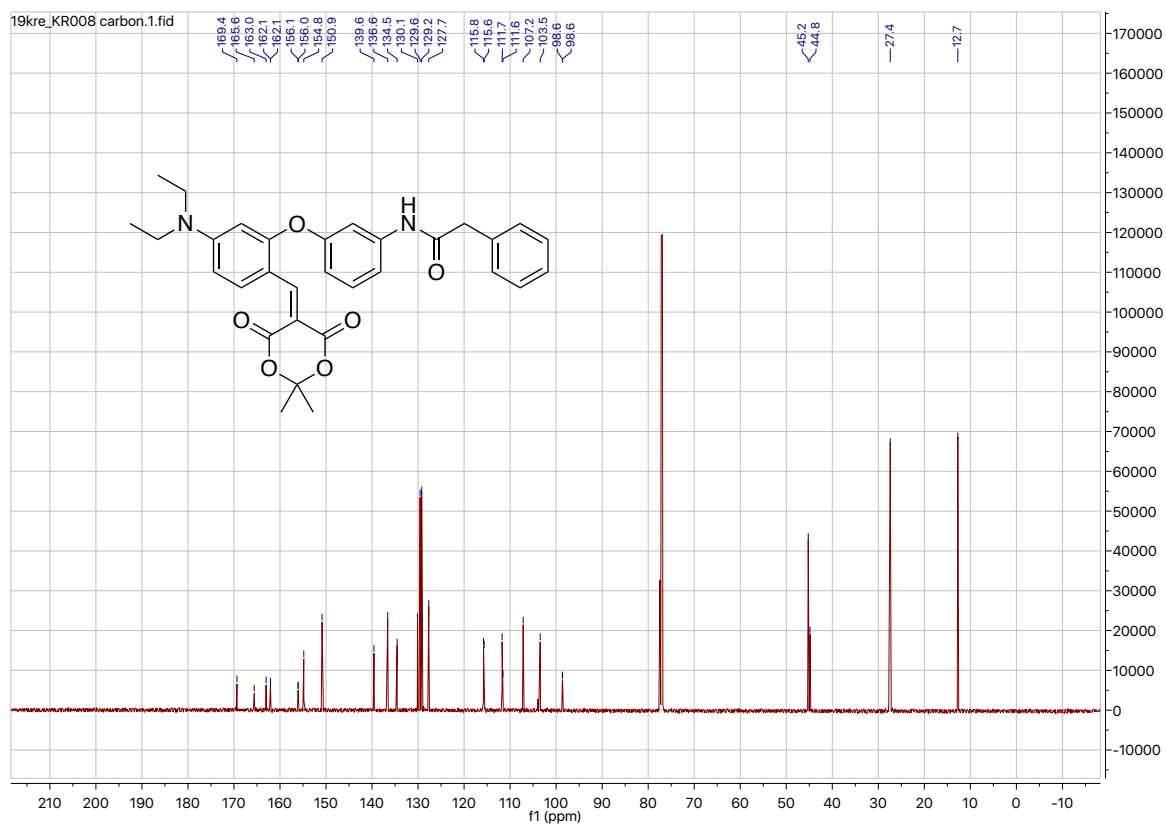
IR-ATR spectrum of compound 5



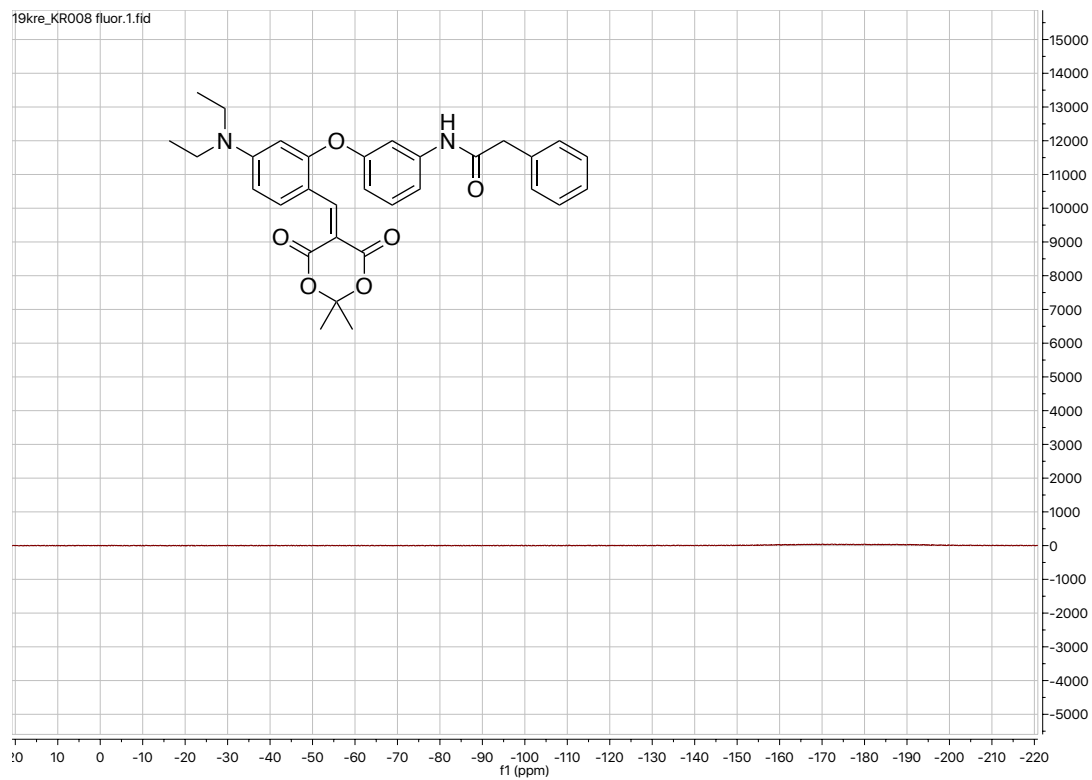
¹H NMR spectrum of compound 6 in CDCl₃ (500 MHz)



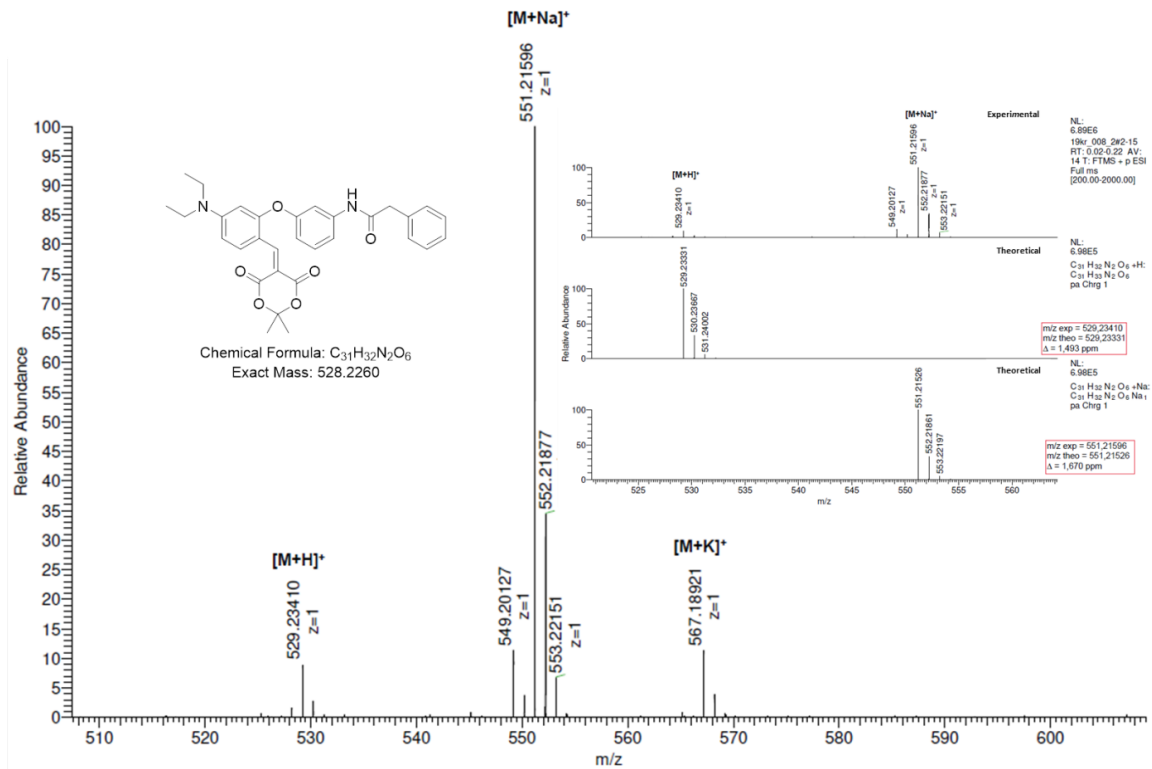
¹³C NMR spectrum of compound 6 in CDCl₃ (126 MHz)



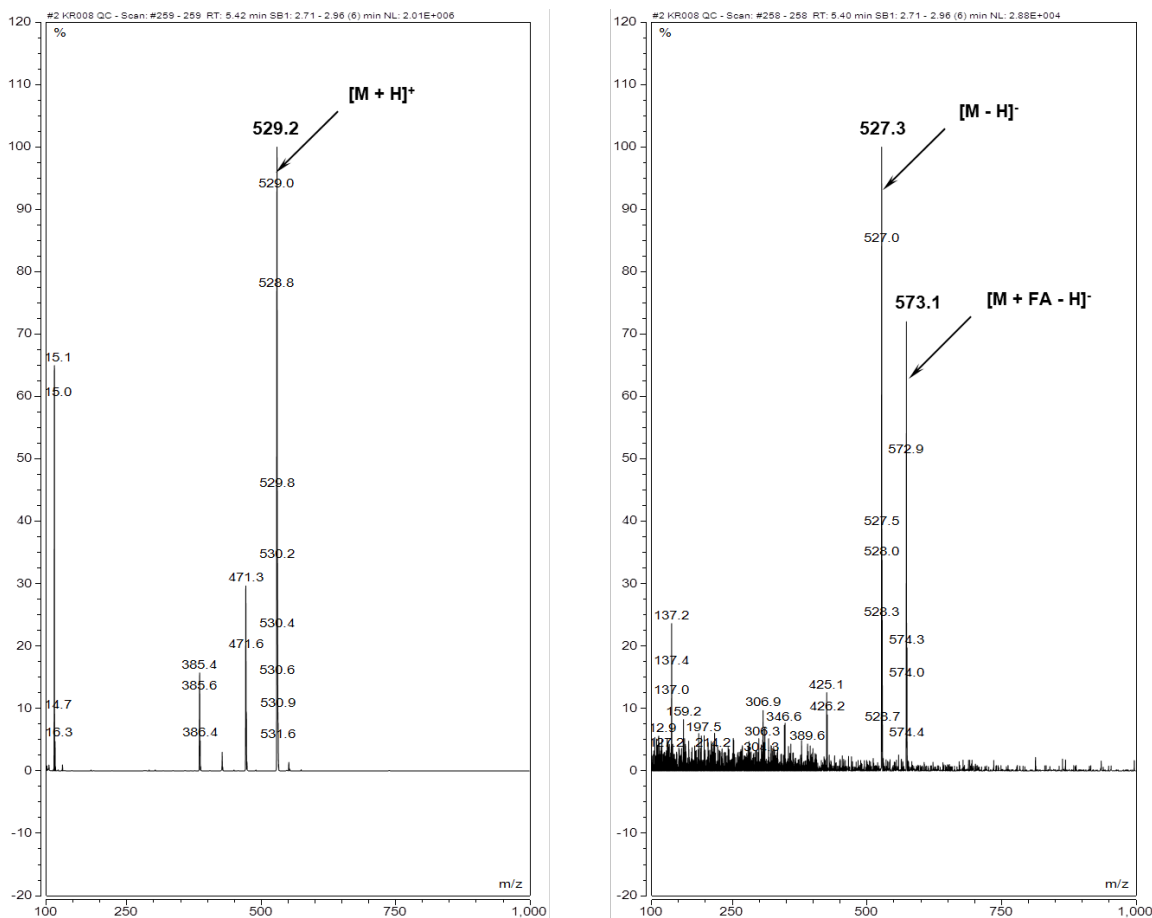
¹⁹F NMR spectrum of compound 6 in CDCl₃ (470 MHz)



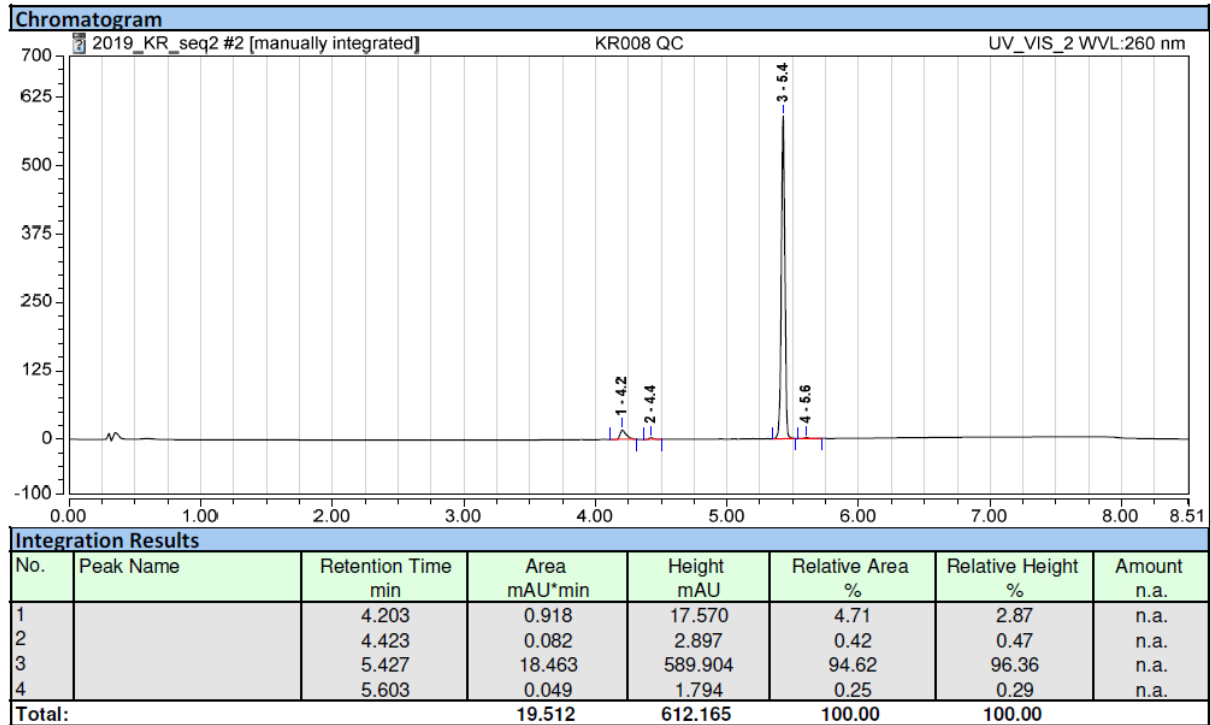
ESI+ mass spectrum (high resolution) of compound 6



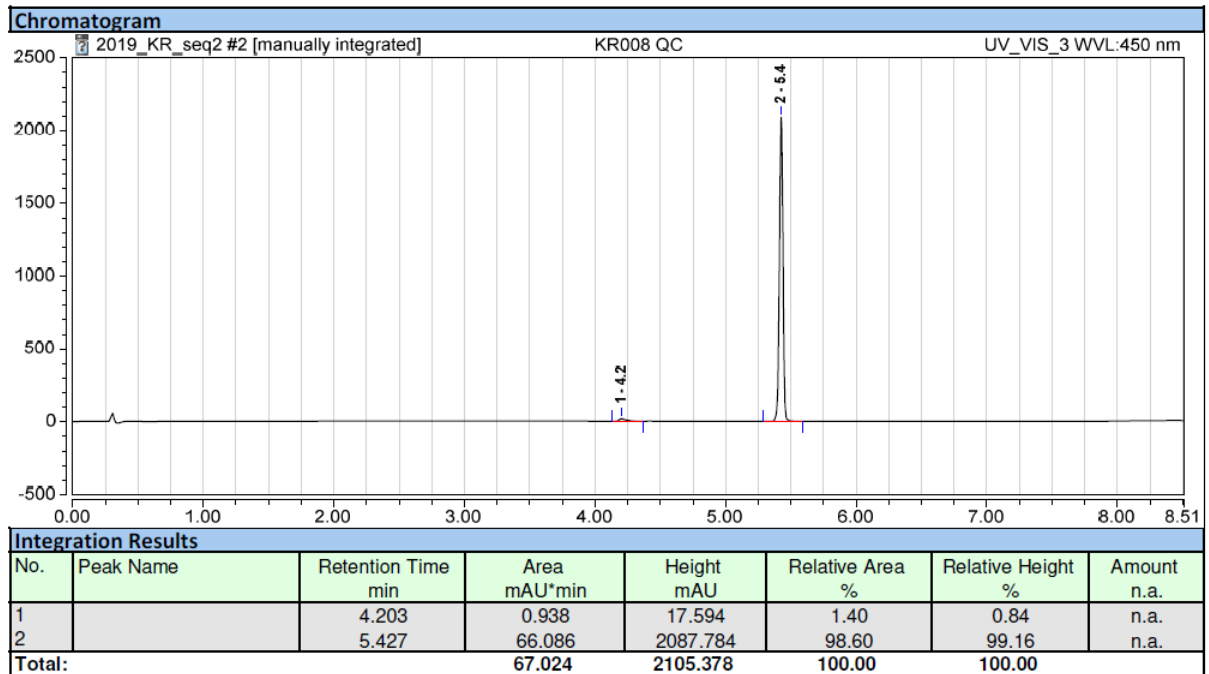
ESI+ (left) / ESI- (right) mass spectrum (low resolution) of compound 6



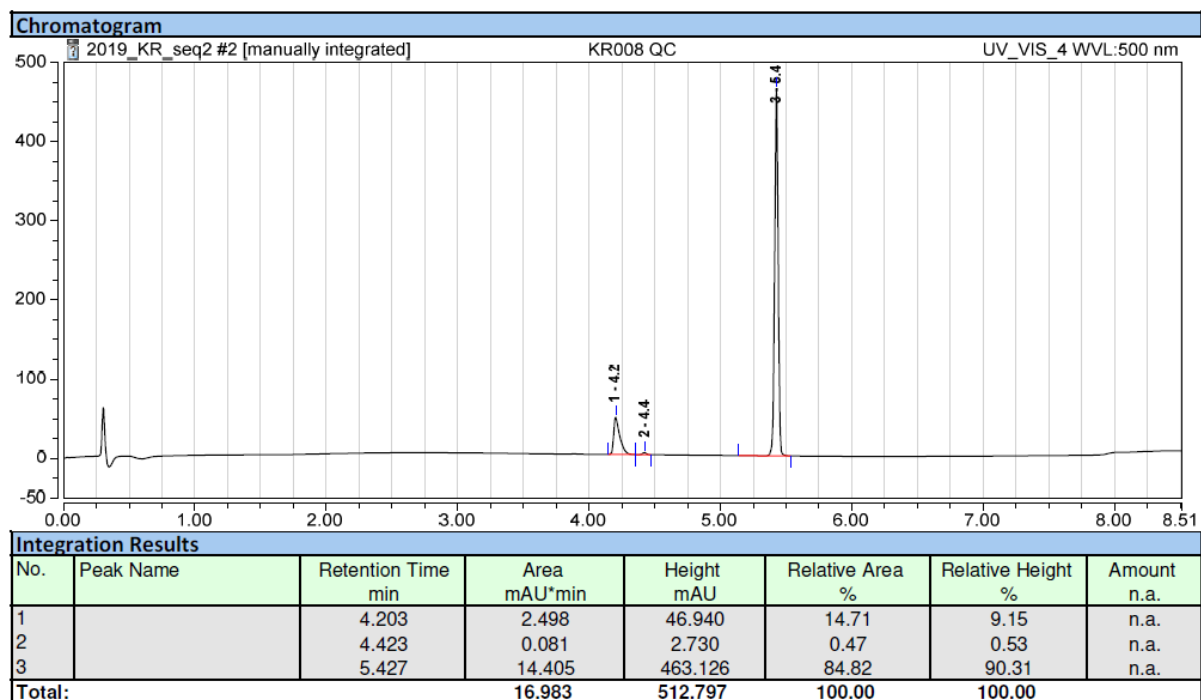
RP-HPLC elution profile of compound 6 (system A, detection at 260 nm)



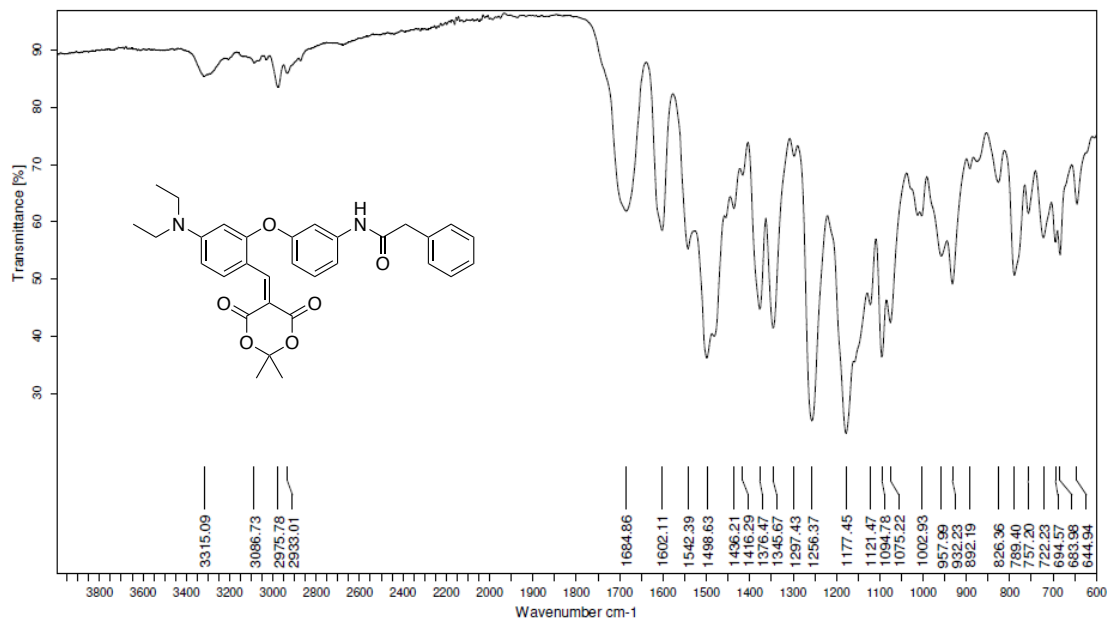
RP-HPLC elution profile of compound 6 (system A, detection at 450 nm)



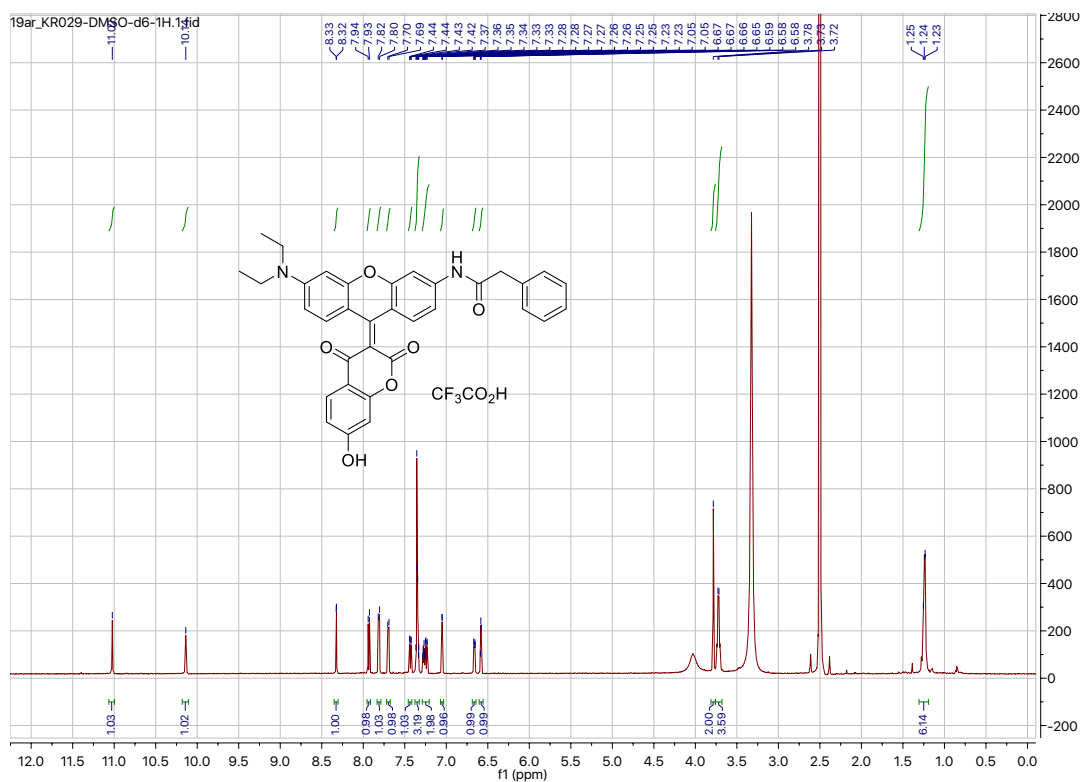
RP-HPLC elution profile of compound 6 (system A, detection at 500 nm)



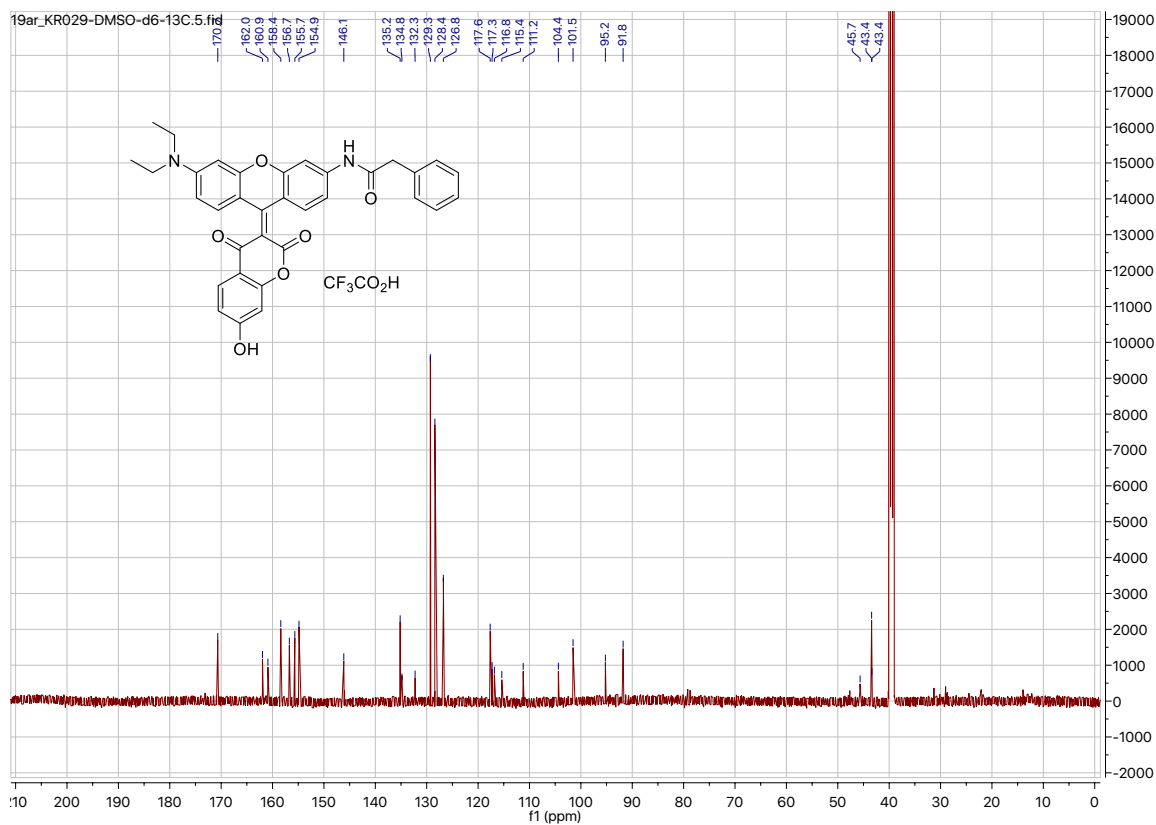
IR-ATR spectrum of compound 6



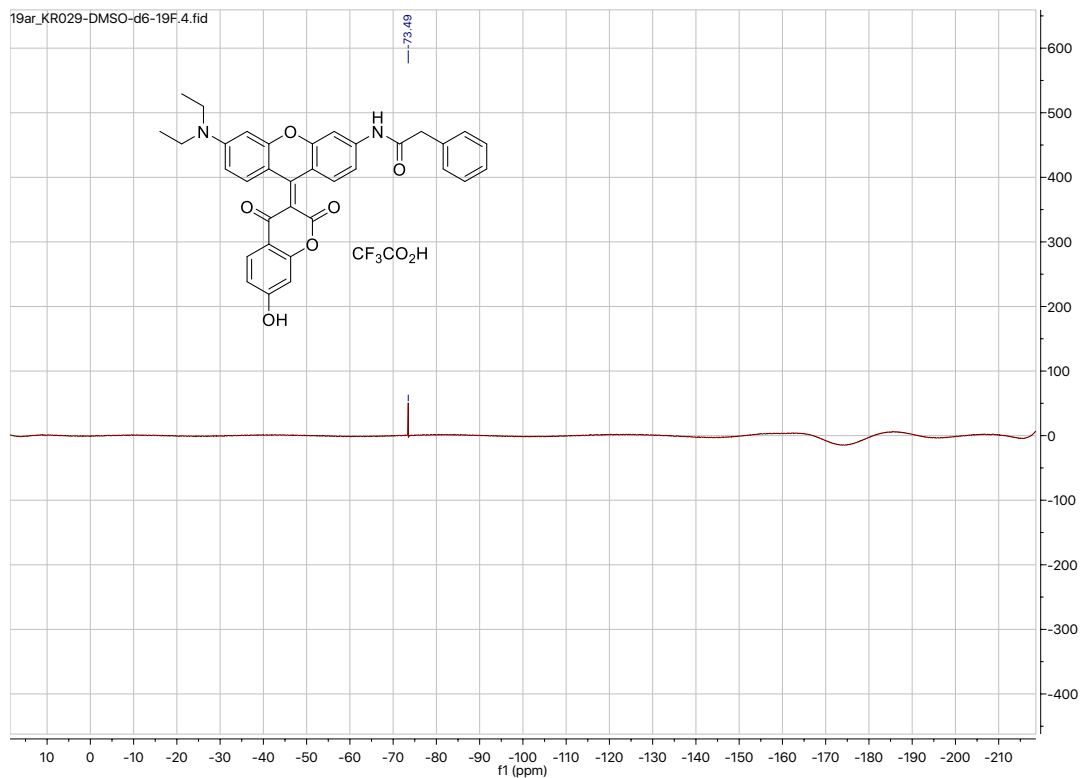
¹H NMR spectrum of compound 7 in CDCl₃ (600 MHz)



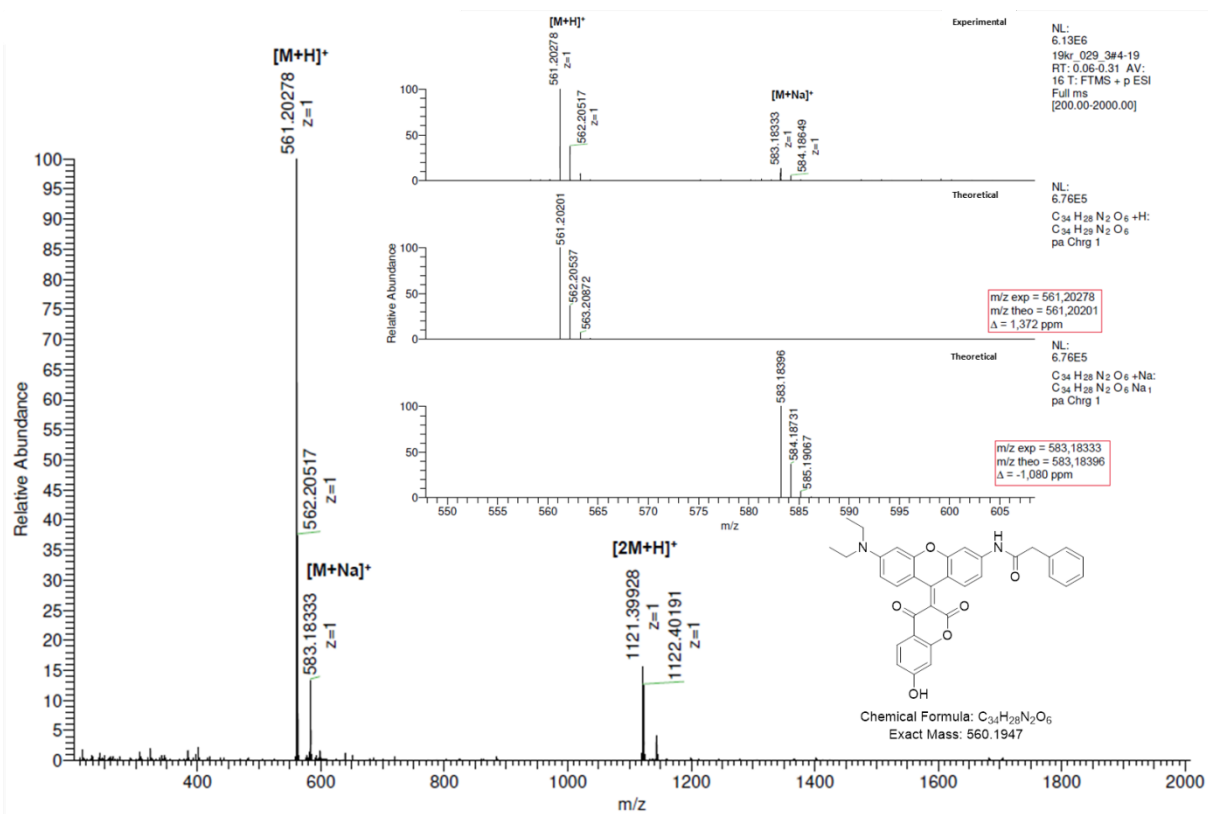
¹³C NMR spectrum of compound 7 in CDCl₃ (151 MHz)



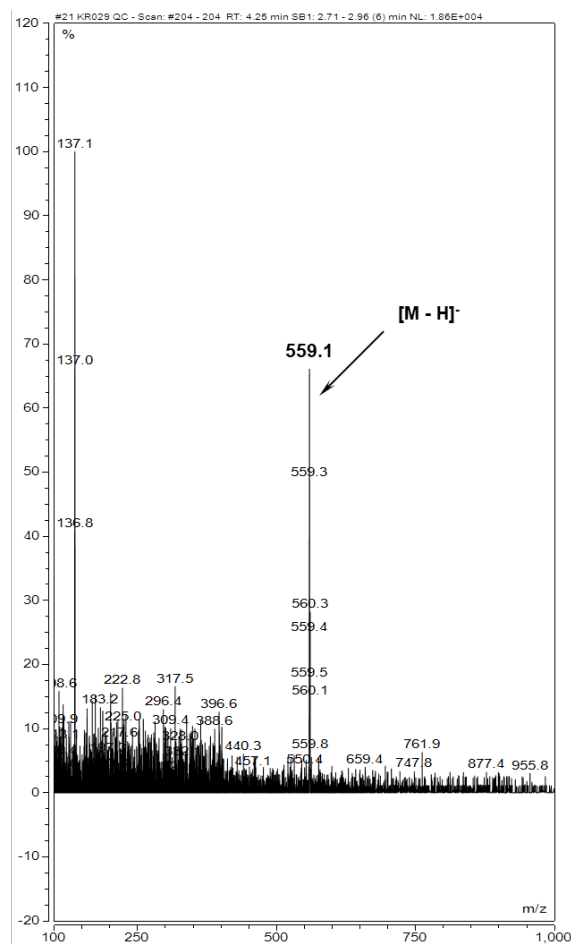
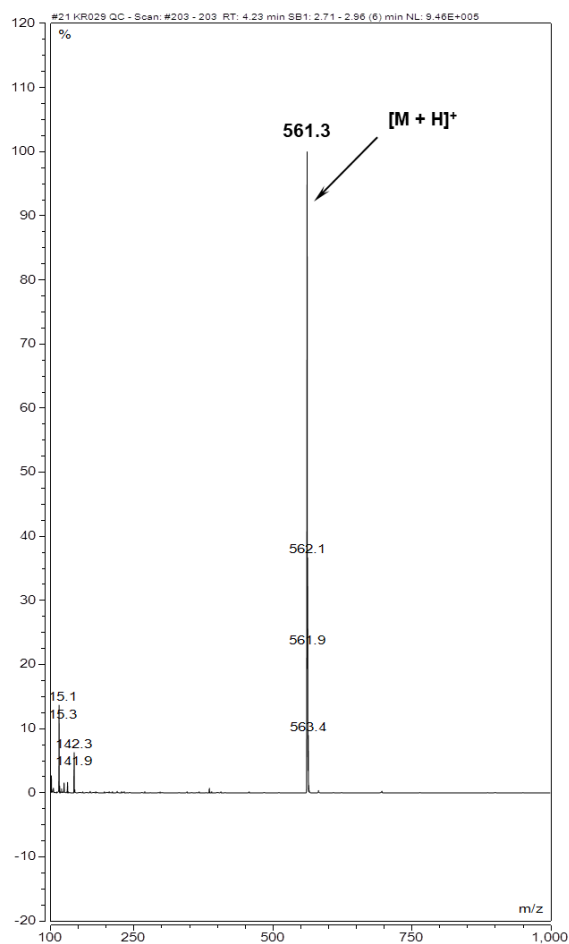
¹⁹F NMR spectrum of compound 7 in CDCl₃ (565 MHz)



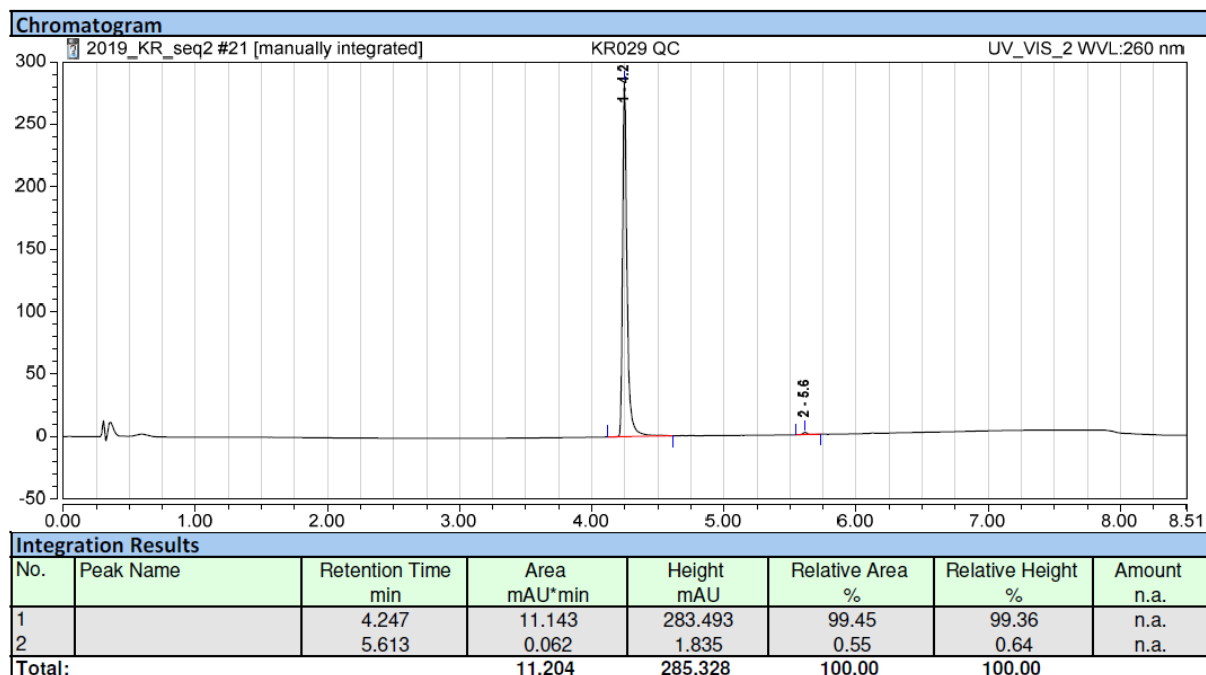
ESI+ mass spectrum (high resolution) of compound 7



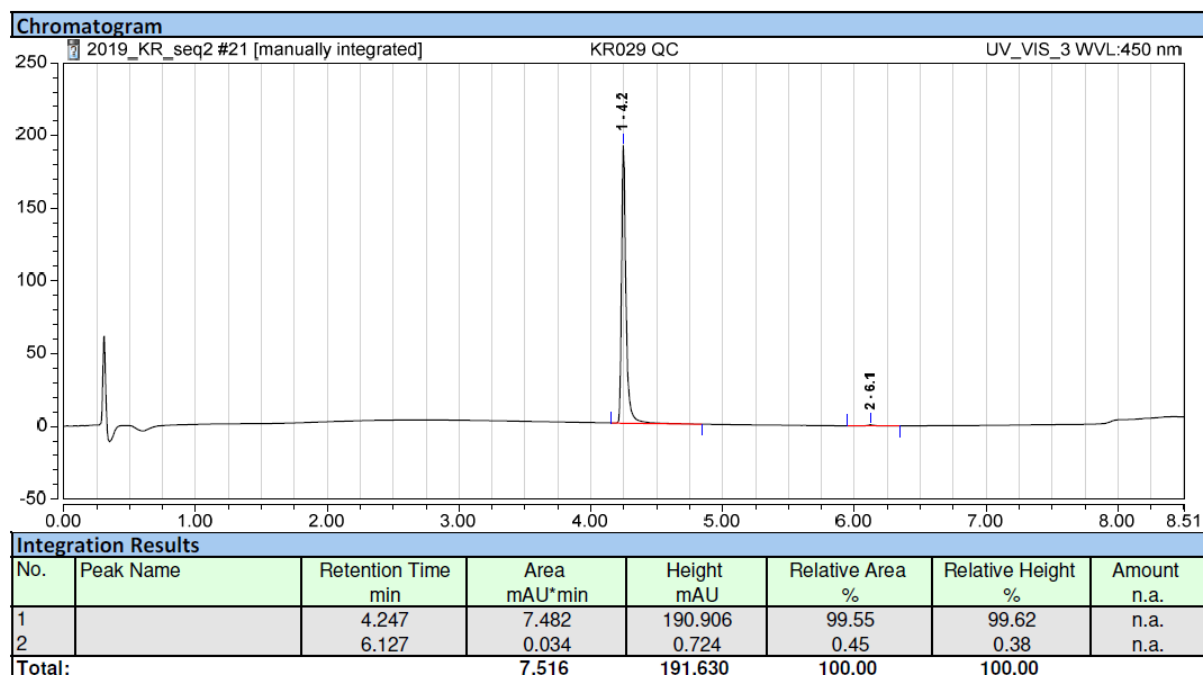
ESI+ (left) / ESI- (right) mass spectrum (low resolution) of compound 7



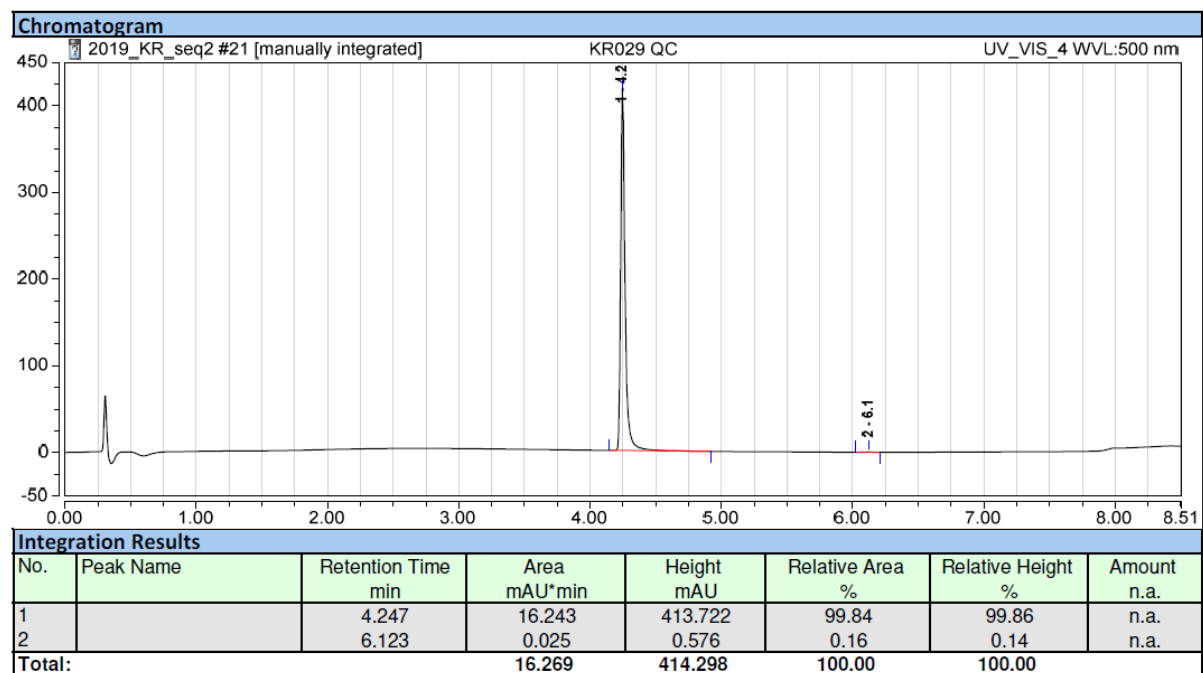
RP-HPLC elution profile of compound 7 (system A, detection at 260 nm)



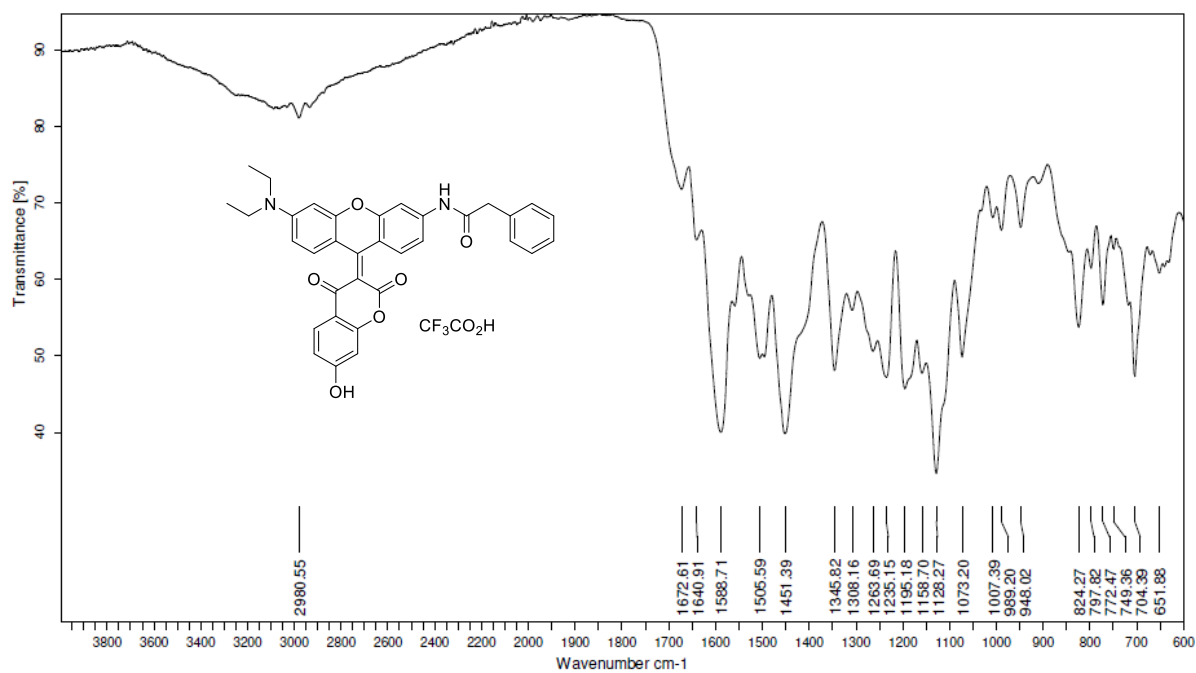
RP-HPLC elution profile of compound 7 (system A, detection at 450 nm)



RP-HPLC elution profile of compound 7 (system A, detection at 500 nm)



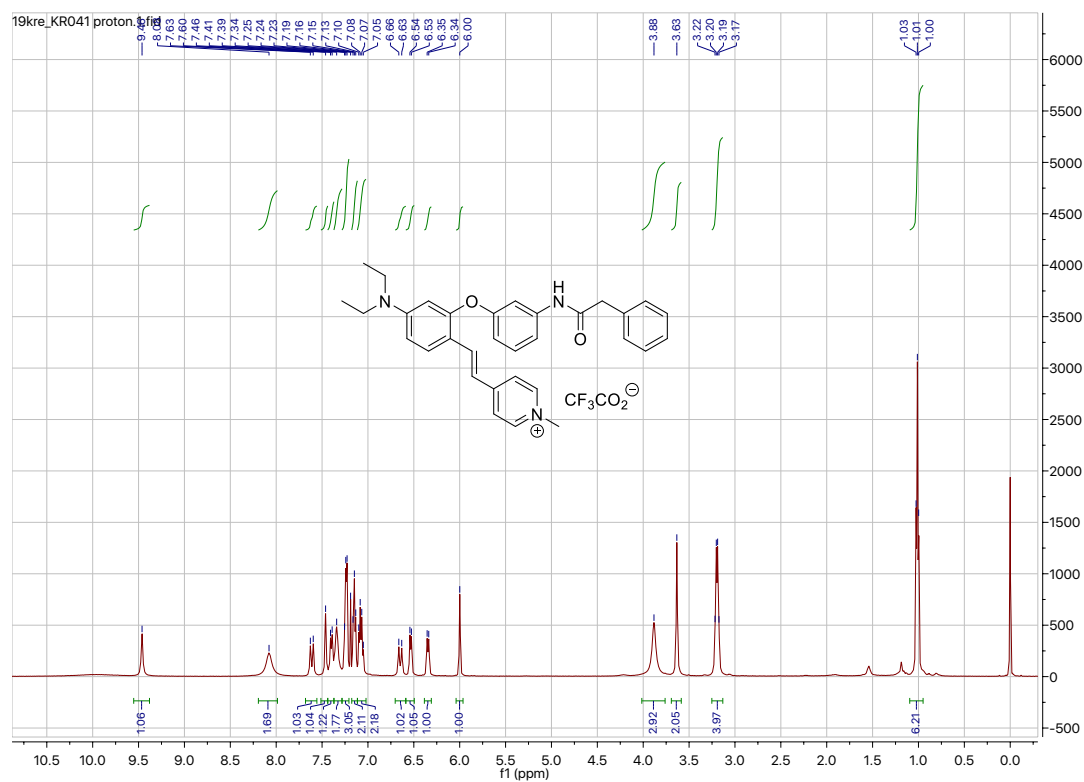
IR-ATR spectrum of compound 7



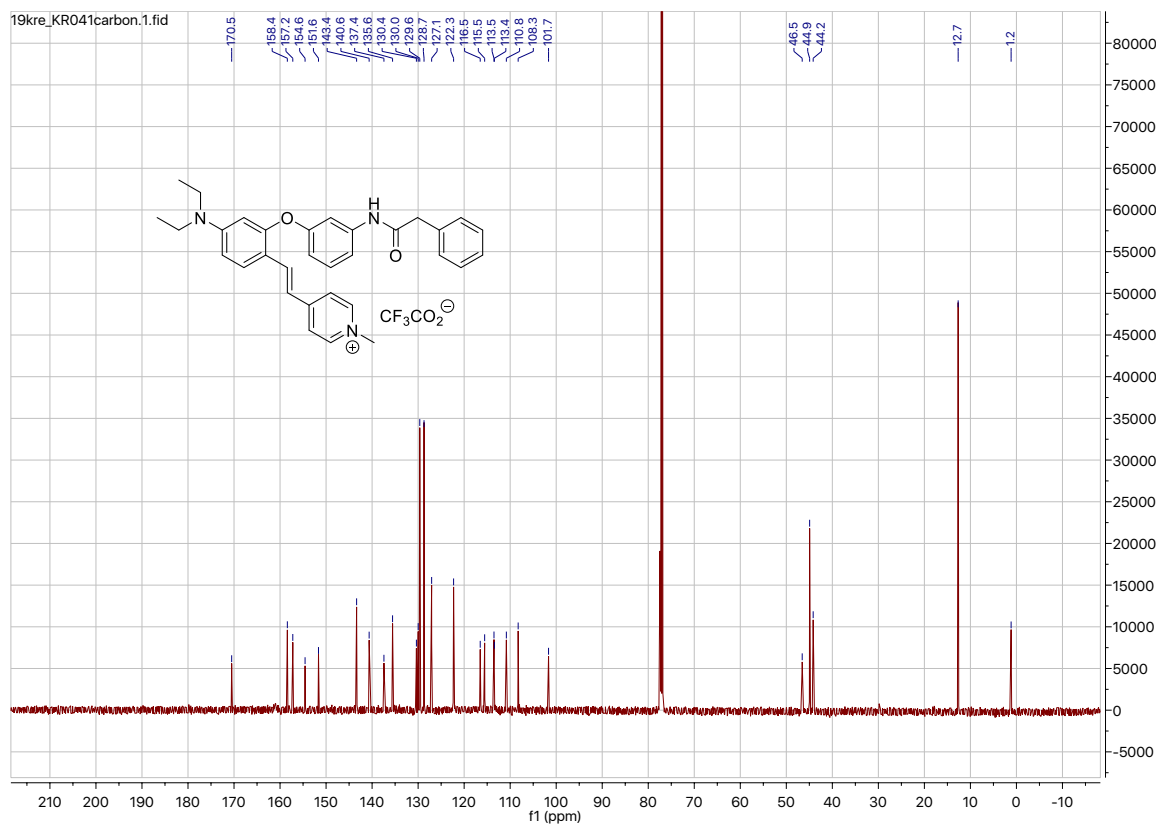
TFA determination by ionic chromatography - results

Concentration	1.0 mg/mL in DMSO	
Sample dilution factor	100	50
Raw data ppm	1.057	2.310
Content in wt %	10.57	11.55
Average content in wt %	11.06	

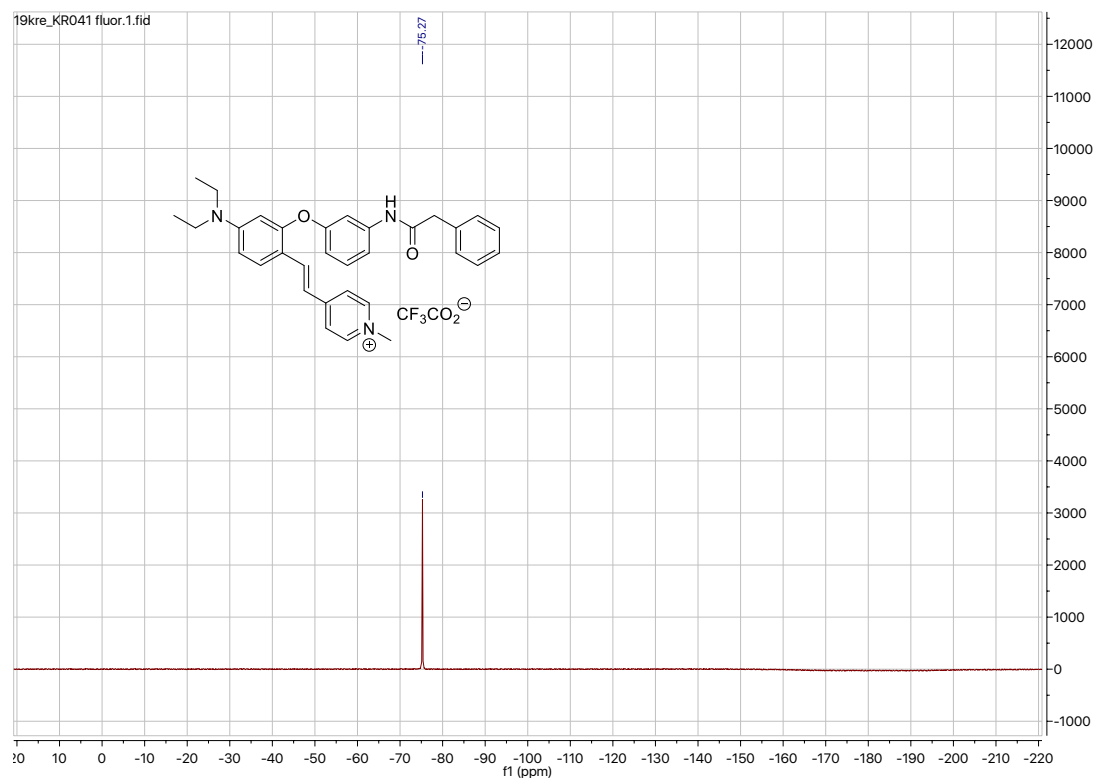
¹H NMR spectrum of compound 8 in CDCl₃ (500 MHz)



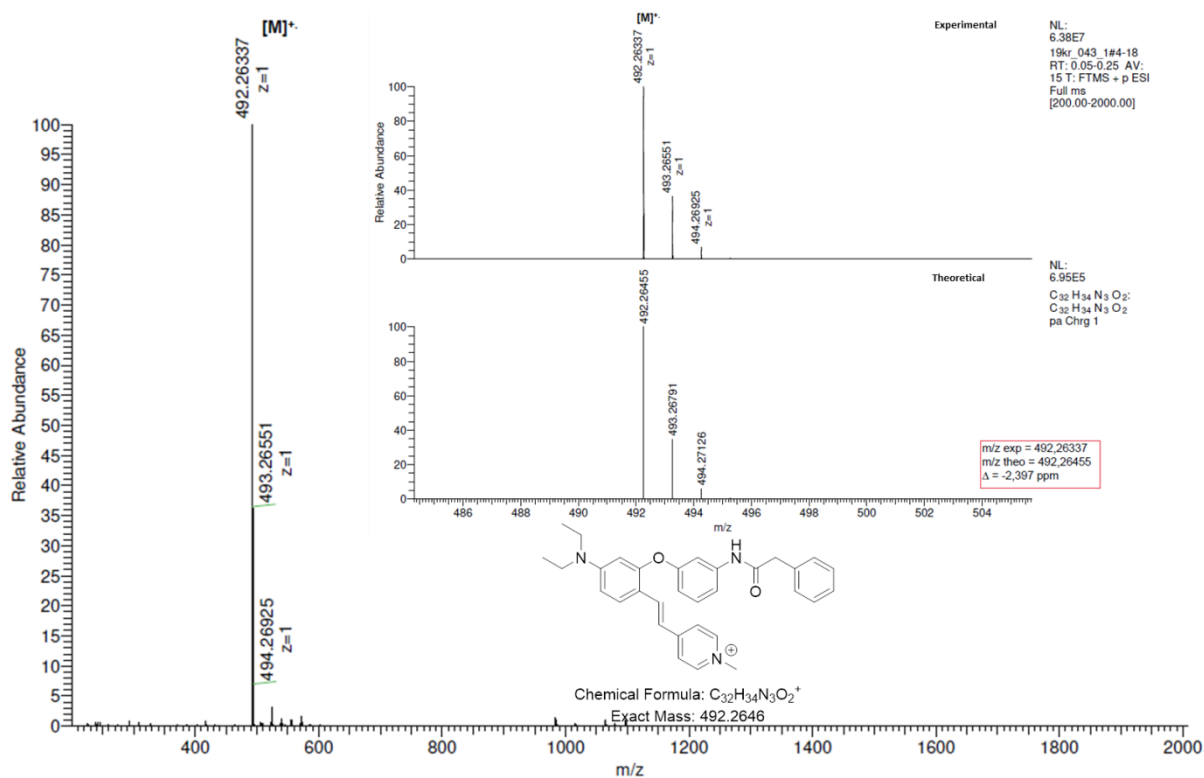
¹³C NMR spectrum of compound 8 in CDCl₃ (126 MHz)



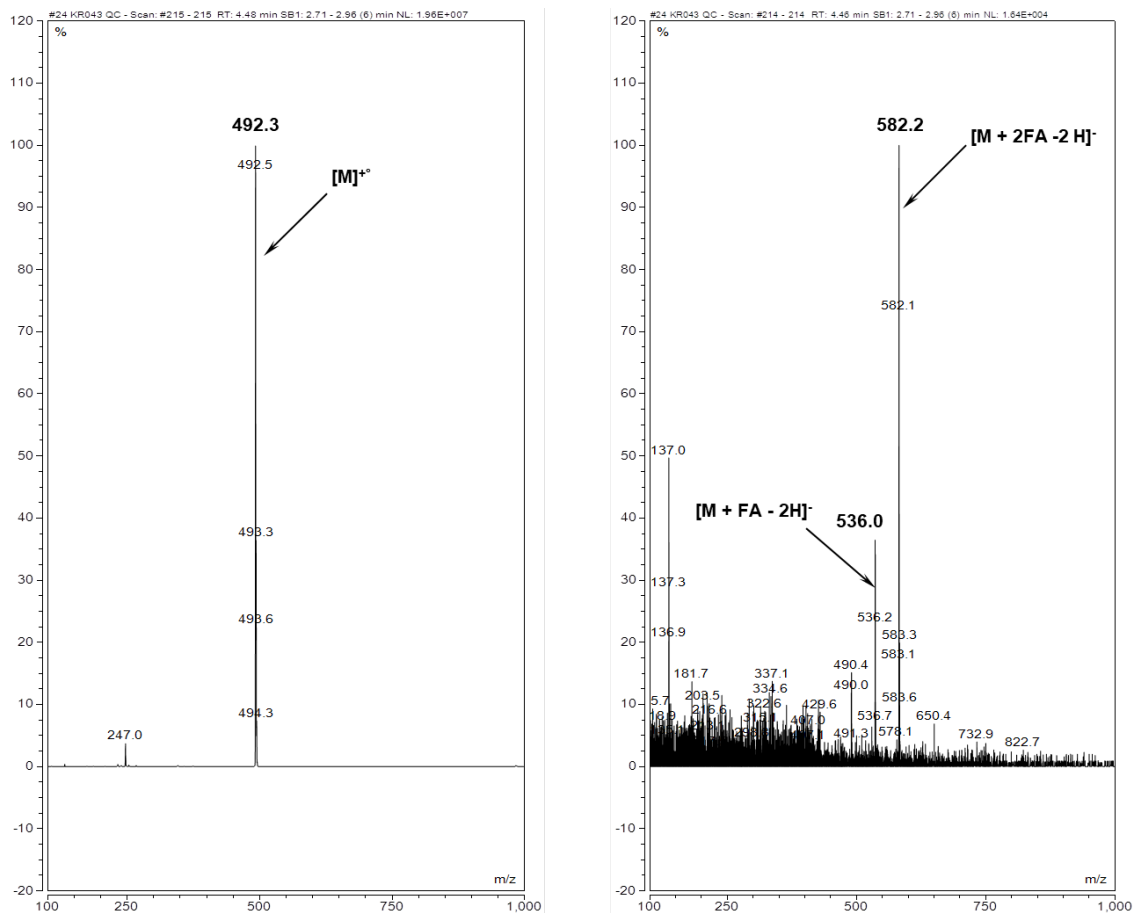
^{19}F NMR spectrum of compound 8 in CDCl_3 (470 MHz)



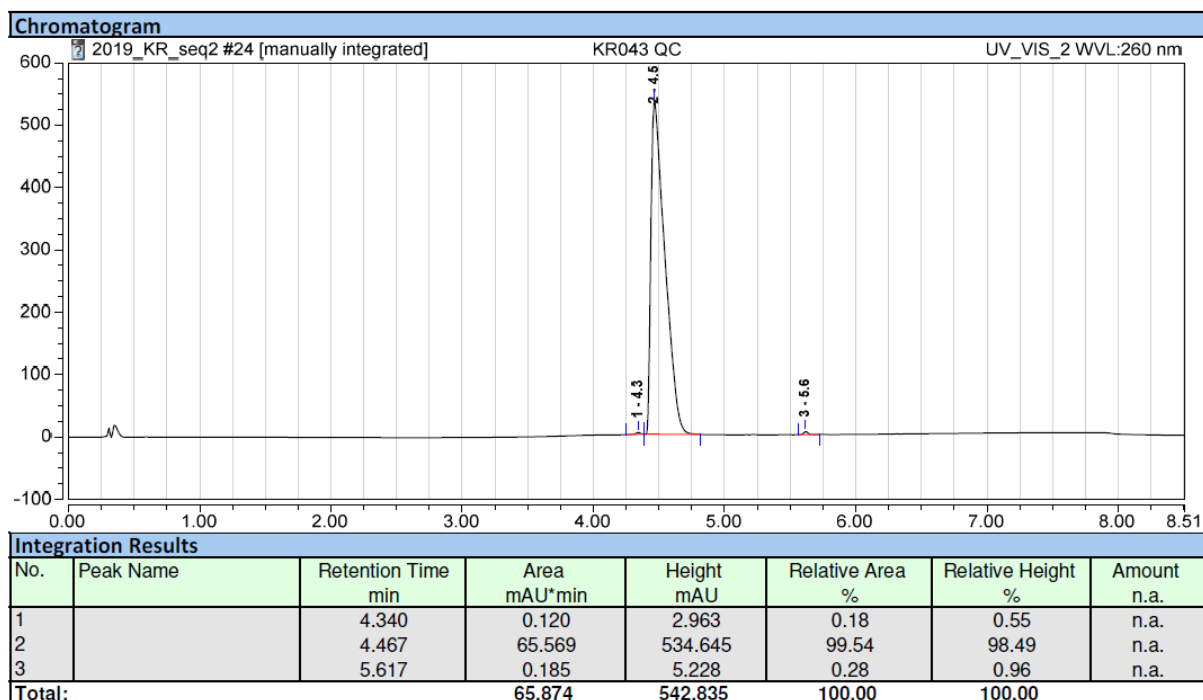
ESI+ mass spectrum (high resolution) of compound 8



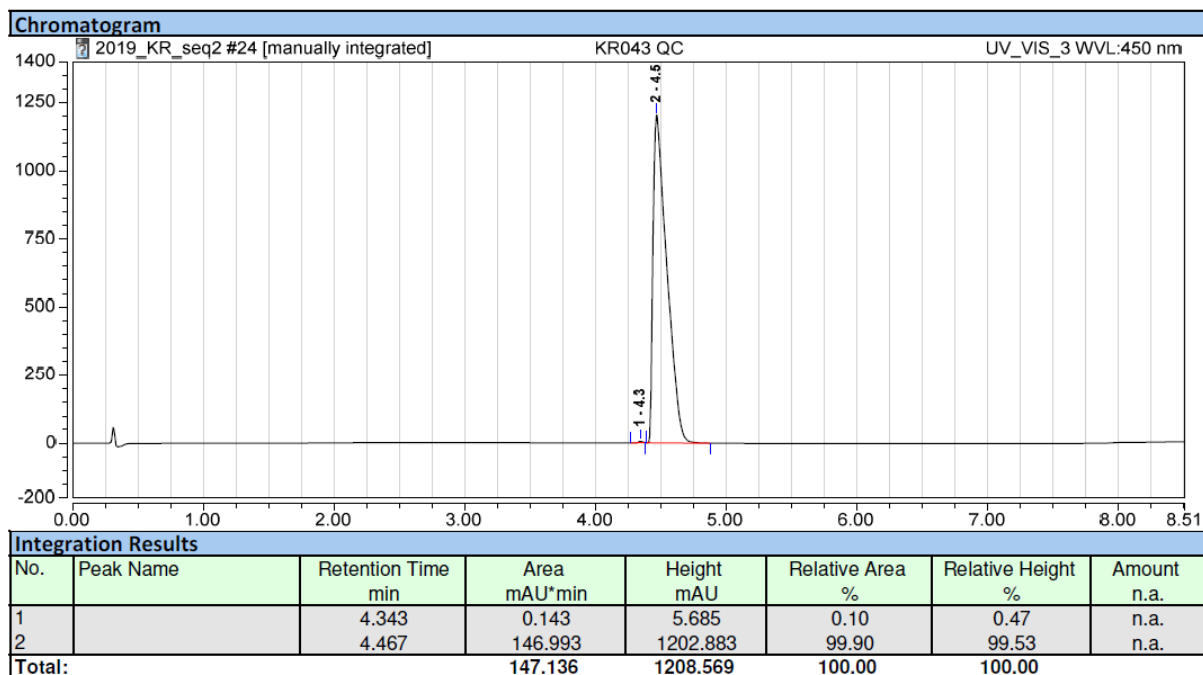
ESI+ (left) / ESI- (right) mass spectrum (low resolution) of compound 8



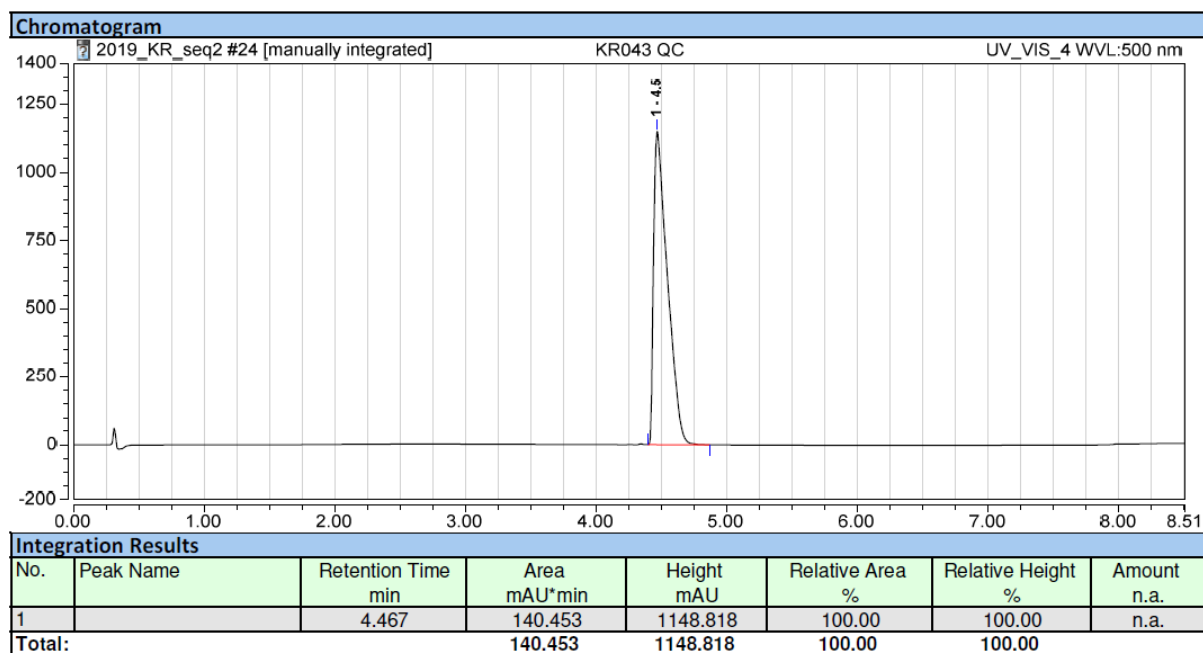
RP-HPLC elution profile of compound 8 (system A, detection at 260 nm)



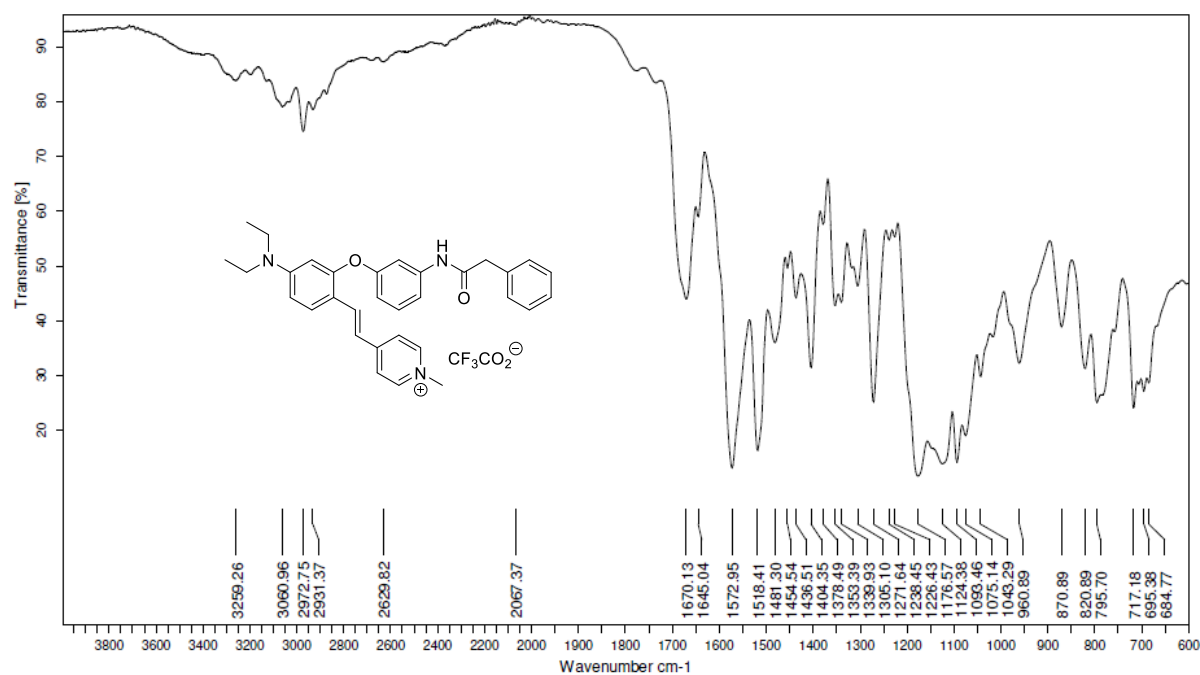
RP-HPLC elution profile of compound 8 (system A, detection at 450 nm)



RP-HPLC elution profile of compound 8 (system A, detection at 500 nm)



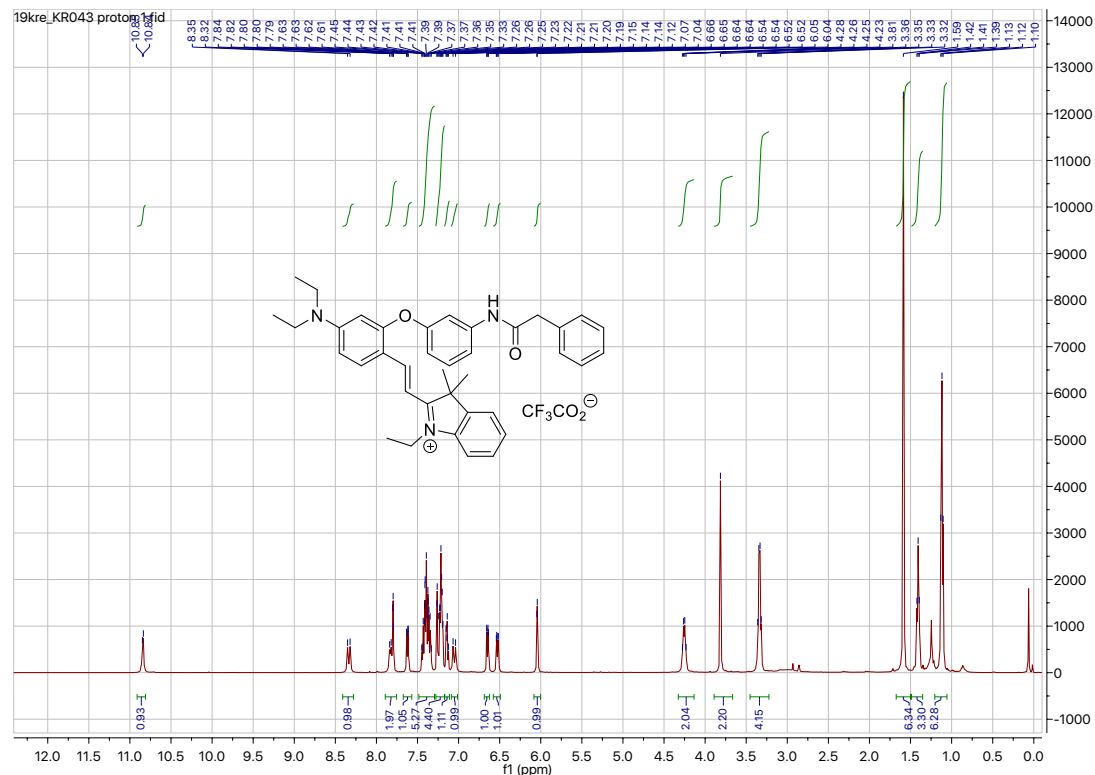
IR-ATR spectrum of compound 8



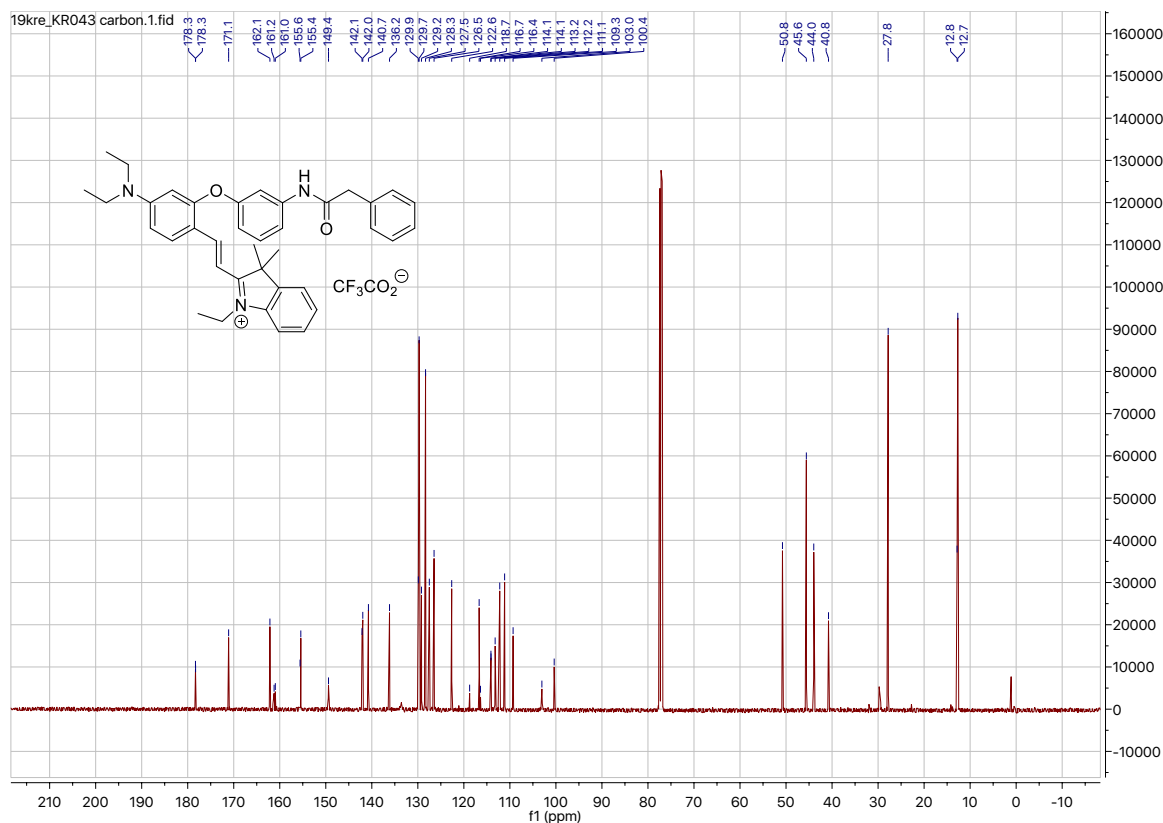
TFA determination by ionic chromatography - results

Concentration	1.78 mg/mL in DMSO	
Sample dilution factor	100	50
Raw data ppm	4.534	8.628
Content in wt %	25.47	24.24
Average content in wt %	24.85	

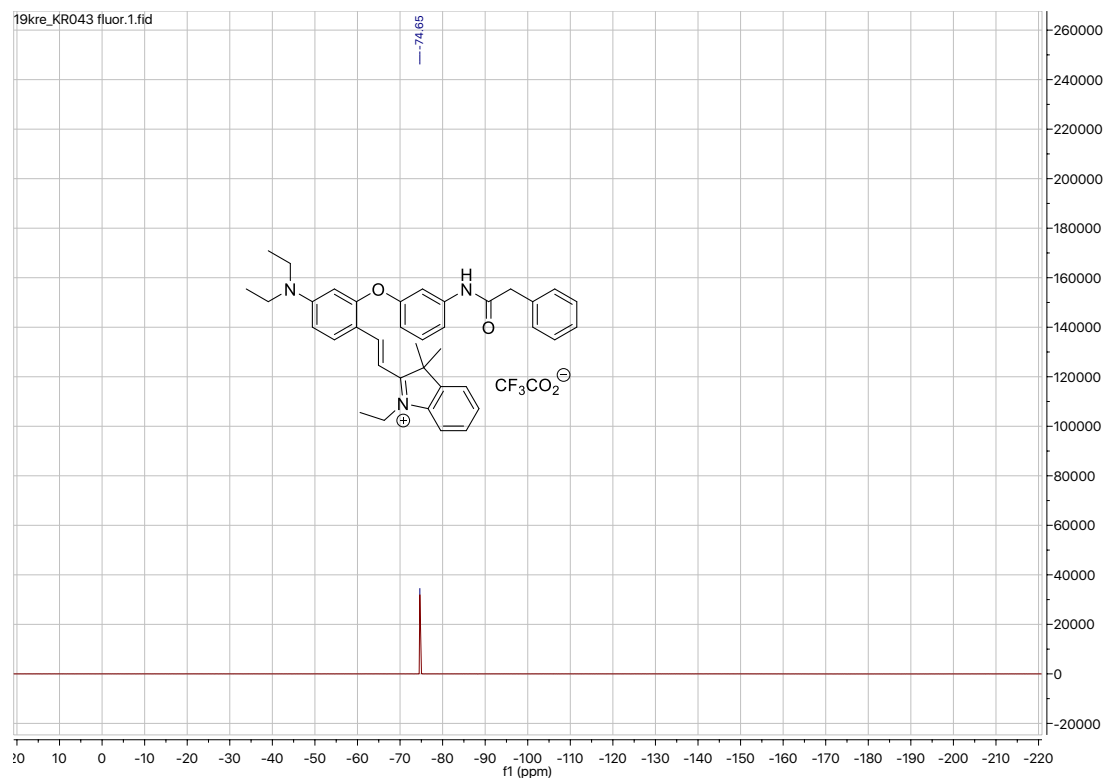
¹H NMR spectrum of compound 9 in CDCl₃ (500 MHz)



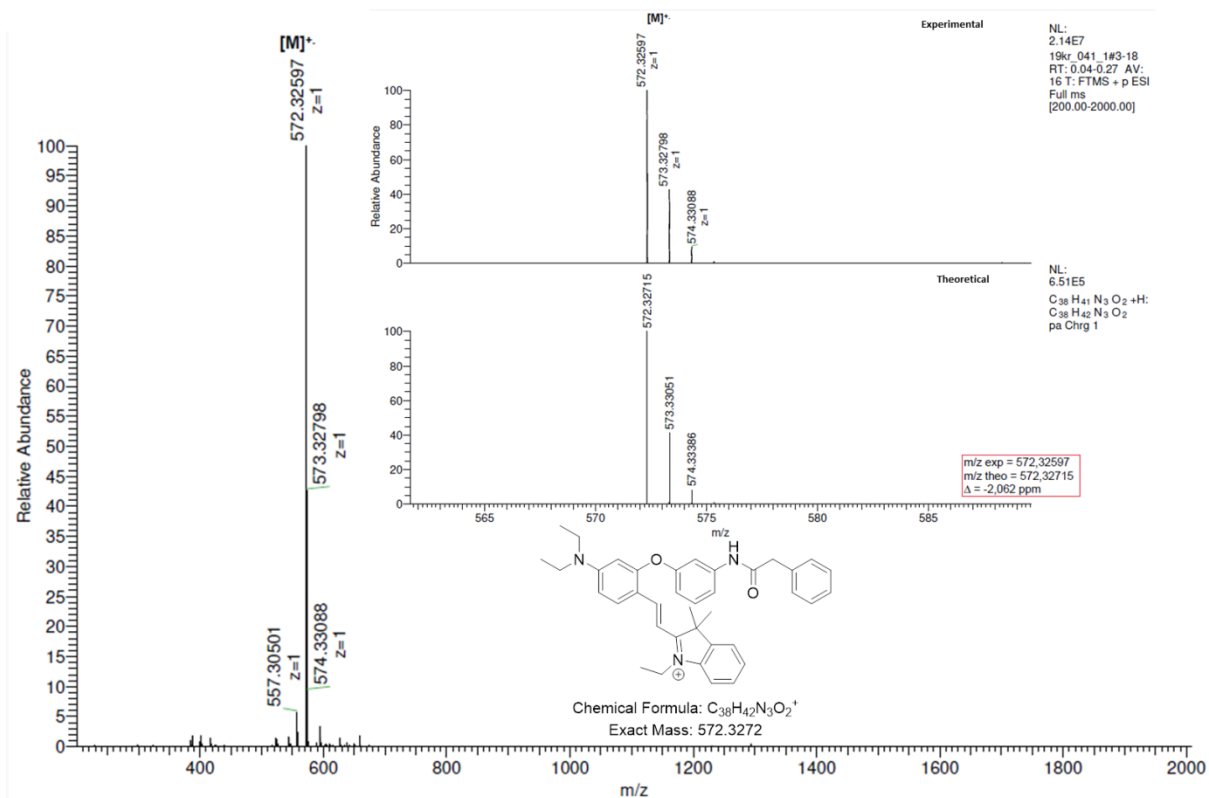
¹³C NMR spectrum of compound 9 in CDCl₃ (126 MHz)



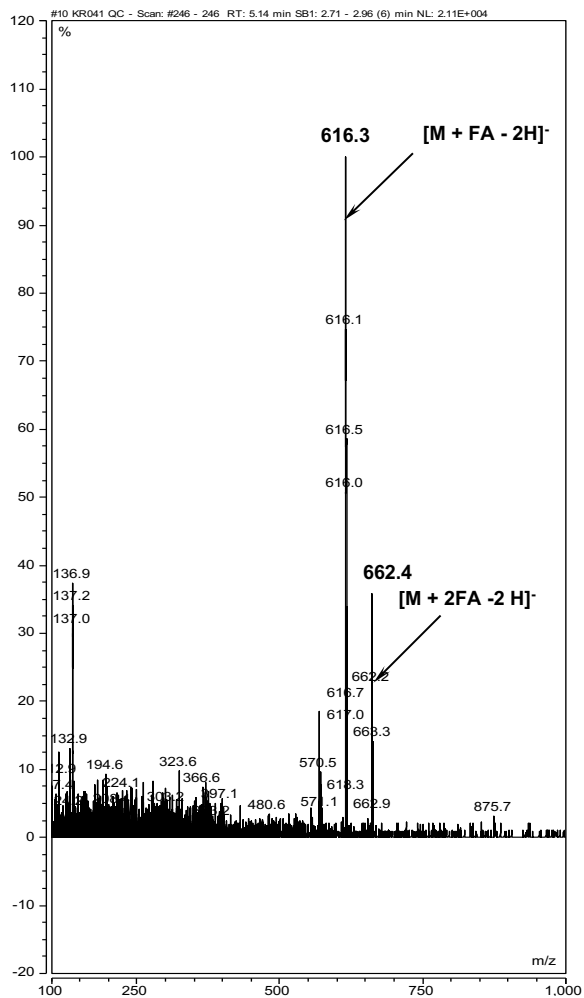
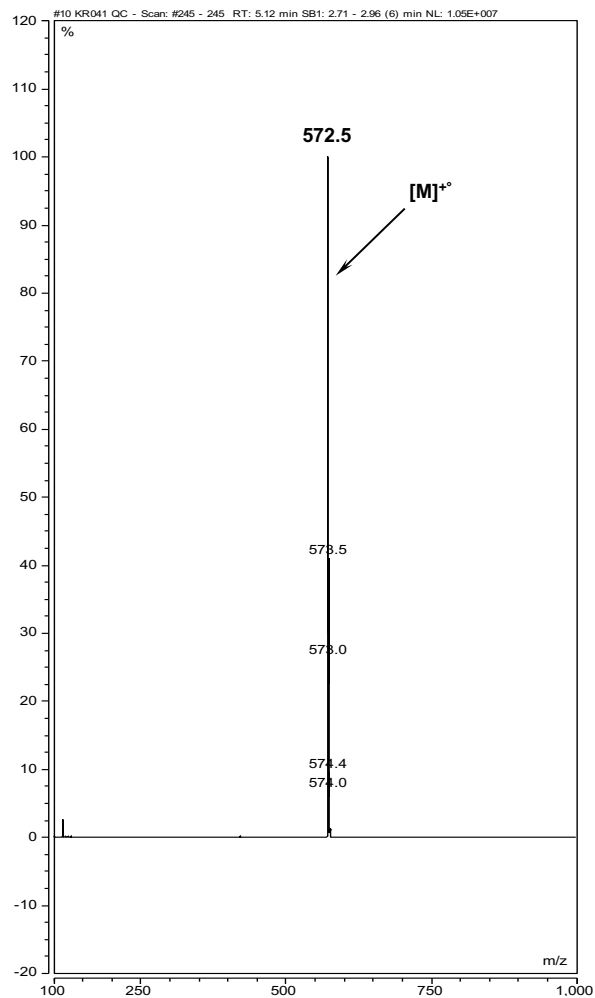
^{19}F NMR spectrum of compound 9 in CDCl_3 (470 MHz)



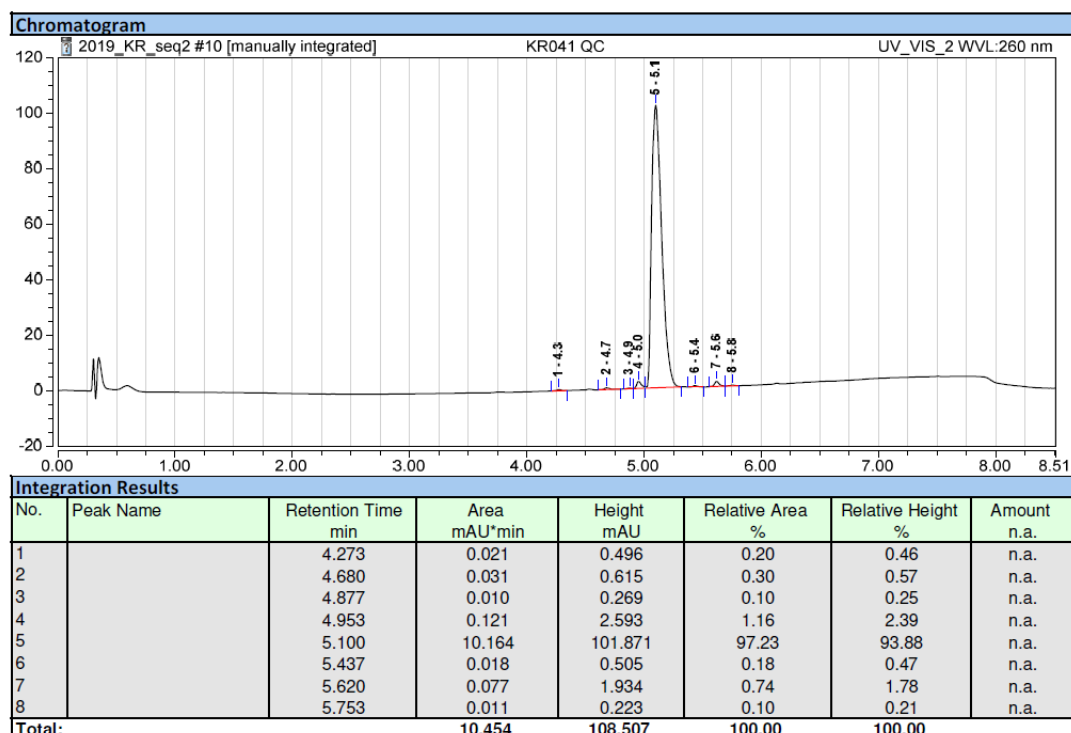
ESI+ mass spectrum (high resolution) of compound 9



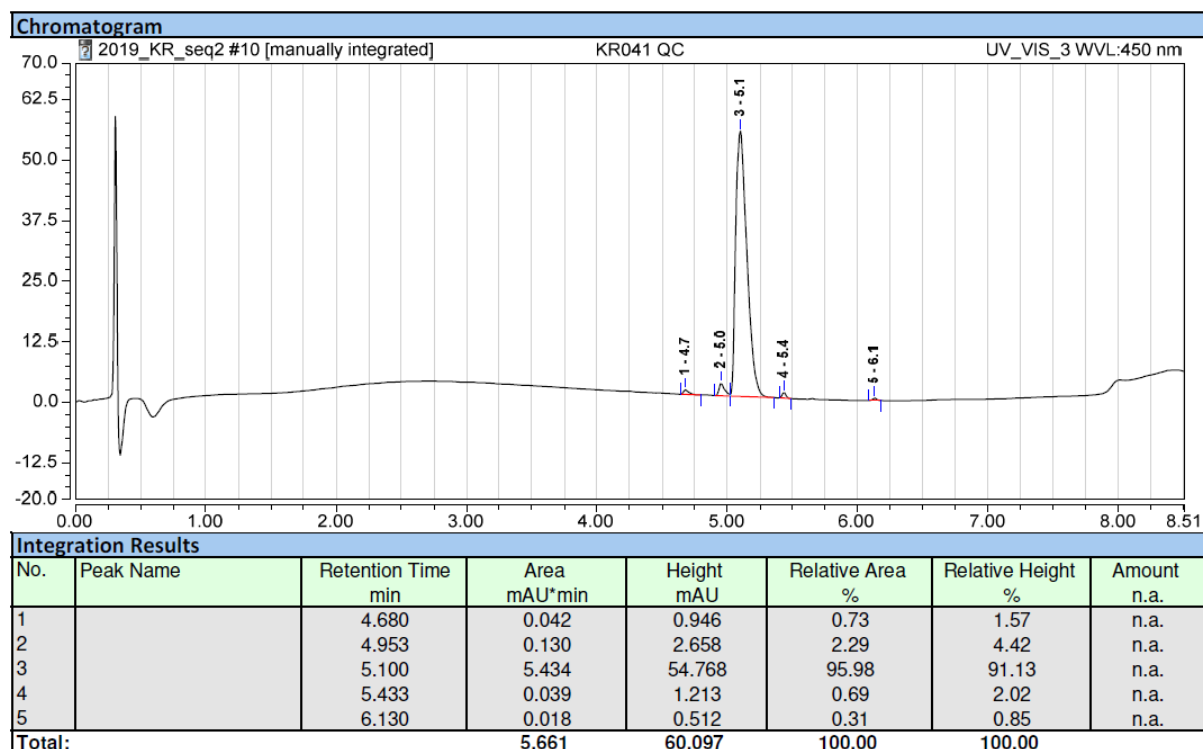
ESI+ (left) / ESI- (right) mass spectrum (low resolution) of compound 9



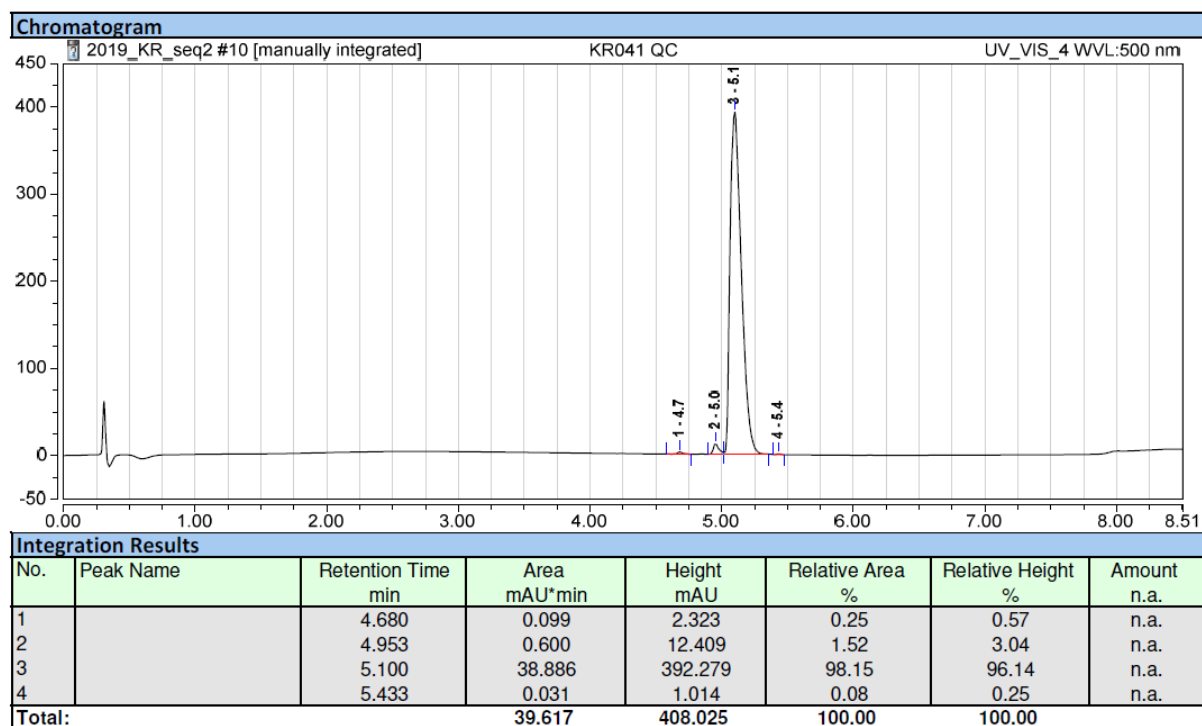
RP-HPLC elution profile of compound 9 (system A, detection at 260 nm)



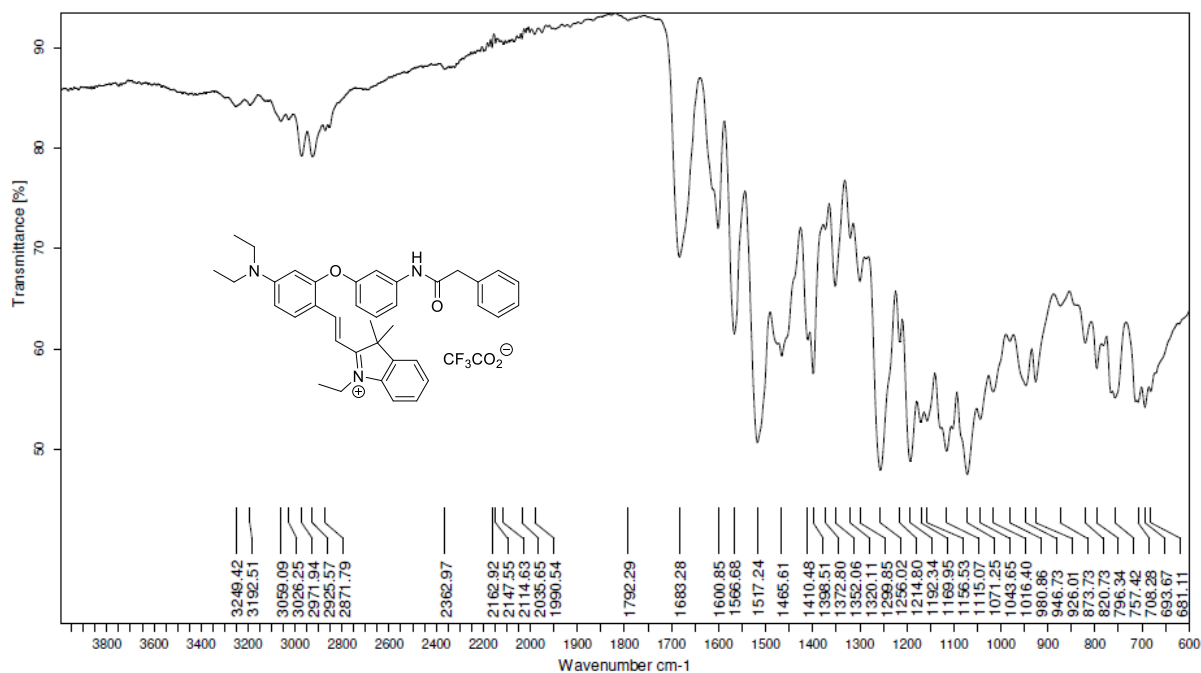
RP-HPLC elution profile of compound 9 (system A, detection at 450 nm)



RP-HPLC elution profile of compound 9 (system A, detection at 500 nm)



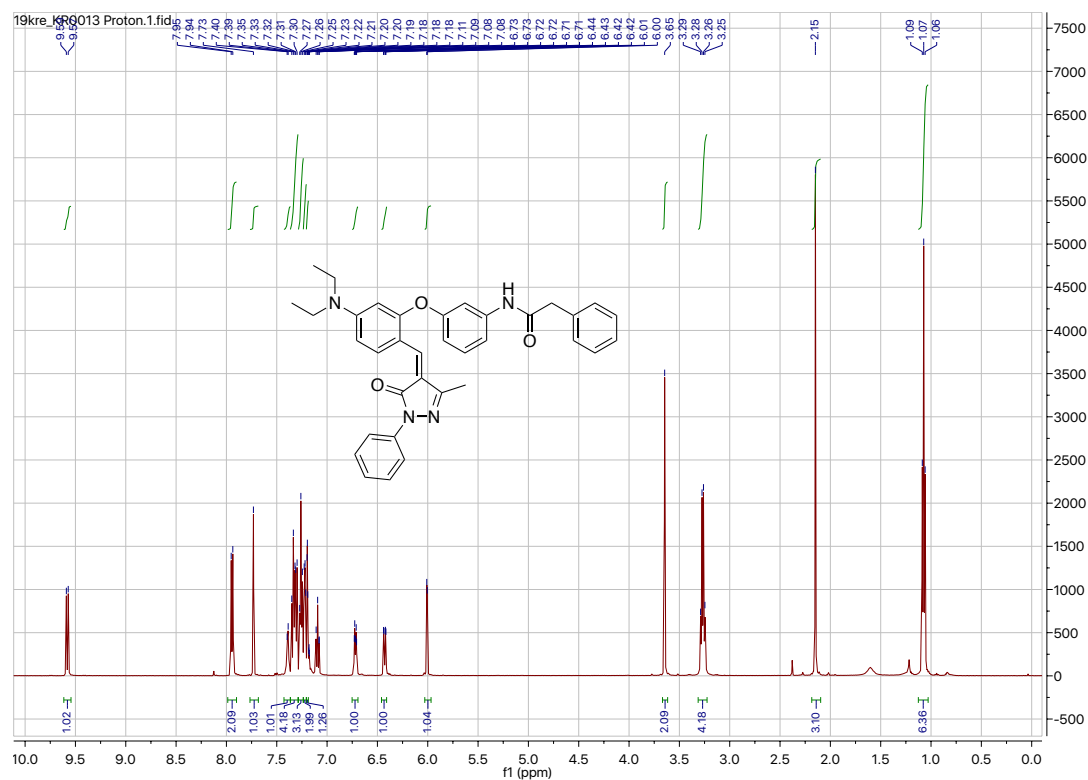
IR-ATR spectrum of compound 9



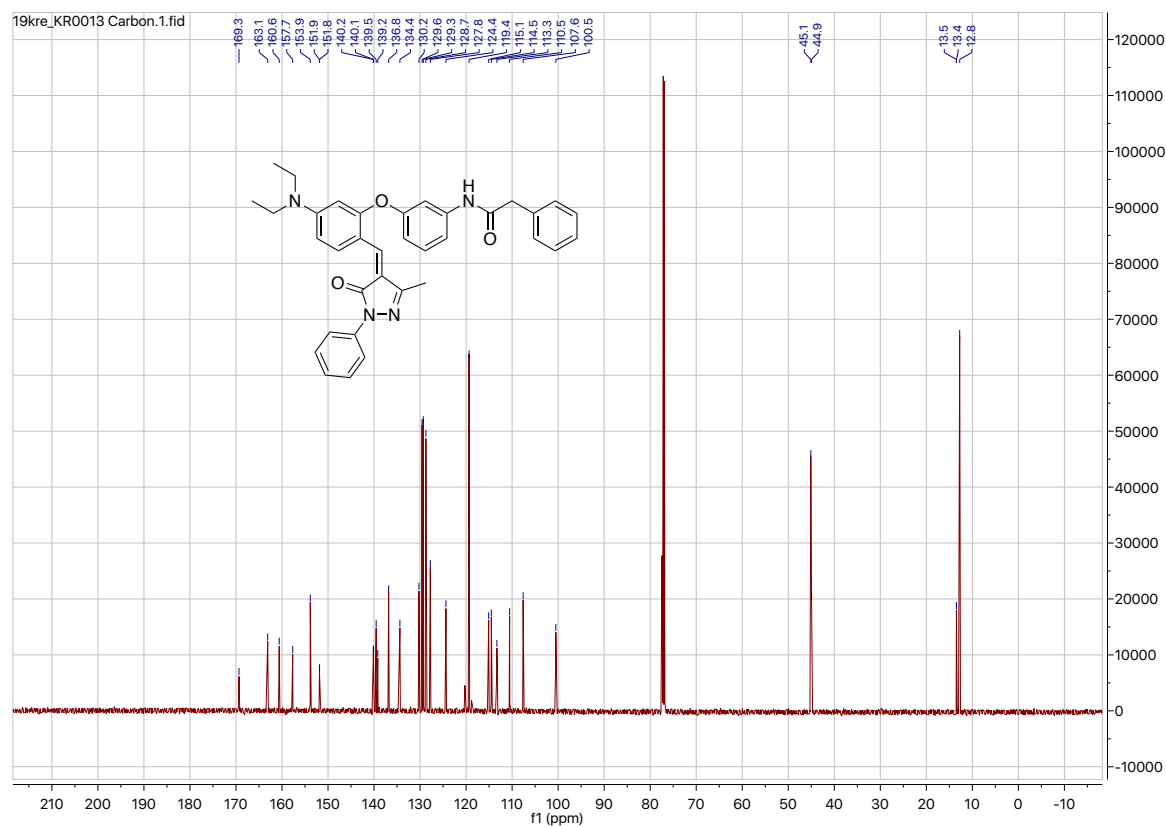
TFA determination by ionic chromatography - results

Concentration	1.68 mg/mL in DMSO	
Sample dilution factor	100	50
Raw data ppm	2.209	4.796
Content in wt %	13.15	14.27
Average content in wt %	13.71	

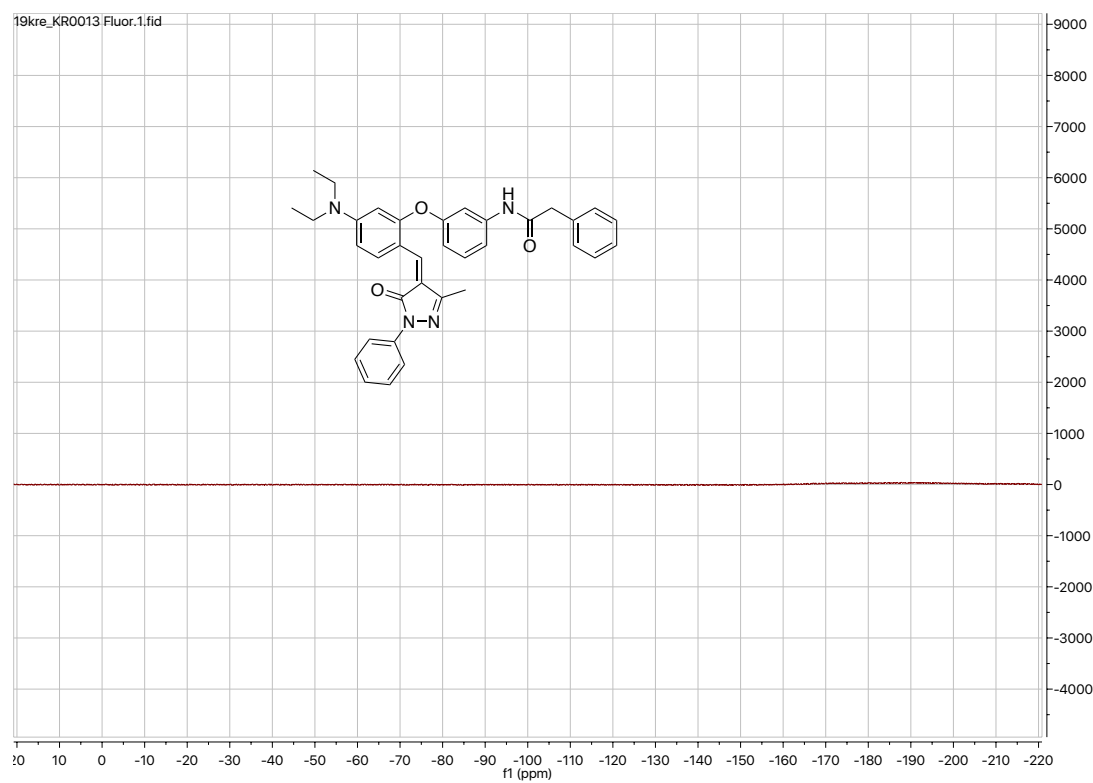
¹H NMR spectrum of compound 10 in CDCl₃ (500 MHz)



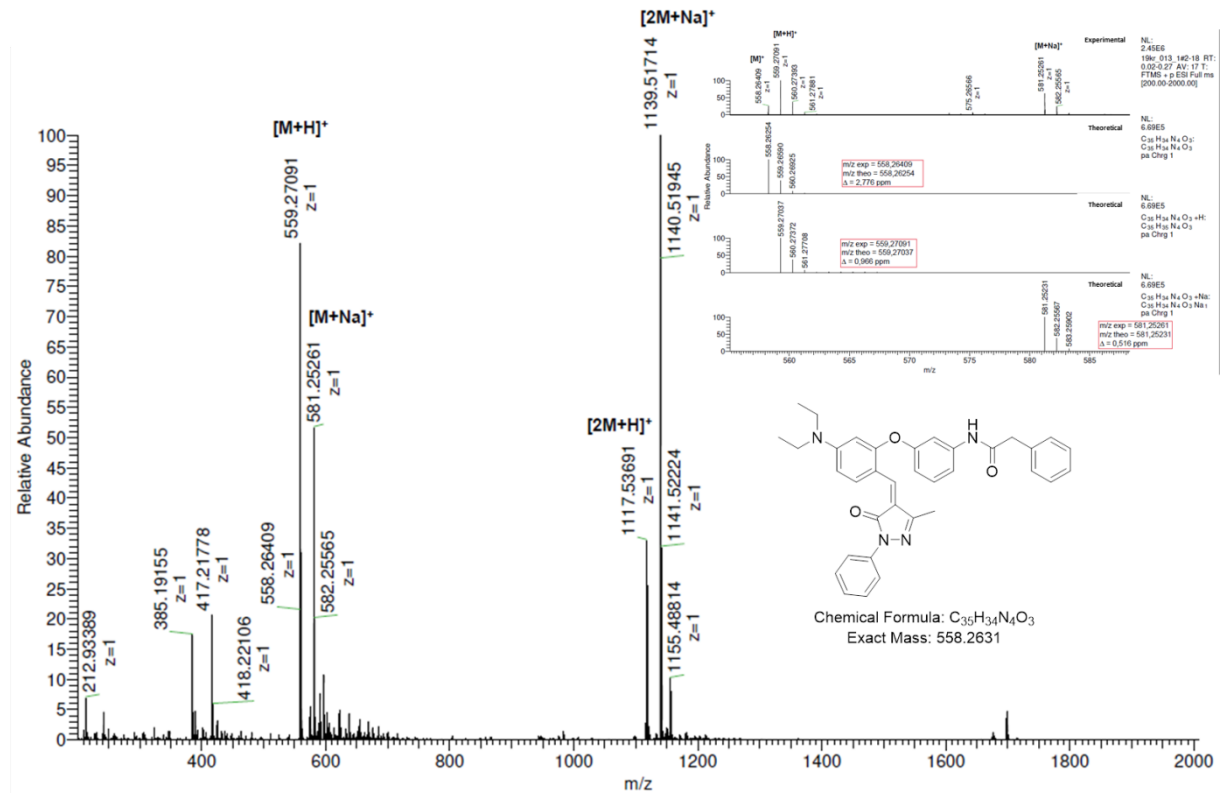
^{13}C NMR spectrum of compound 10 in CDCl_3 (126 MHz)



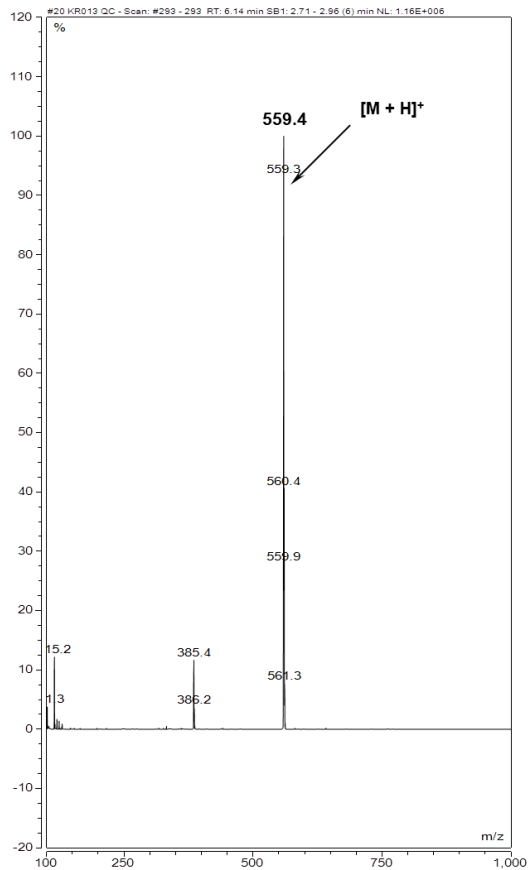
^{19}F NMR spectrum of compound 10 in CDCl_3 (470 MHz)



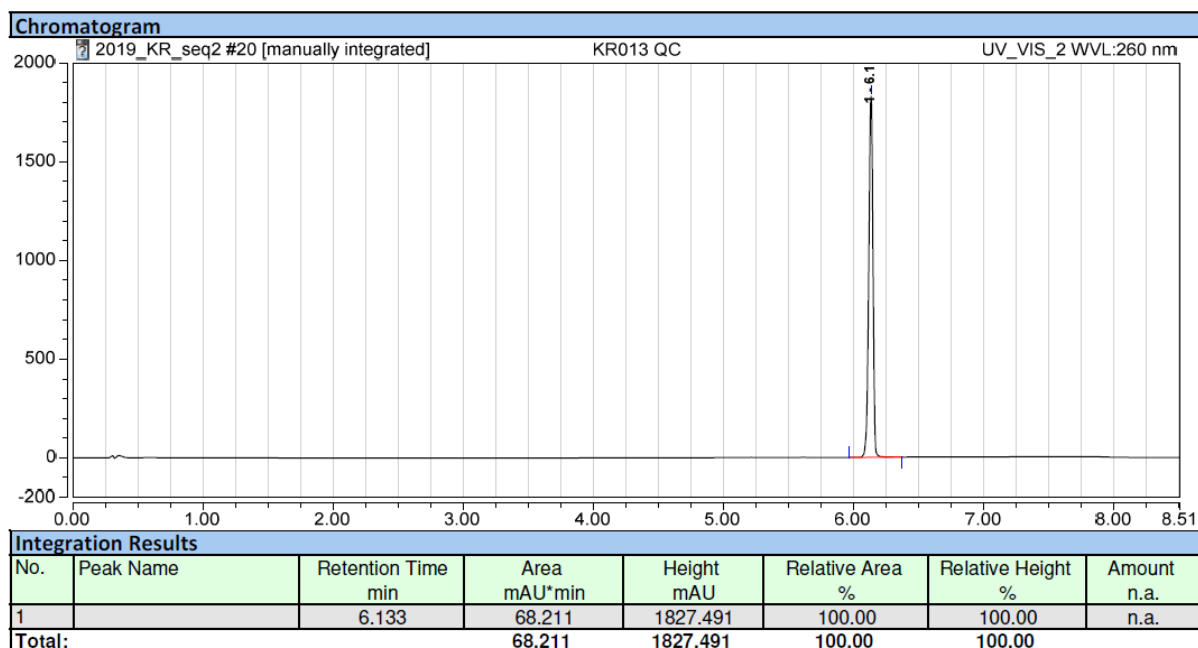
ESI+ mass spectrum (high resolution) of compound 10



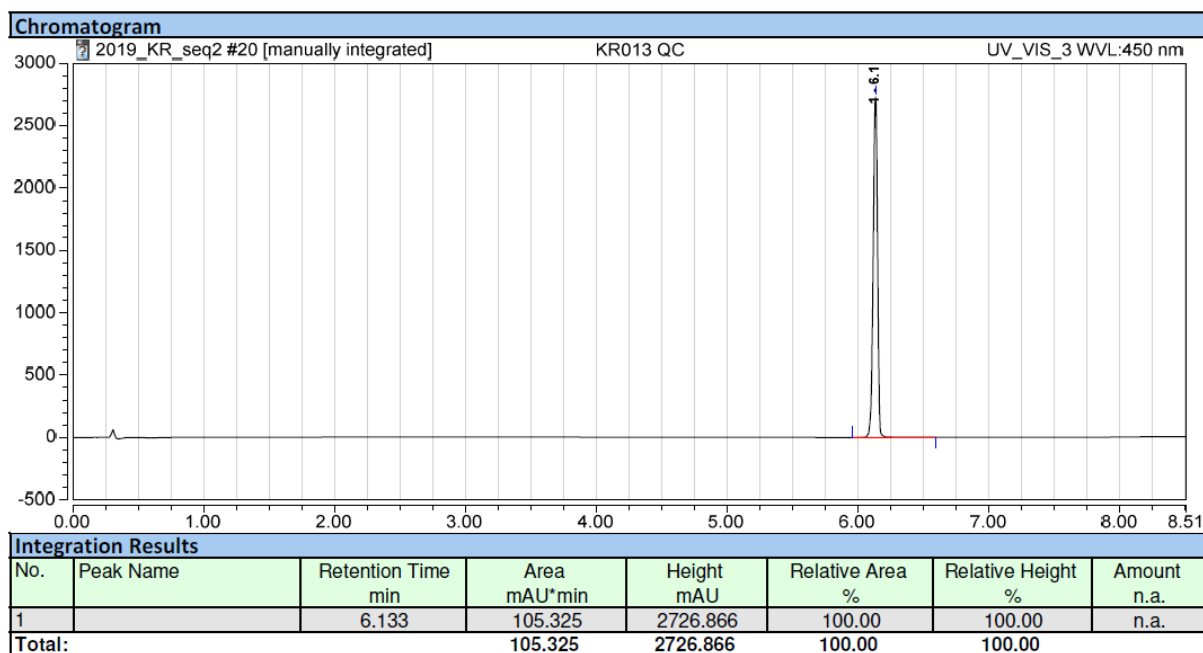
ESI+ mass spectrum (low resolution) of compound 10



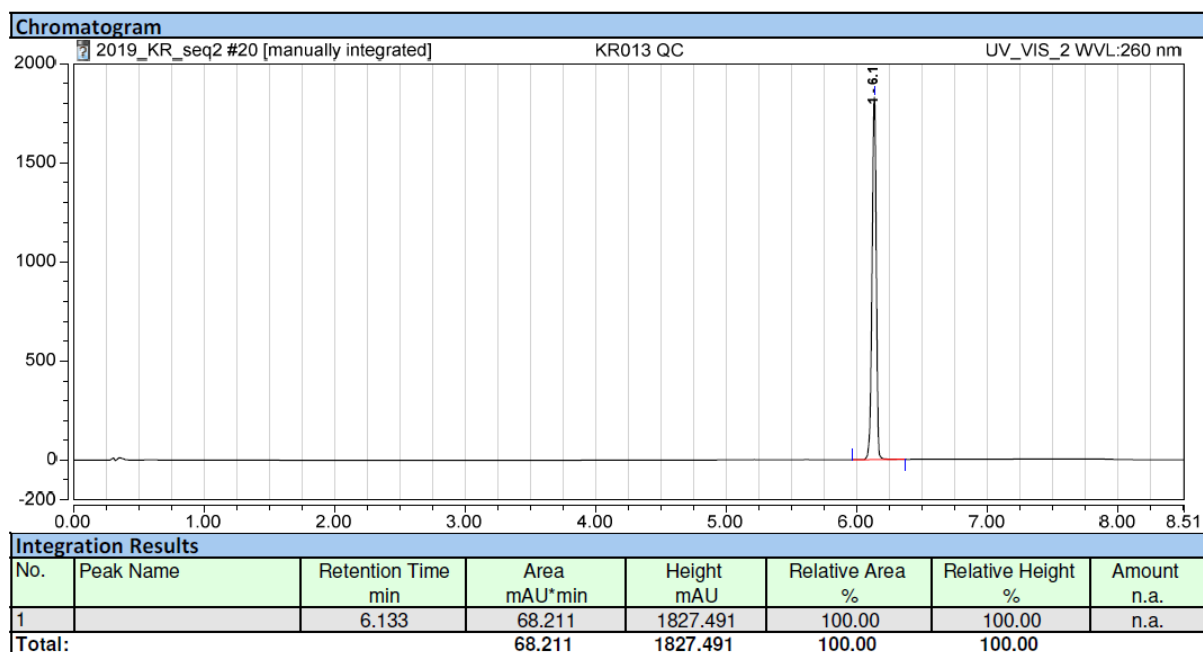
RP-HPLC elution profile of compound 10 (system A, detection at 260 nm)



RP-HPLC elution profile of compound 10 (system A, detection at 450 nm)



RP-HPLC elution profile of compound 10 (system A, detection at 500 nm)



IR-ATR spectrum of compound 10

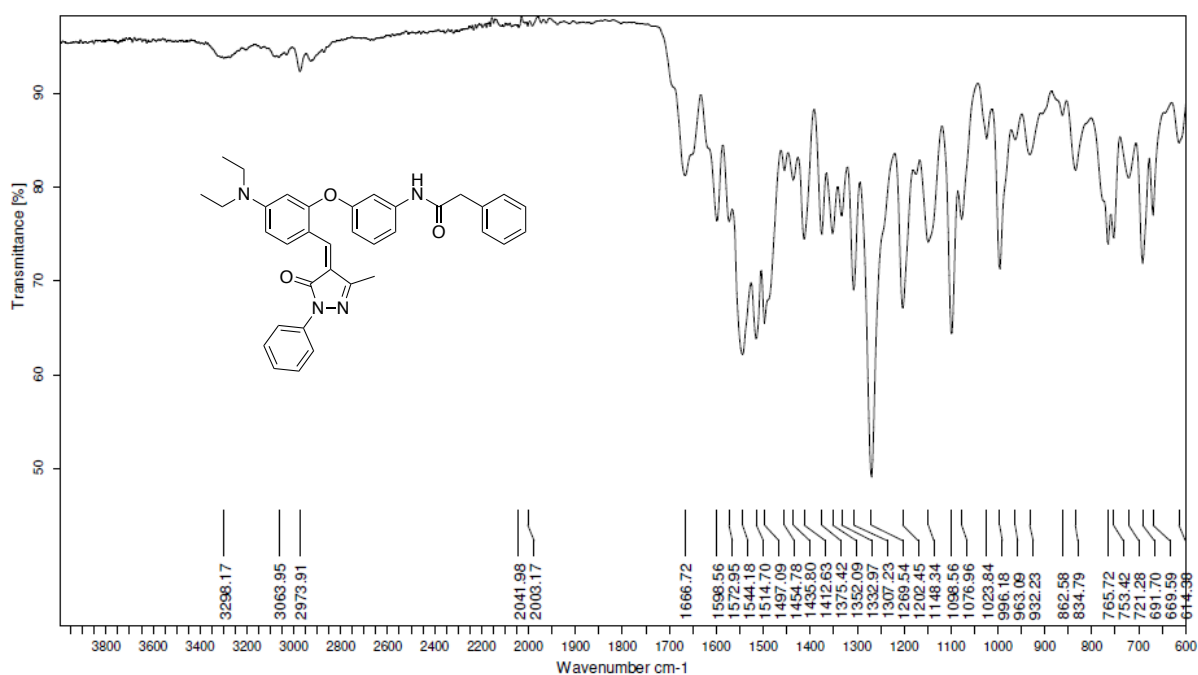
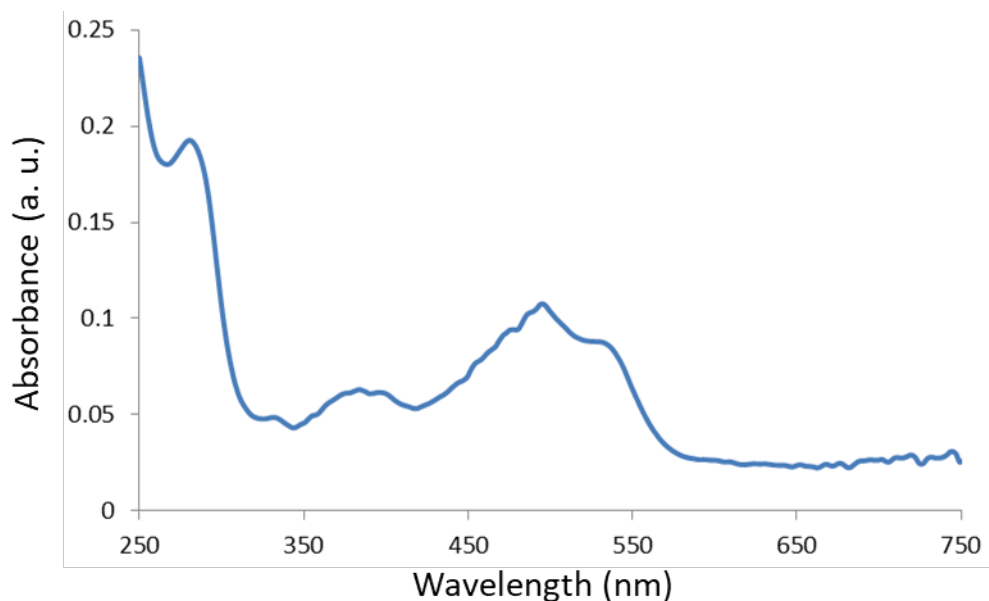


Fig. S1 UV-vis absorption spectrum of dimedone-based probes 4 in PB (concentration: 9.0 μM)^a at 25 °C.



^aPlease note: rapid hydrolysis of this probe was occurred during the preparation of solution and the recording of its absorption spectrum. That explains both the low value of absorbance at $\lambda_{max} = 495$ nm and the poor quality of spectrum.

Fig. S2 UV-vis absorption spectrum of barbiturate-based probes 5 in PB (concentration: 11 μM) at 25 °C.

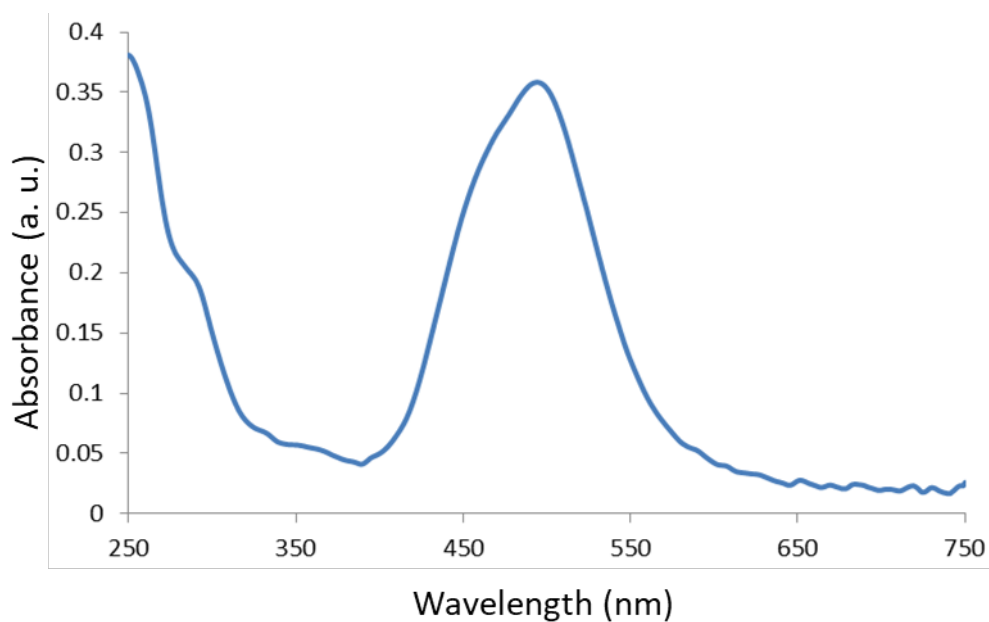


Fig. S3 UV-vis absorption spectrum of Meldrum's acid-based probes 6 in PB (concentration: 20 μM) at 25 $^{\circ}\text{C}$.

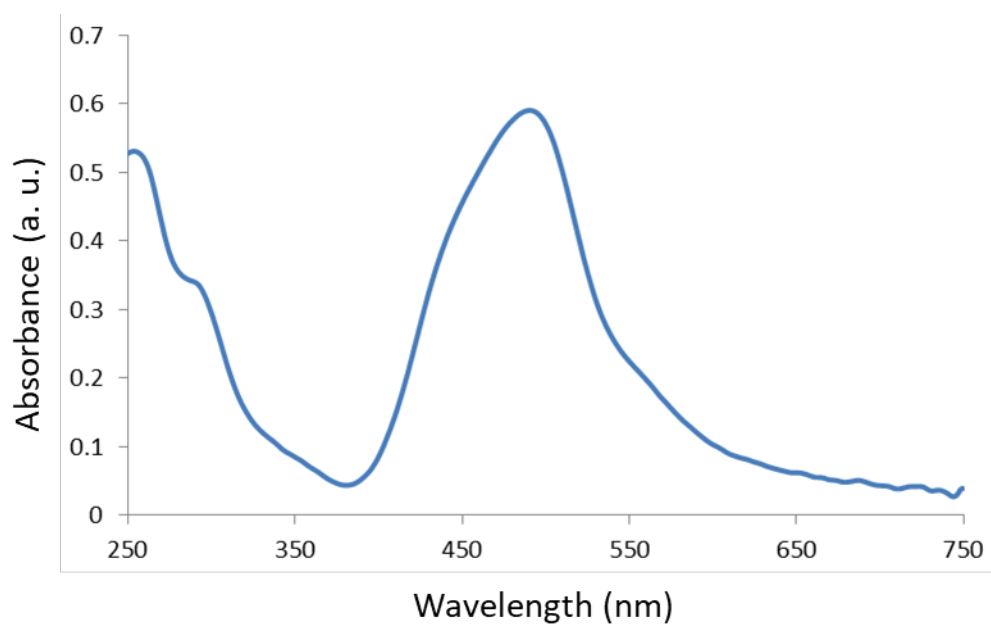


Fig. S4 UV-vis absorption spectrum of rosamine-based probes 7 in PB (concentration: 25 μM) at 25 $^{\circ}\text{C}$.

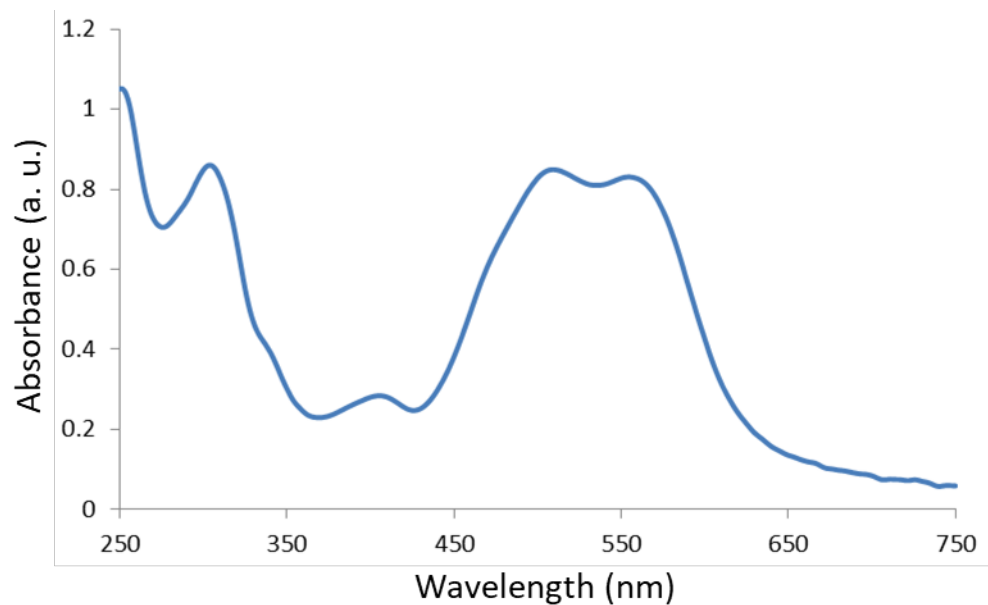


Fig. S5 UV-vis absorption spectrum of hemicyanine-based probes 8 in PB (concentration: 29 μ M) at 25 $^{\circ}$ C.

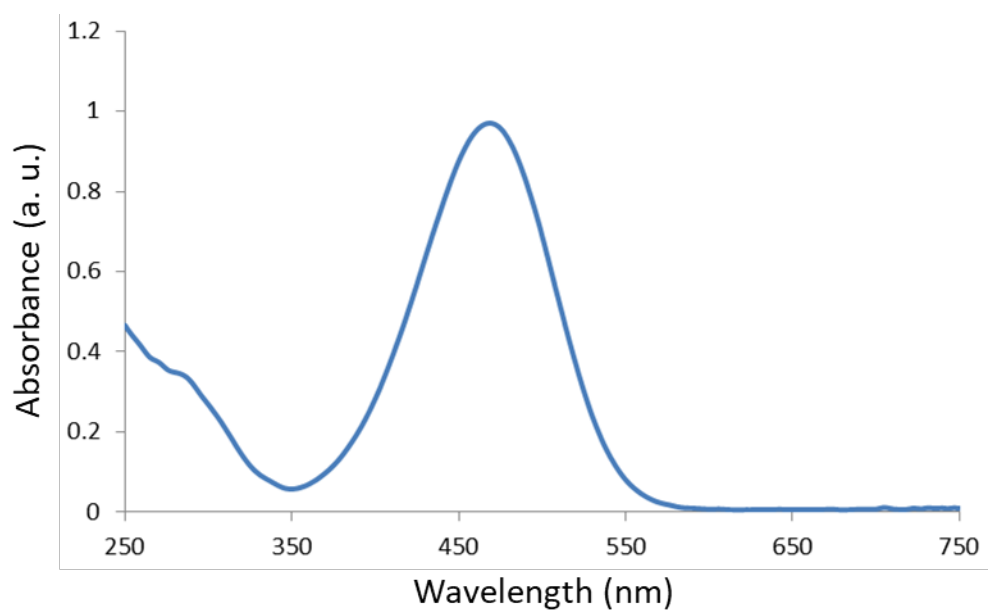


Fig. S6 UV-vis absorption spectrum of hemicyanine-based probes 9 in PB (concentration: 25 μ M) at 25 $^{\circ}$ C.

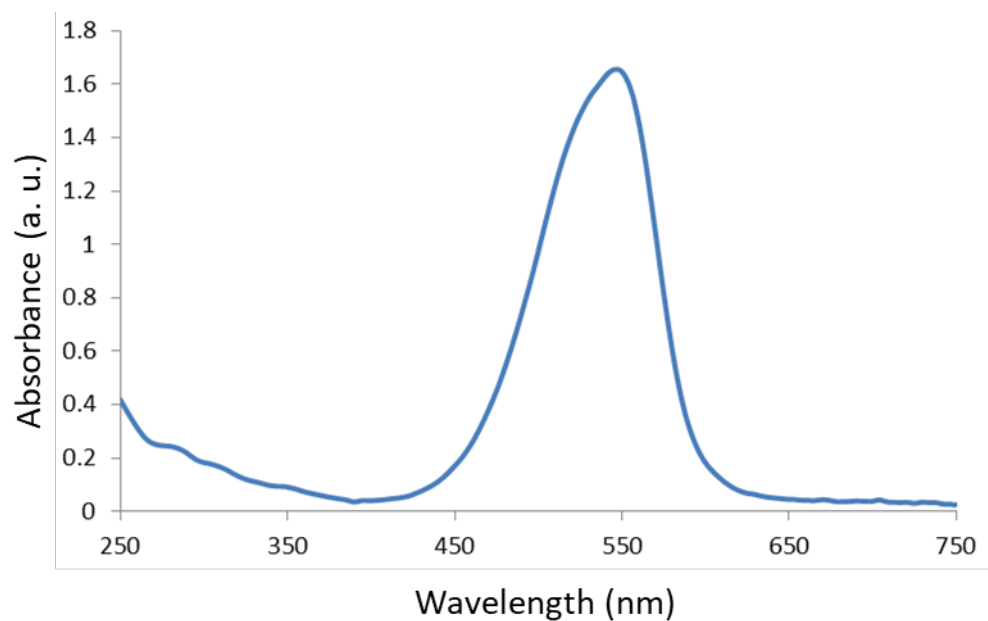


Fig. S7 UV-vis absorption spectrum of edaravone-based probes 10 in PB (concentration: 16 μ M) at 25 $^{\circ}$ C.

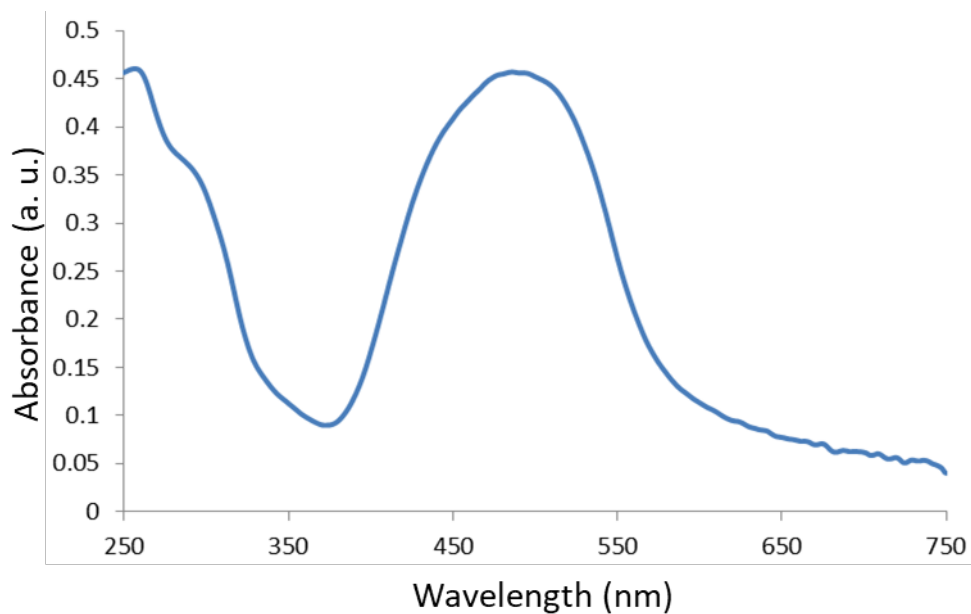


Fig. S8 UV-vis Normalised absorption, excitation (Em. 615 nm, slit 5 nm), emission (Ex. 440 nm, slit 7 nm) spectra of Meldrum's acid-based probes 10 in PB at 25 $^{\circ}$ C.

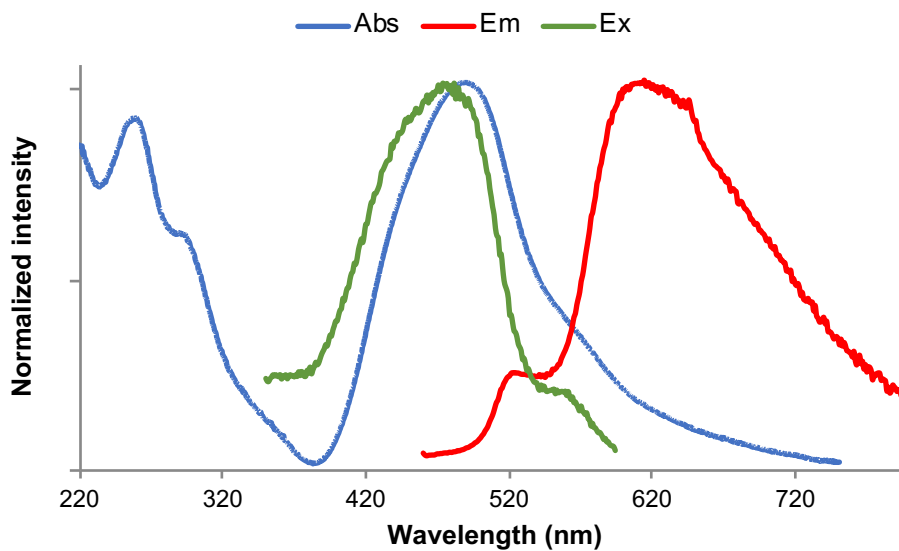
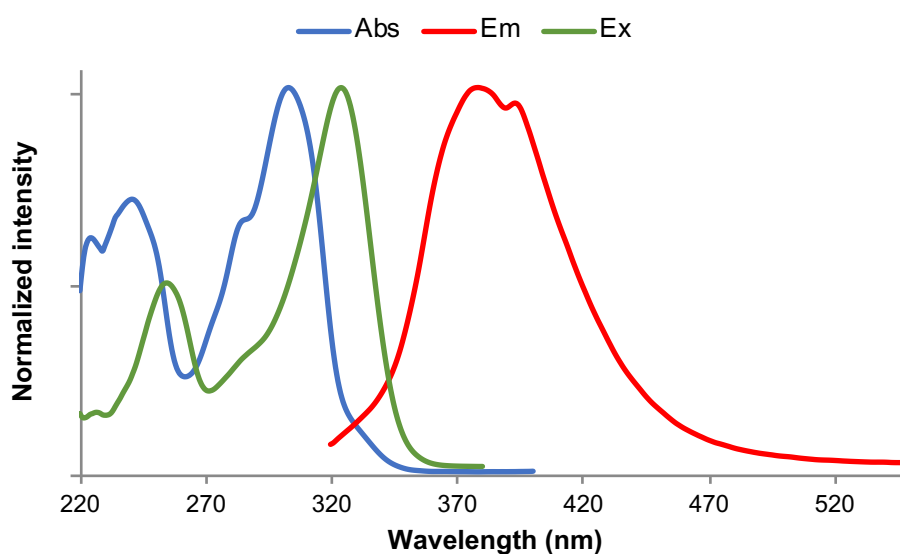


Fig. S9 UV-vis Normalised absorption, excitation (Em. 400 nm, bandwidth 5 nm)^a, emission (Ex. 300 nm, bandwidth 5 nm) spectra of 4,7-dihydroxycoumarin in PB at 25 °C.



^aPlease note: the non-perfect matching observed between Abs and Ex. spectrum is explained by the fact that emissive form (phenolate form, $\lambda_{max} = 324$ nm) is not prevalent at pH 7.6 ($\lambda_{max} = 241$ and 303 nm for the phenol form).

Fig. S10 Time-dependent changes in the green-yellow fluorescence intensity (Ex./Em. 525/545 nm, slit 5 nm) of fluorogenic probe 4 (concentration: 1.0 μ M) in the presence of PGA (1 U) in PB (100 mM, pH 7.6) at 37 °C.

Please note: for all enzymatic kinetics, PGA was added after 5 min of incubation of probe in PB alone. Kinetics of probes 2 and 3 (PGA and blank) are not shown because they are similar to those already reported in ref. 10.

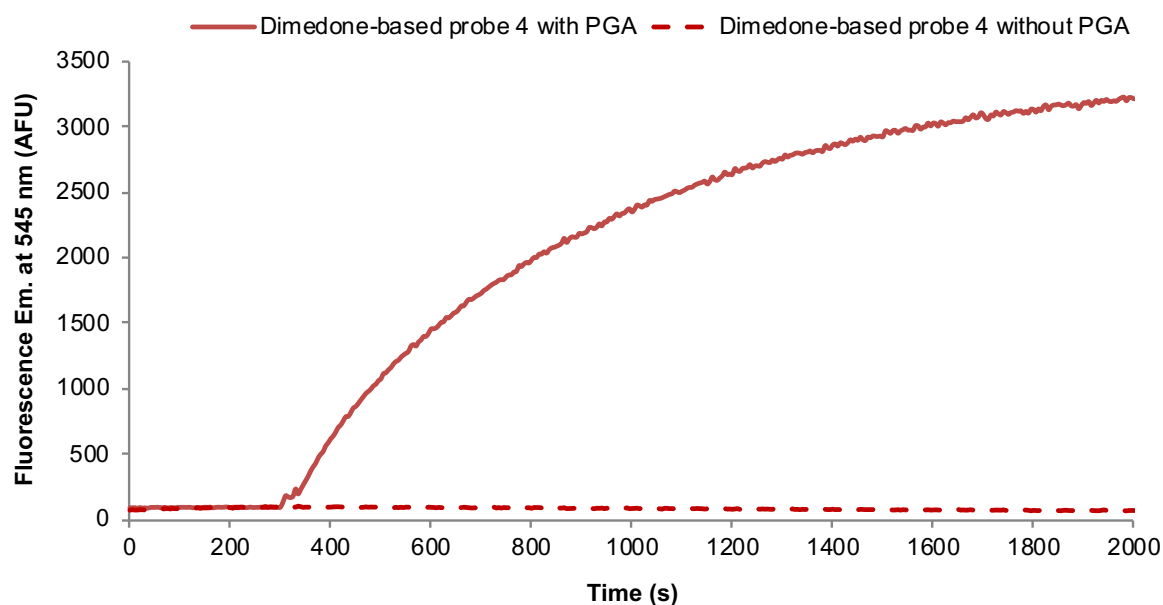


Fig. S11 Time-dependent changes in the green-yellow fluorescence intensity (Ex./Em. 525/545 nm, slit 5 nm) of fluorogenic probe 5 (concentration: 1.0 μM) in the presence of PGA (1 U) in PB (100 mM, pH 7.6) at 37 $^{\circ}\text{C}$.

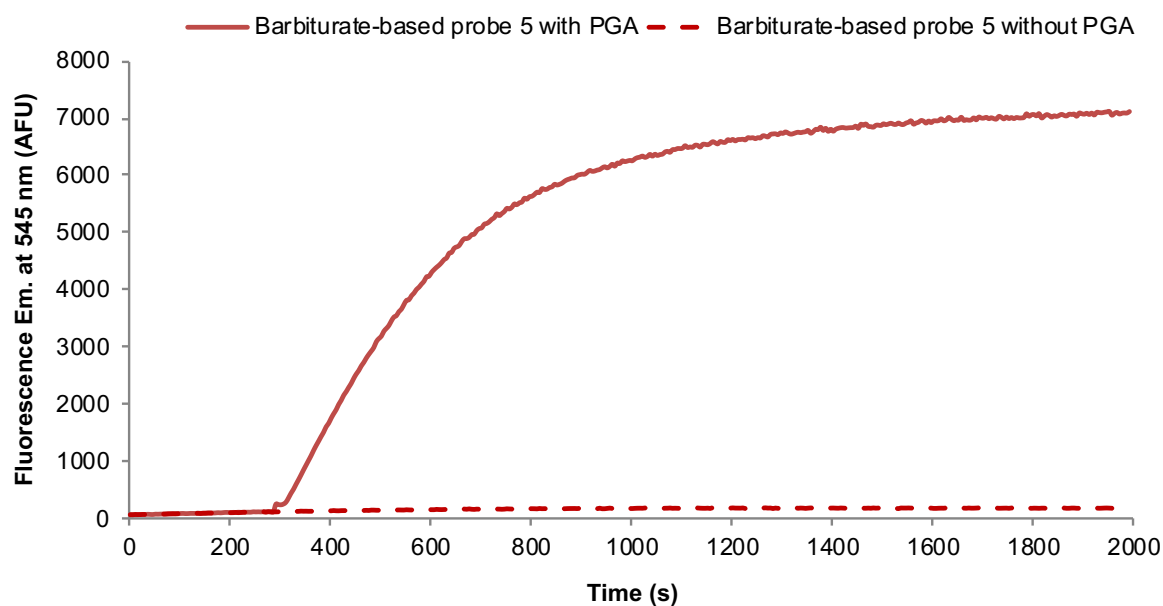


Fig. S12 Time-dependent changes in the green-yellow fluorescence intensity (Ex./Em. 525/545 nm, slit 5 nm) of fluorogenic probe 6 (concentration: 1.0 μM) in the presence of PGA (1 U) in PB (100 mM, pH 7.6) at 37 $^{\circ}\text{C}$.

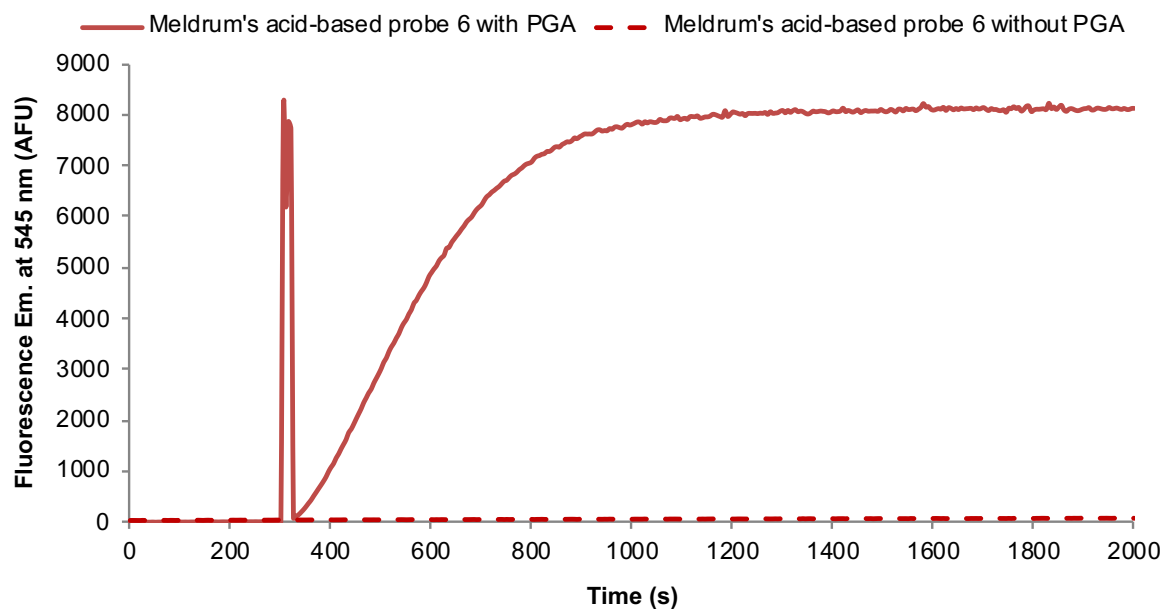


Fig. S13 Time-dependent changes in the green-yellow fluorescence intensity (Ex./Em. 525/545 nm, slit 5 nm) of fluorogenic probe 7 (concentration: 1.0 μM) in the presence of PGA (1 U) in PB (100 mM, pH 7.6) at 37 $^{\circ}\text{C}$.

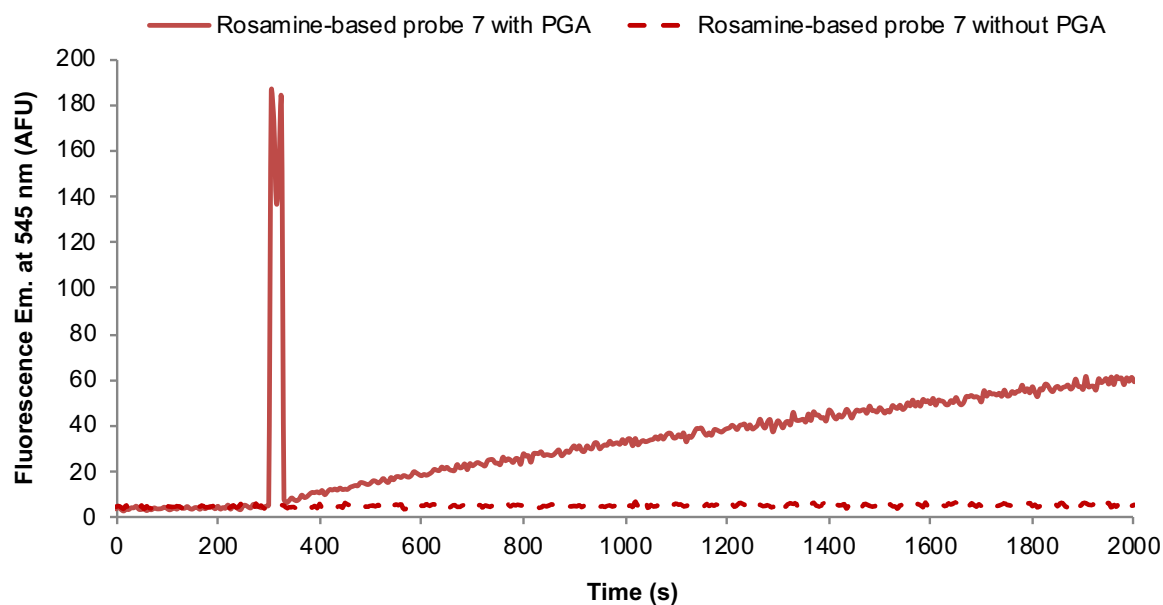


Fig. S14 Time-dependent changes in the green-yellow fluorescence intensity (Ex./Em. 525/545 nm, slit 5 nm) of fluorogenic probe 8 (concentration: 1.0 μM) in the presence of PGA (1 U) in PB (100 mM, pH 7.6) at 37 $^{\circ}\text{C}$.

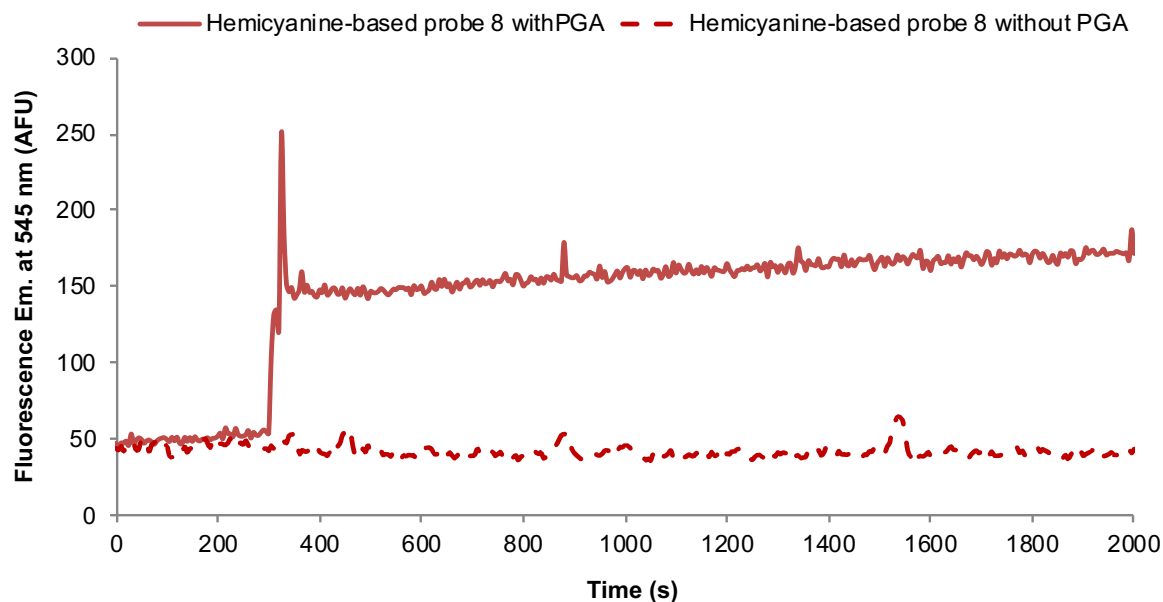


Fig. S15 Time-dependent changes in the green-yellow fluorescence intensity (Ex./Em. 525/545 nm, slit 5 nm) of fluorogenic probe 9 (concentration: 1.0 μ M) in the presence of PGA (1 U) in PB (100 mM, pH 7.6) at 37 $^{\circ}$ C.

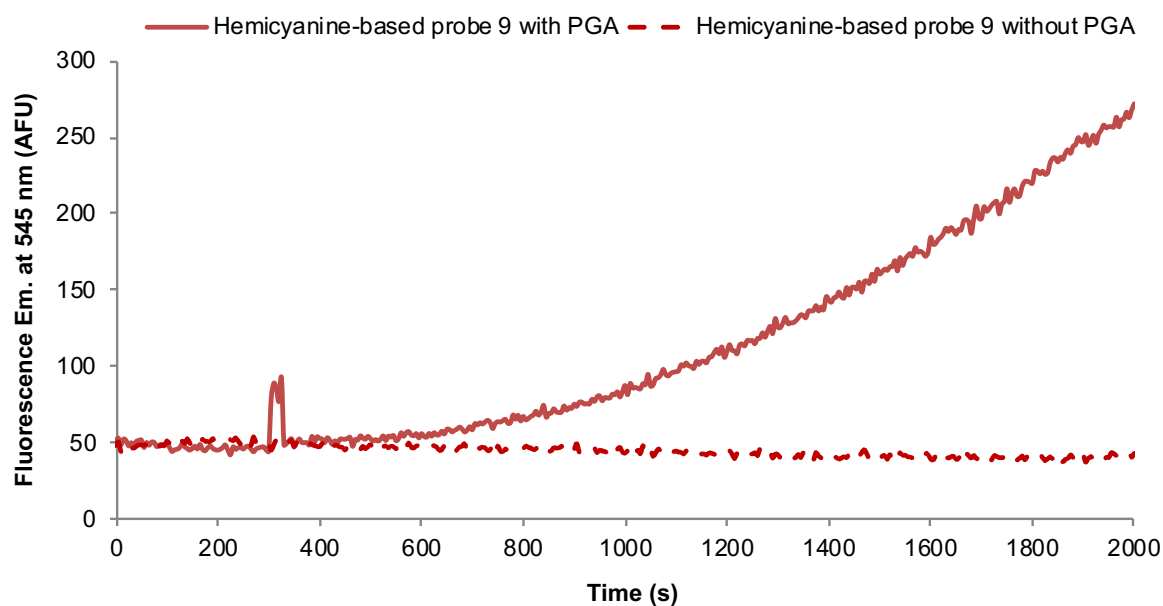


Fig. S16 Time-dependent changes in the green-yellow fluorescence intensity (Ex./Em. 525/545 nm, slit 5 nm) of fluorogenic probe 10 (concentration: 1.0 μ M) in the presence of PGA (1 U) in PB (100 mM, pH 7.6) at 37 $^{\circ}$ C.

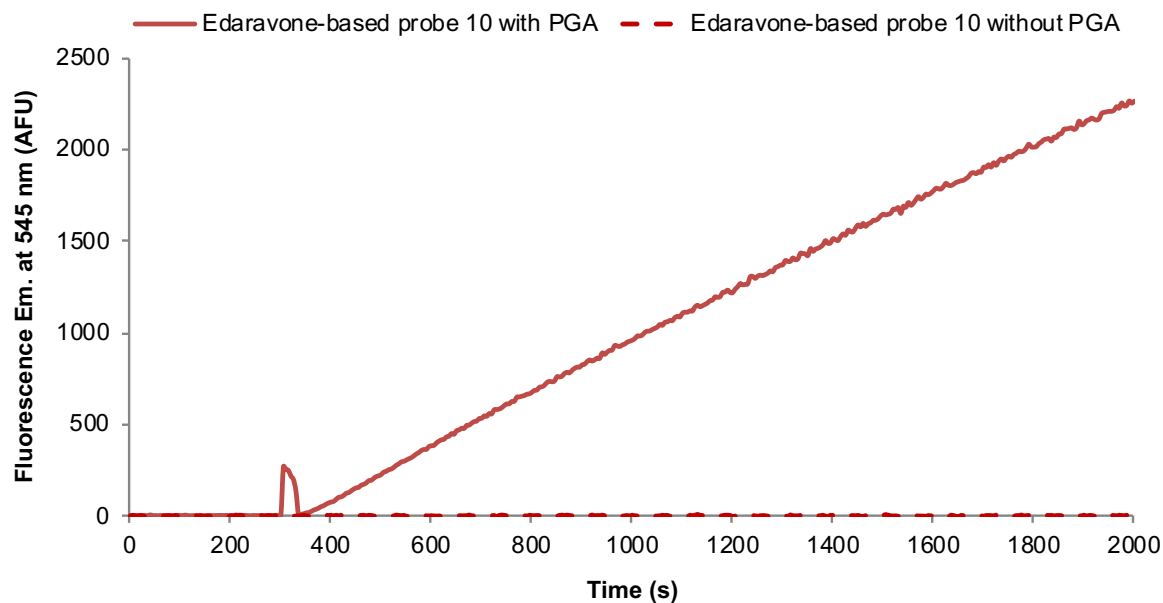


Fig. S17 Time-dependent changes in the green-yellow fluorescence intensity (Ex./Em. 525/545 nm, slit 5 nm) of fluorogenic probe 3 (concentration: 1.0 μ M) in the presence of PGA (1 U) with or without GSH (50 equiv.), in PB (100 mM, pH 7.6) at 37 $^{\circ}$ C.

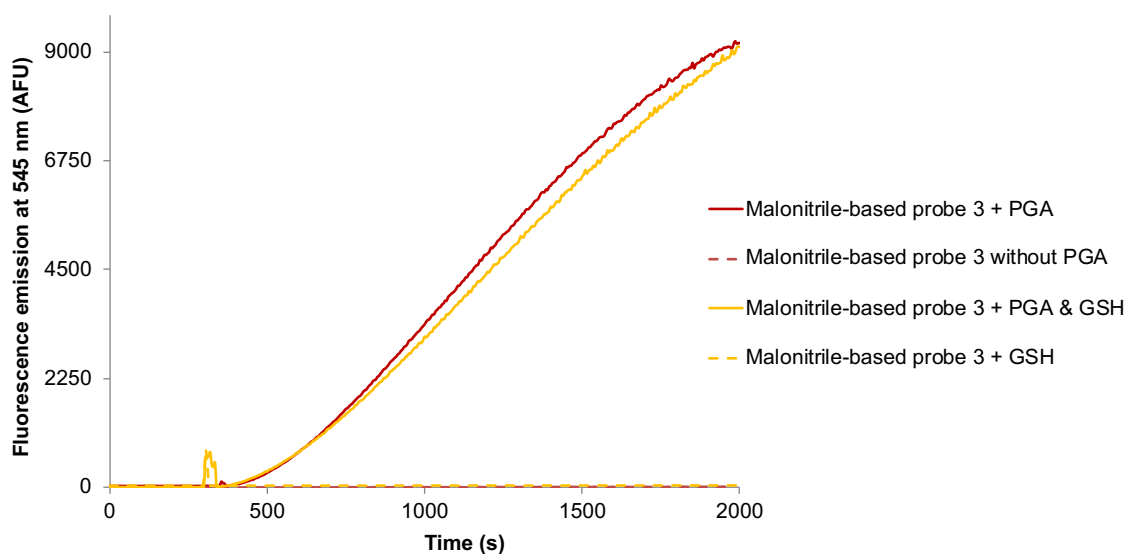


Fig. S18 Time-dependent changes in the green-yellow fluorescence intensity (Ex./Em. 525/545 nm, slit 5 nm) of fluorogenic probe 6 (concentration: 1.0 μ M) in the presence of PGA (1 U) with or without GSH (50 equiv.), in PB (100 mM, pH 7.6) at 37 $^{\circ}$ C.

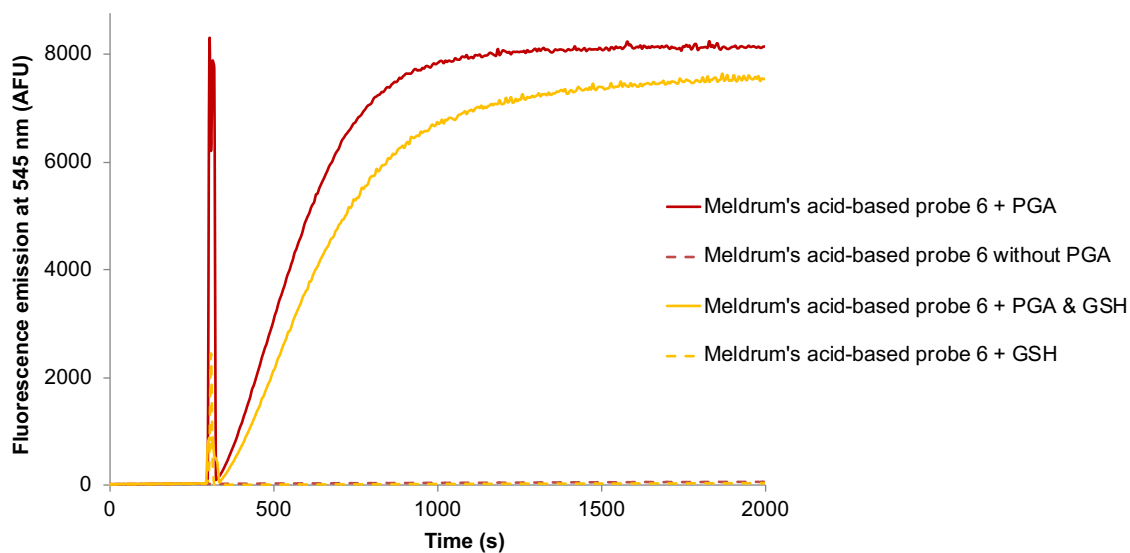


Fig. S19 Time-dependent changes in the green-yellow fluorescence intensity (Ex./Em. 525/545 nm, slit 5 nm) of fluorogenic probe 10 (concentration: 1.0 μ M) in the presence of PGA (1 U) with or without GSH (50 equiv.), in PB (100 mM, pH 7.6) at 37 $^{\circ}$ C.

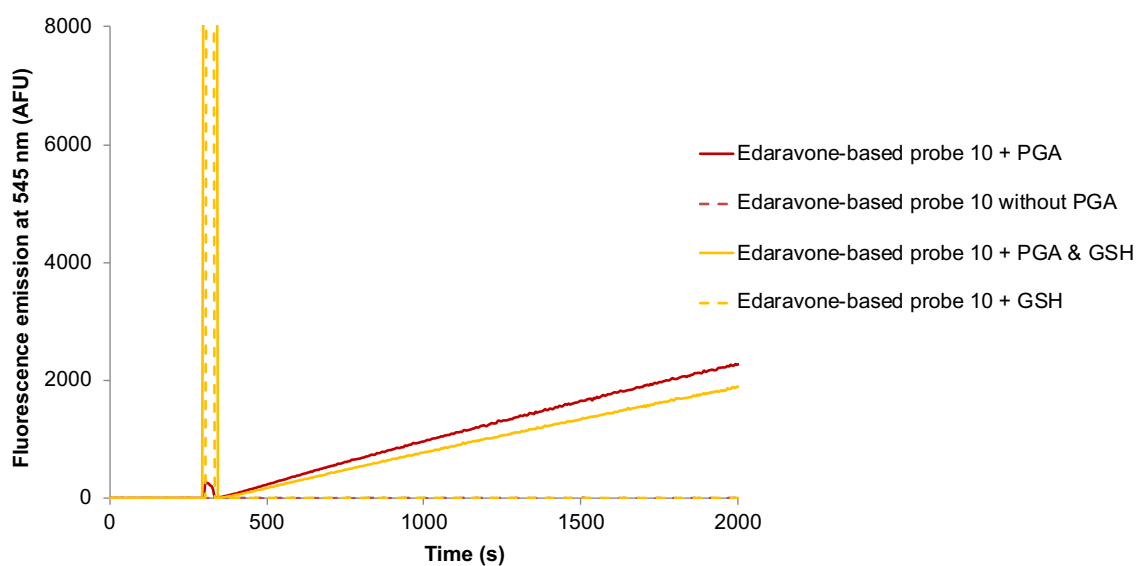


Fig. S20 Bar charts related to UV-vis absorbance changes (at λ_{\max}) of fluorogenic probes 2-10 (concentration: 2.0 μ M) after 30 min incubation with GSH (50 equiv.), in PB (100 mM, pH 7.6) at 25 $^{\circ}$ C.

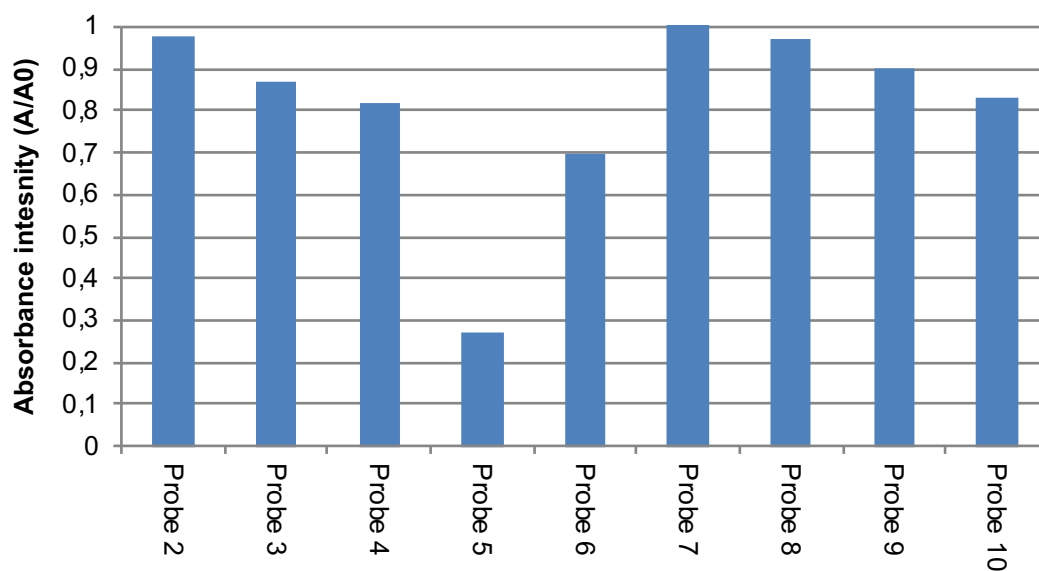


Fig. S21 RP-HPLC elution profile (system J, fluorescence detection Ex./Em. 525/545 nm) of fluorogenic probe 3 before enzymatic activation

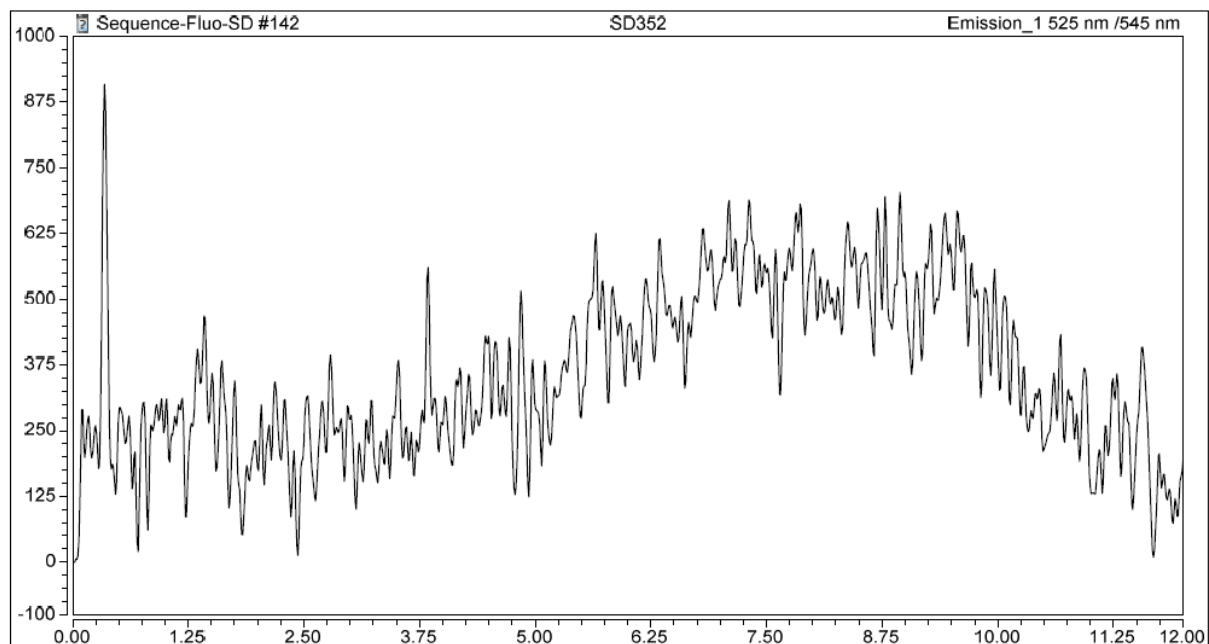
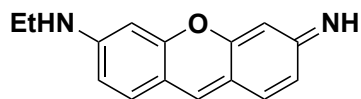


Fig. S22 RP-HPLC elution profile (system J, fluorescence detection Ex./Em. 525/545 nm) of fluorogenic probe 3 after incubation with PGA (1 U, 30 min, 37 °C)

Please note: for all RP-HPLC elution profiles, peak at $t_R = 3.8$ is assigned to pyronin AR116 and peak at $t_R = 3.5$ min is assigned to mono-dealkylated pyronin S1 (structure below).



pyronin S1

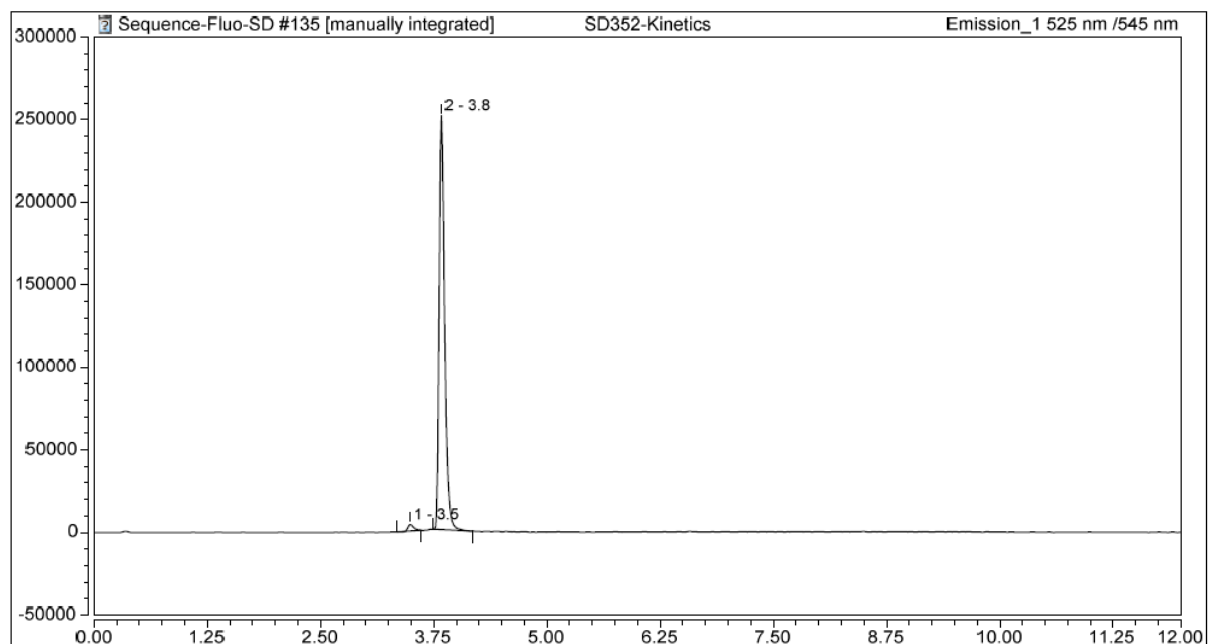


Fig. S23 RP-HPLC elution profile (system J, fluorescence detection Ex./Em. 525/545 nm) of fluorogenic probe 4 before enzymatic activation

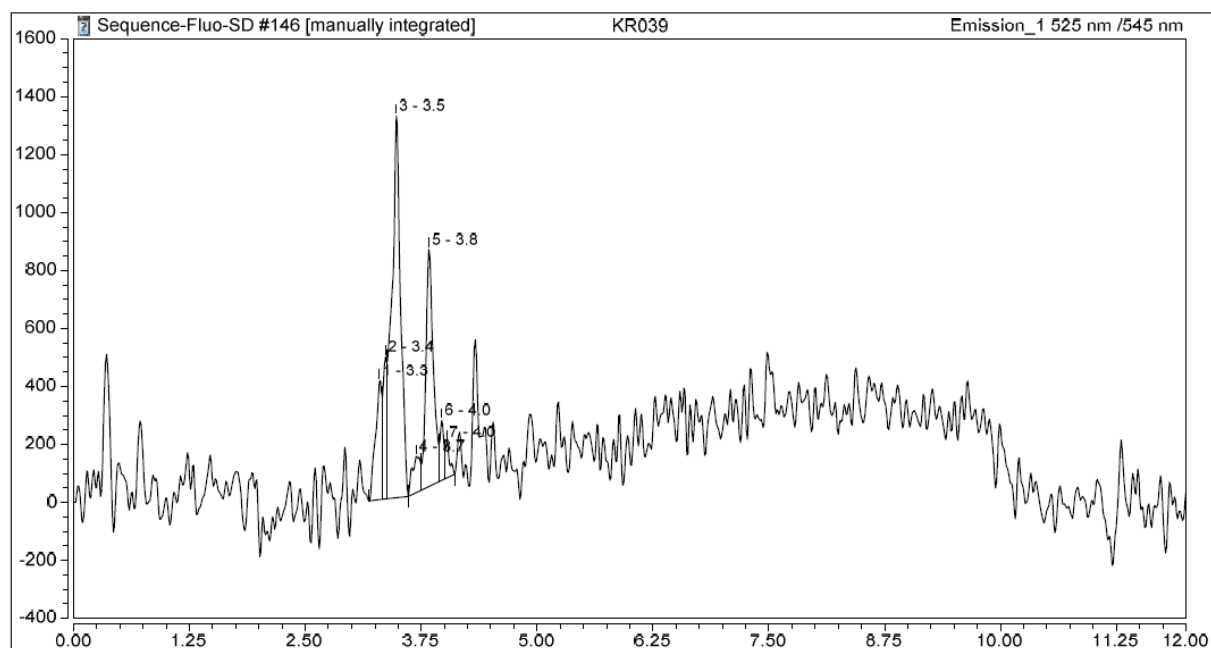


Fig. S24 RP-HPLC elution profile (system J, fluorescence detection Ex./Em. 525/545 nm) of fluorogenic probe 4 after incubation with PGA (1 U, 30 min, 37 °C)

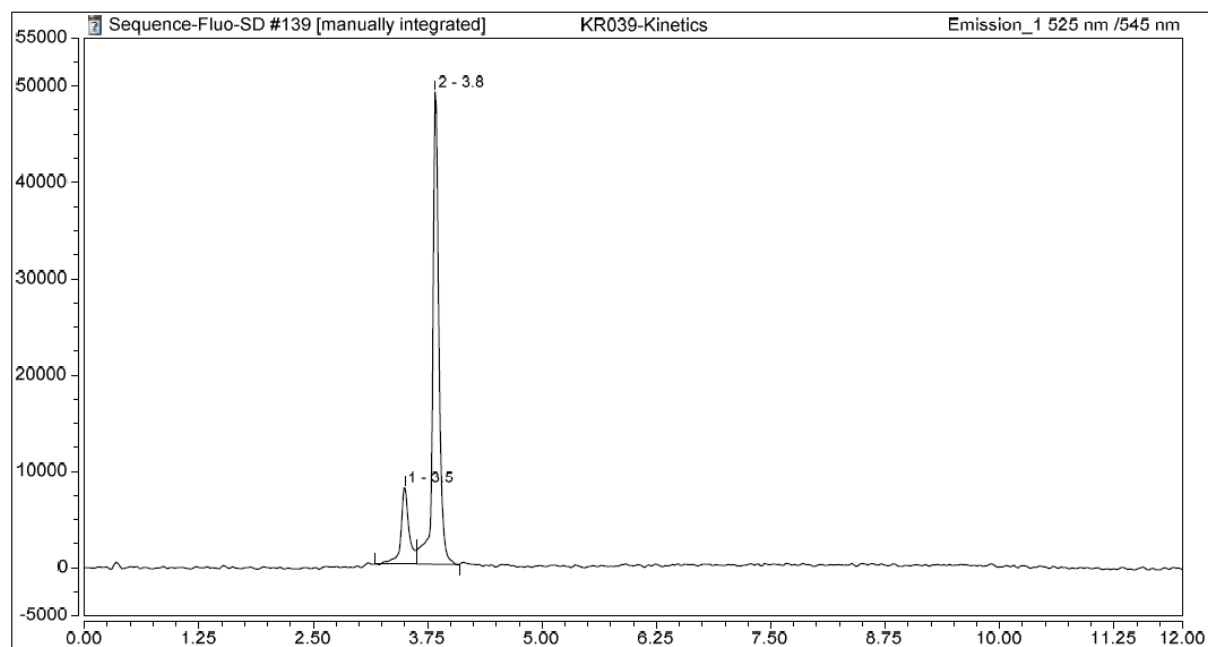


Fig. S25 RP-HPLC elution profile (system J, fluorescence detection Ex./Em. 525/545 nm) of fluorogenic probe 5 before enzymatic activation

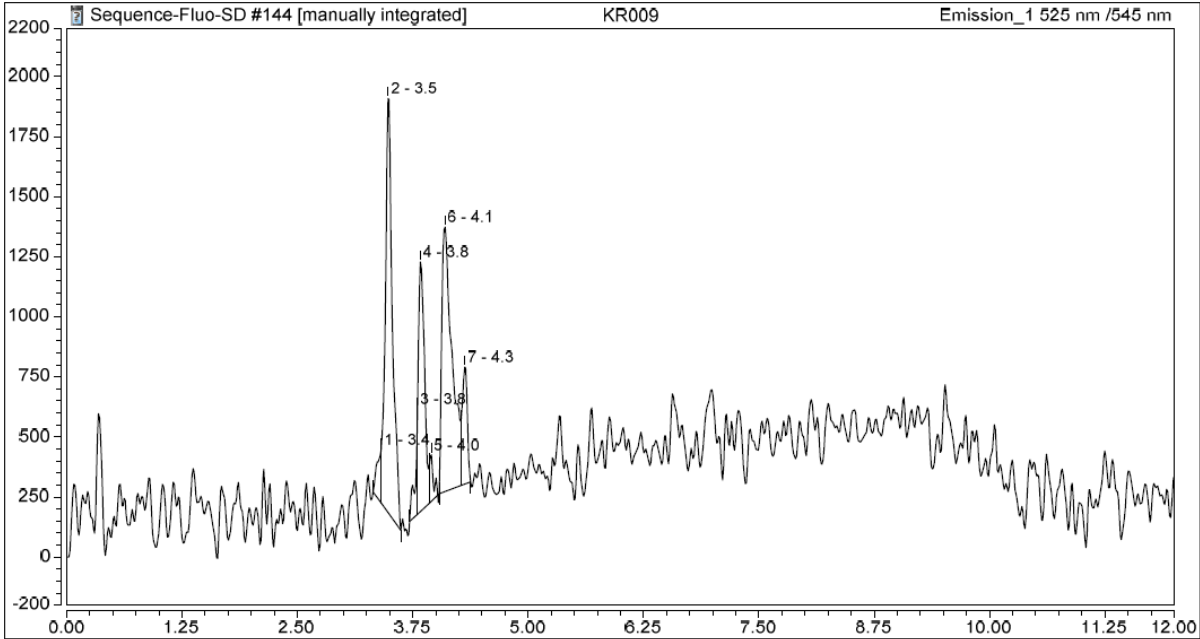


Fig. S26 RP-HPLC elution profile (system J, fluorescence detection Ex./Em. 525/545 nm) of fluorogenic probe 5 after incubation with PGA (1 U, 30 min, 37 °C)

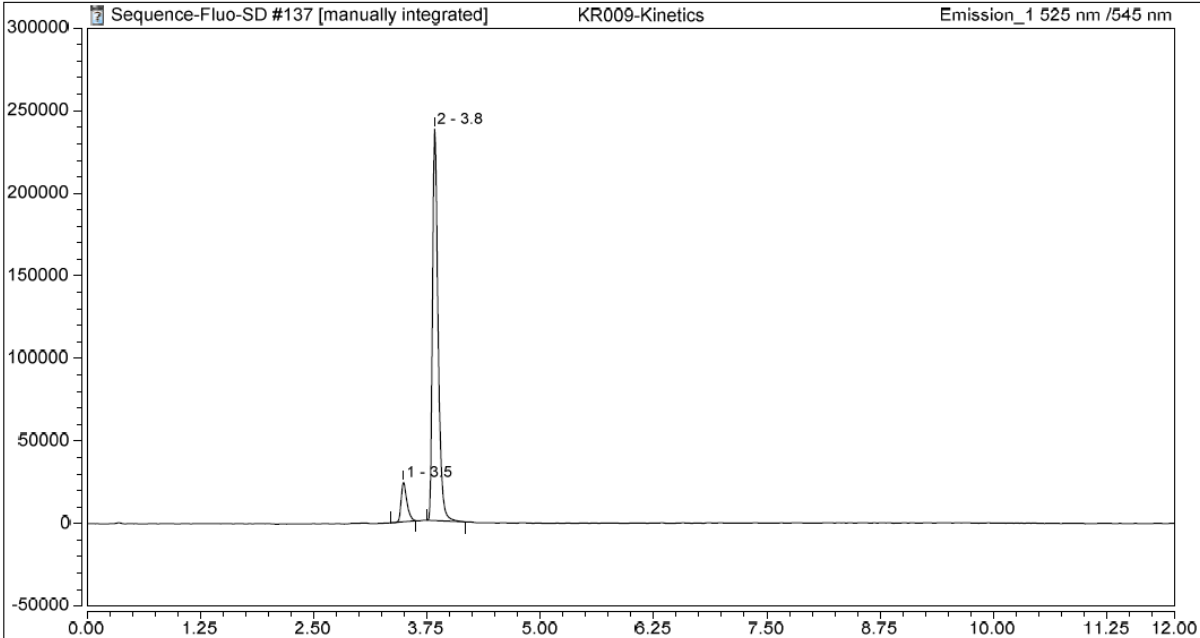


Fig. S27 RP-HPLC elution profile (system J, fluorescence detection Ex./Em. 525/545 nm) of fluorogenic probe 6 before enzymatic activation

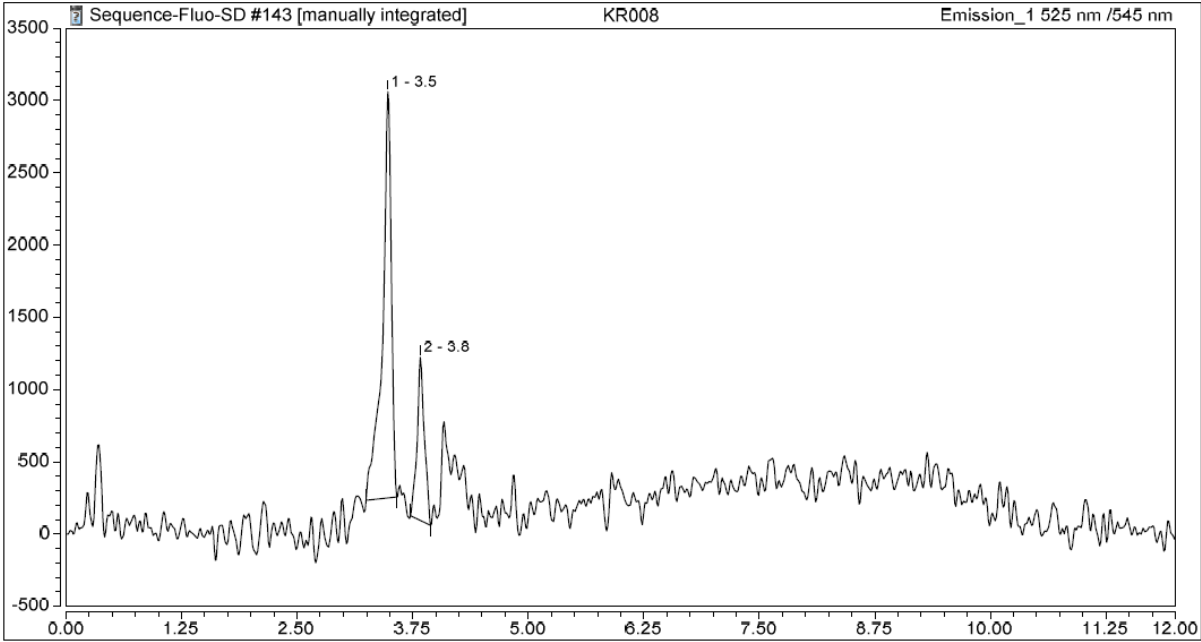


Fig. S28 RP-HPLC elution profile (system J, fluorescence detection Ex./Em. 525/545 nm) of fluorogenic probe 6 after incubation with PGA (1 U, 30 min, 37 °C)

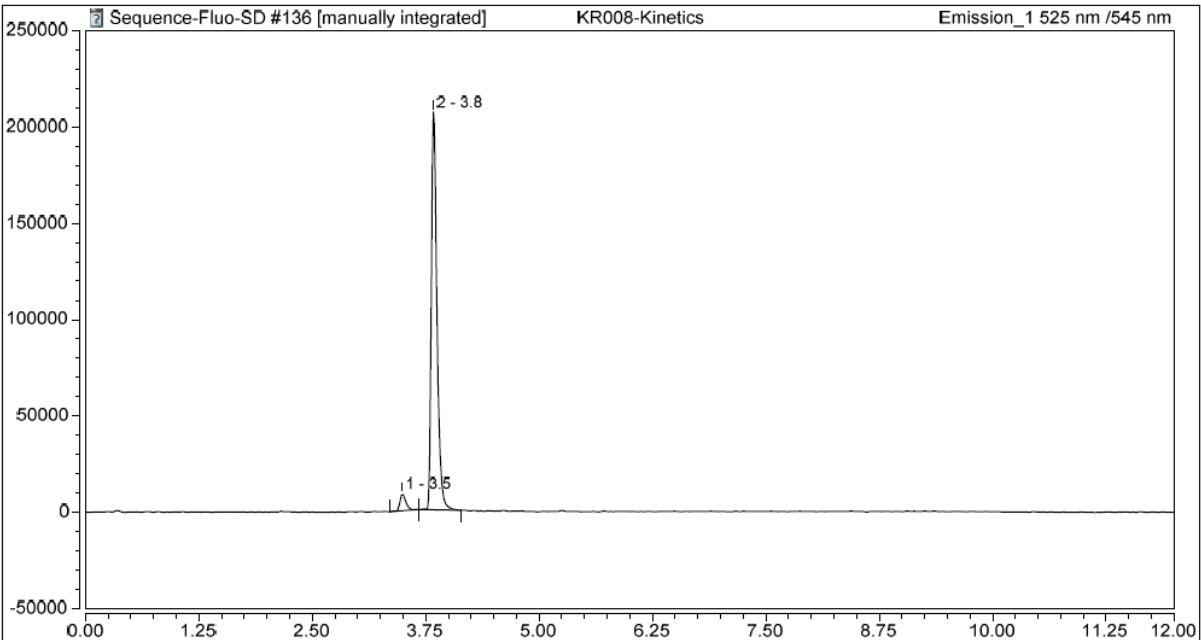


Fig. S29 RP-HPLC elution profile (system J, fluorescence detection Ex./Em. 525/545 nm) of fluorogenic probe 7 before enzymatic activation

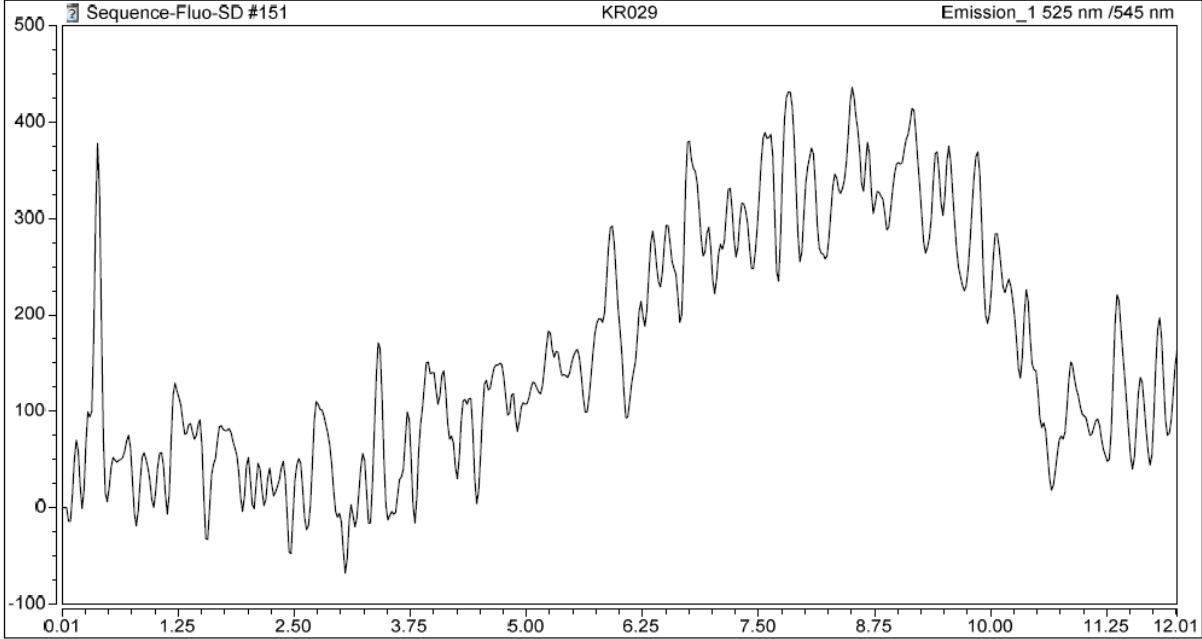


Fig. S30 RP-HPLC elution profile (system J, fluorescence detection Ex./Em. 525/545 nm) of fluorogenic probe 7 after incubation with PGA (1 U, 30 min, 37 °C)

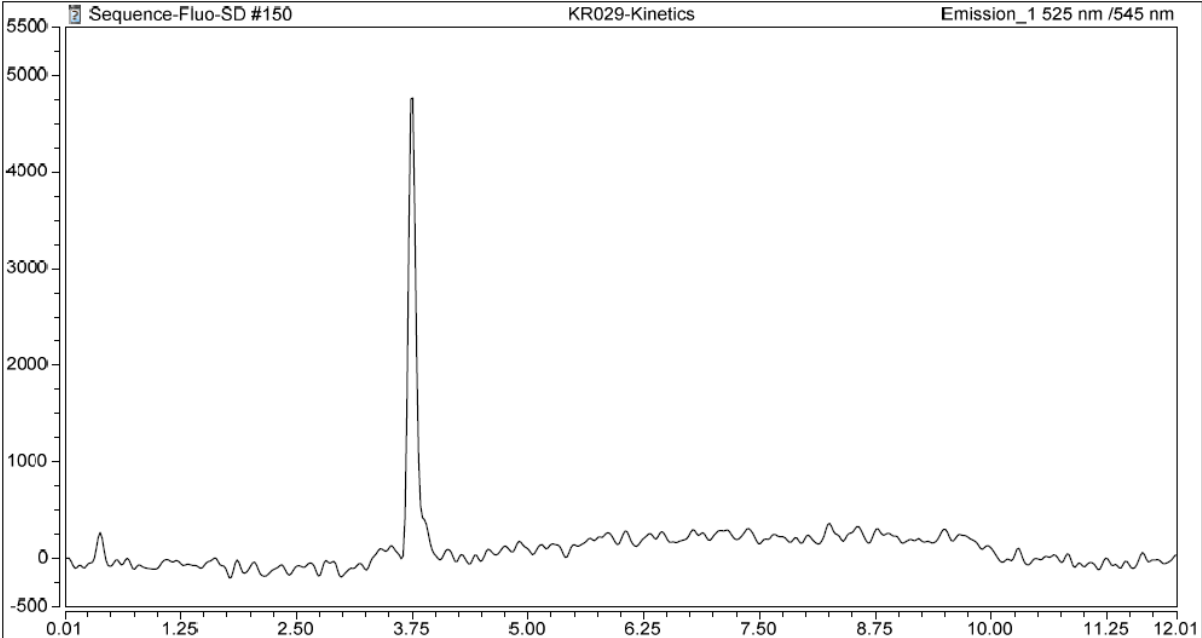


Fig. S31 RP-HPLC elution profile (system J, fluorescence detection Ex./Em. 525/545 nm) of fluorogenic probe 8 before enzymatic activation

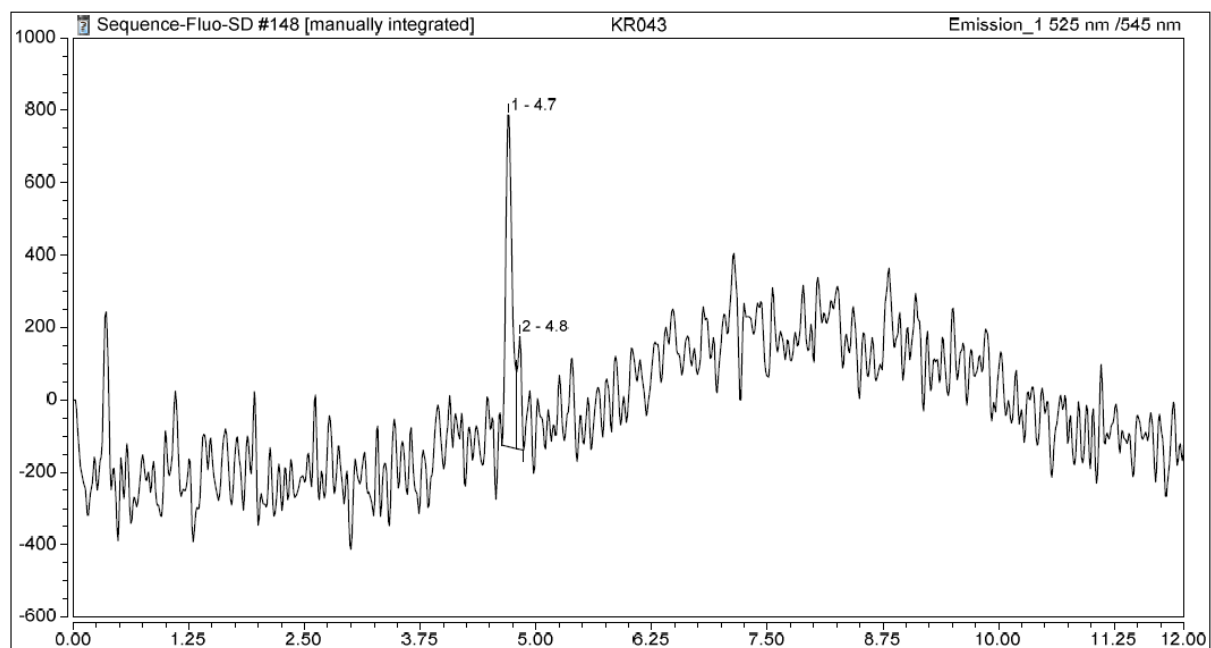


Fig. S32 RP-HPLC elution profile (system J, fluorescence detection Ex./Em. 525/545 nm) of fluorogenic probe 8 after incubation with PGA (1 U, 30 min, 37 °C)

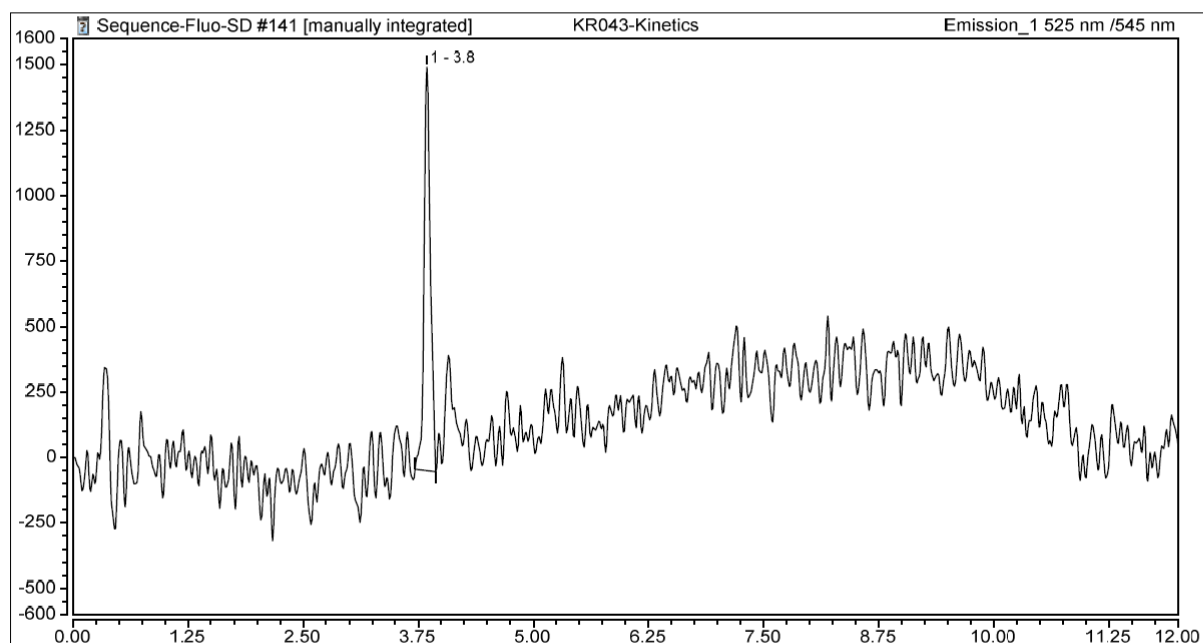


Fig. S33 RP-HPLC elution profile (system J, fluorescence detection Ex./Em. 525/545 nm) of fluorogenic probe 9 before enzymatic activation

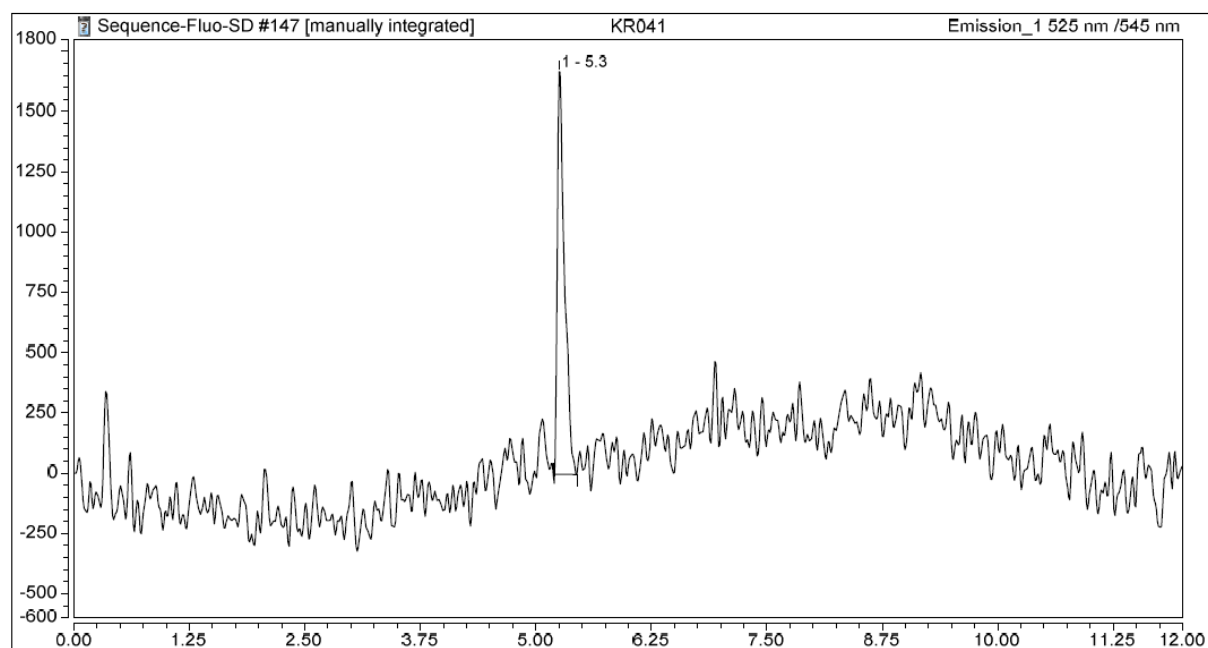


Fig. S34 RP-HPLC elution profile (system J, fluorescence detection Ex./Em. 525/545 nm) of fluorogenic probe 9 after incubation with PGA (1 U, 30 min, 37 °C)

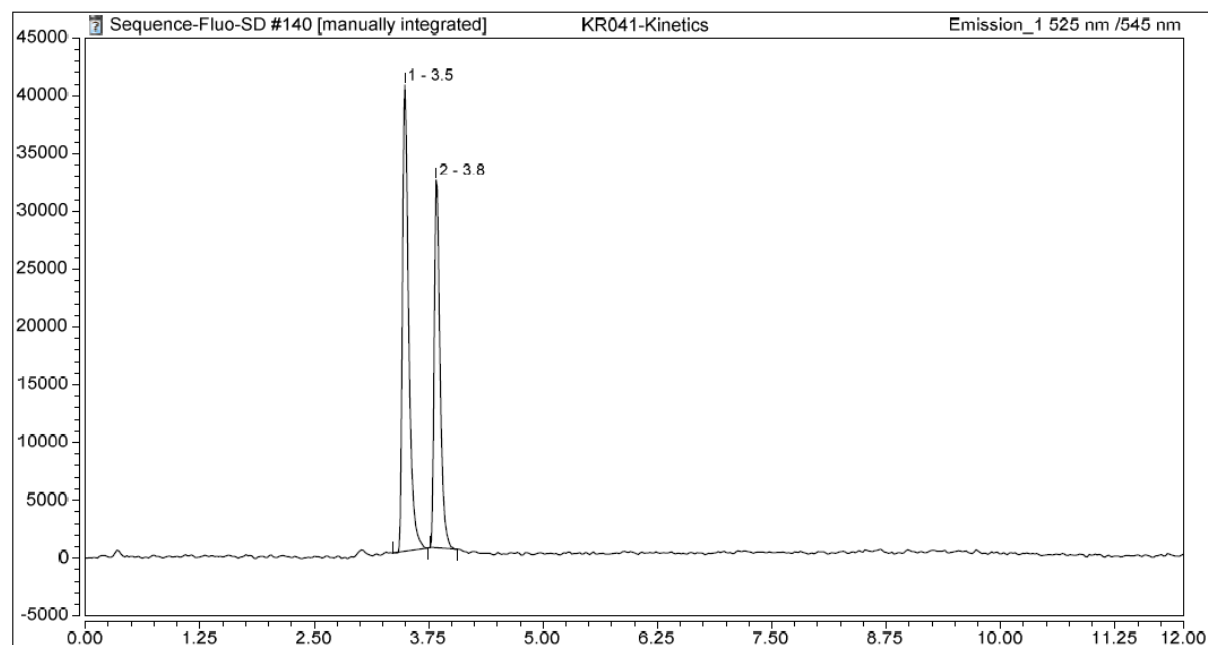


Fig. S35 RP-HPLC elution profile (system J, fluorescence detection Ex./Em. 525/545 nm) of fluorogenic probe 10 before enzymatic activation

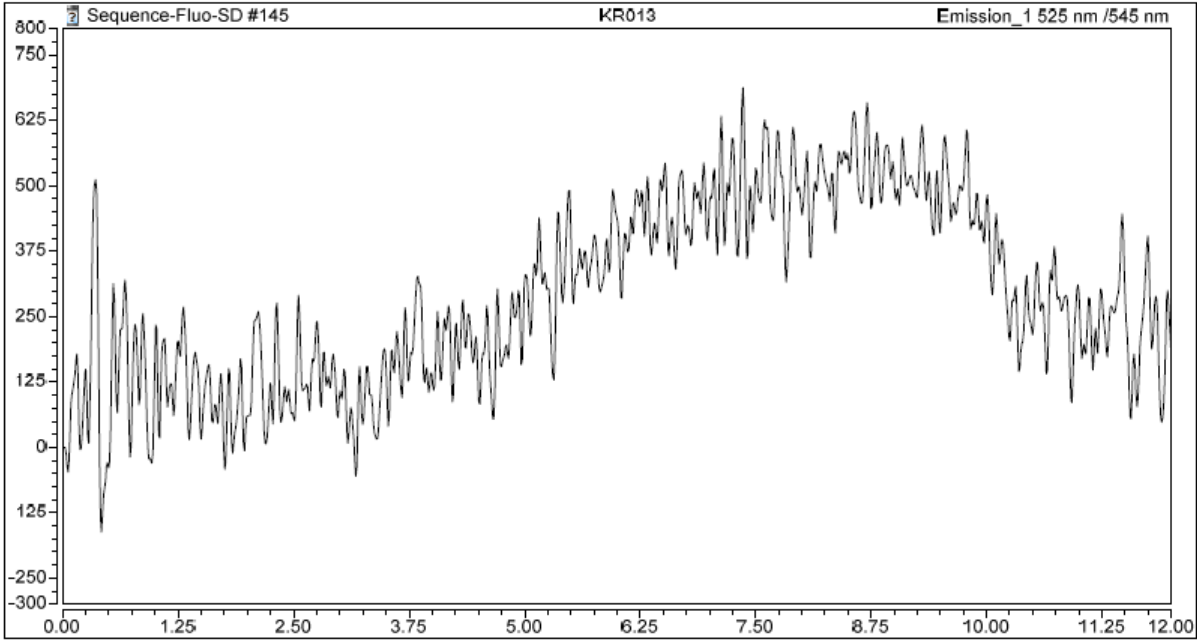


Fig. S36 RP-HPLC elution profile (system J, fluorescence detection Ex./Em. 525/545 nm) of fluorogenic probe 10 after incubation with PGA (1 U, 30 min, 37 °C)

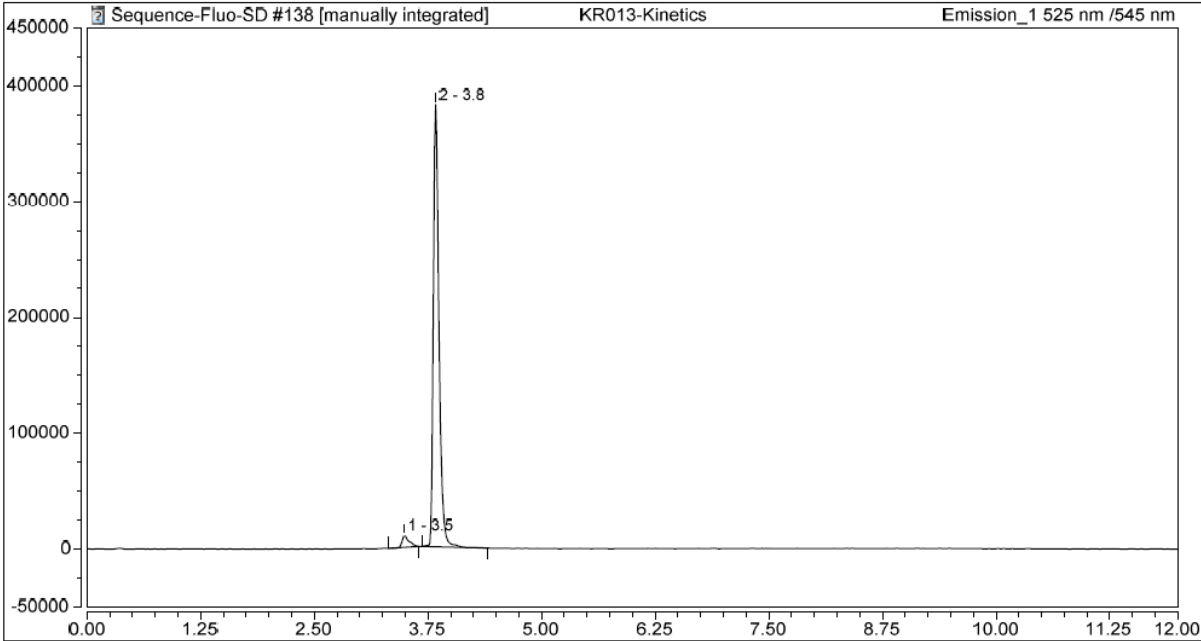


Fig. S37 RP-HPLC elution profile (system J, fluorescence detection Ex./Em. 525/545 nm) of reference pyronin AR116

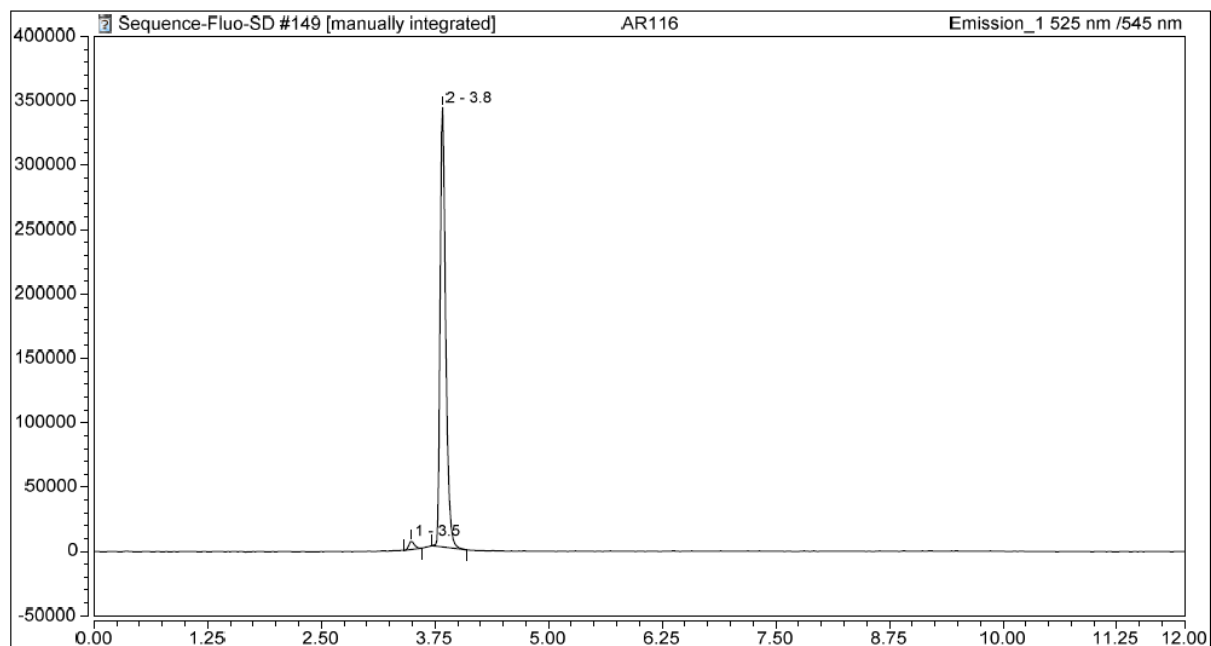
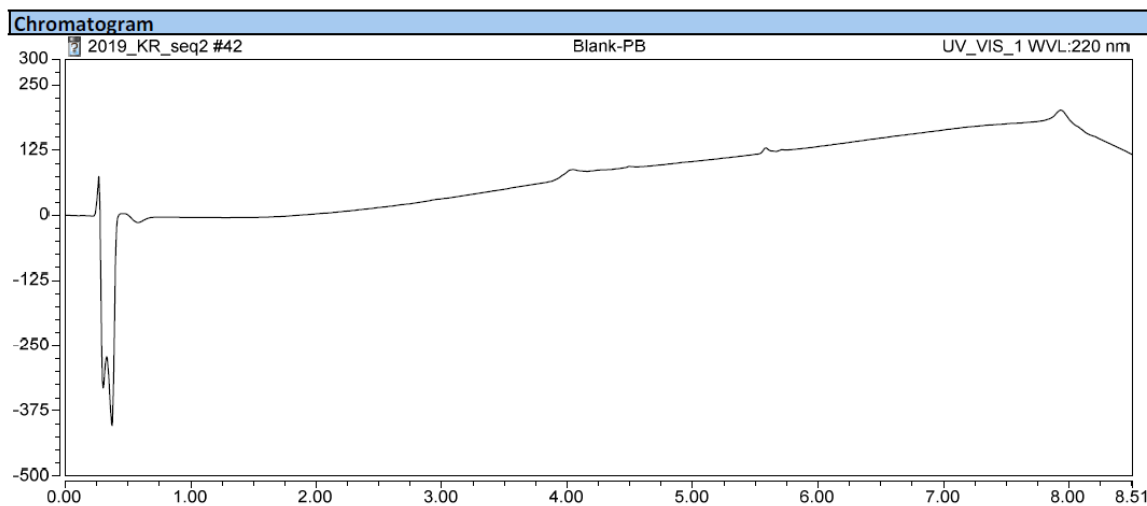
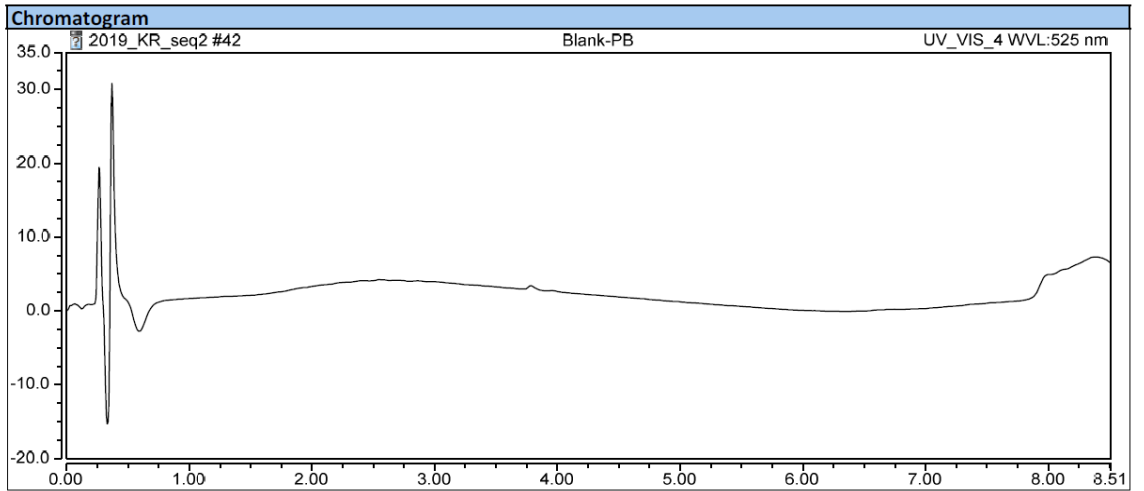
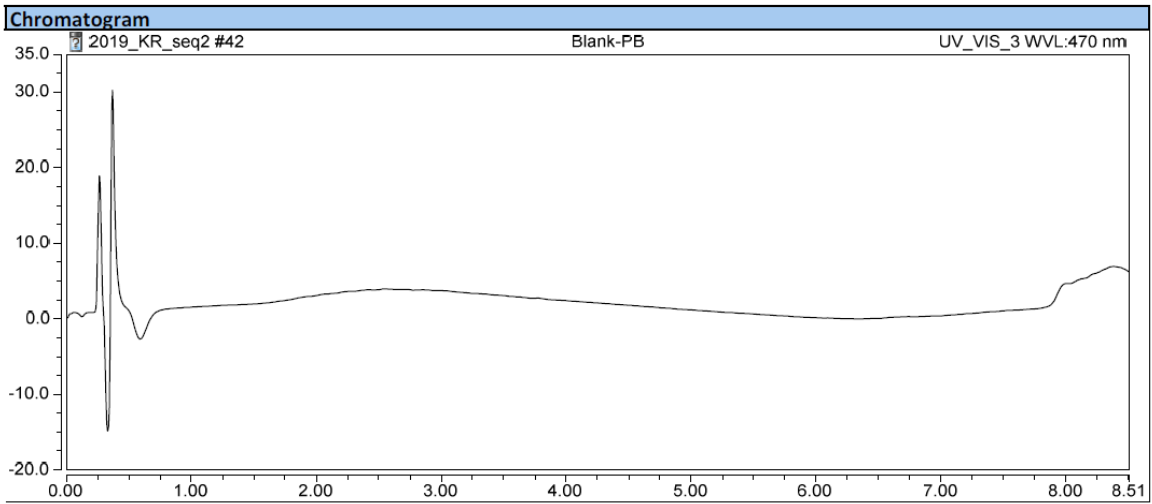
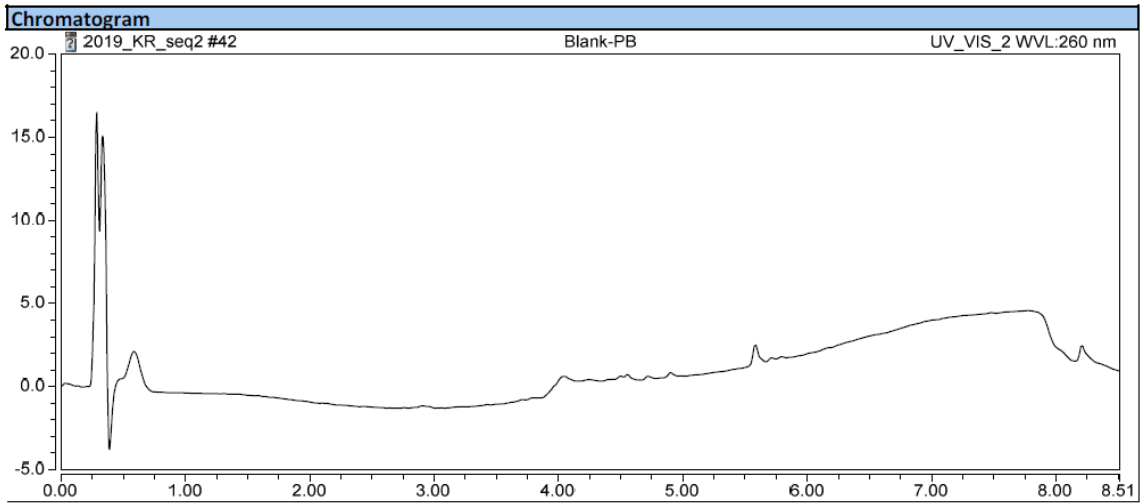


Fig. S38 RP-HPLC elution profiles (system B) of blank (injection of PB alone). UV detection at 220 nm; UV detection at 260 nm; visible detection at 470 nm; visible detection at 525 nm; ESI+ mass detection (SIM mode at $m/z = 175.5 \pm 0.5$) (top-down)





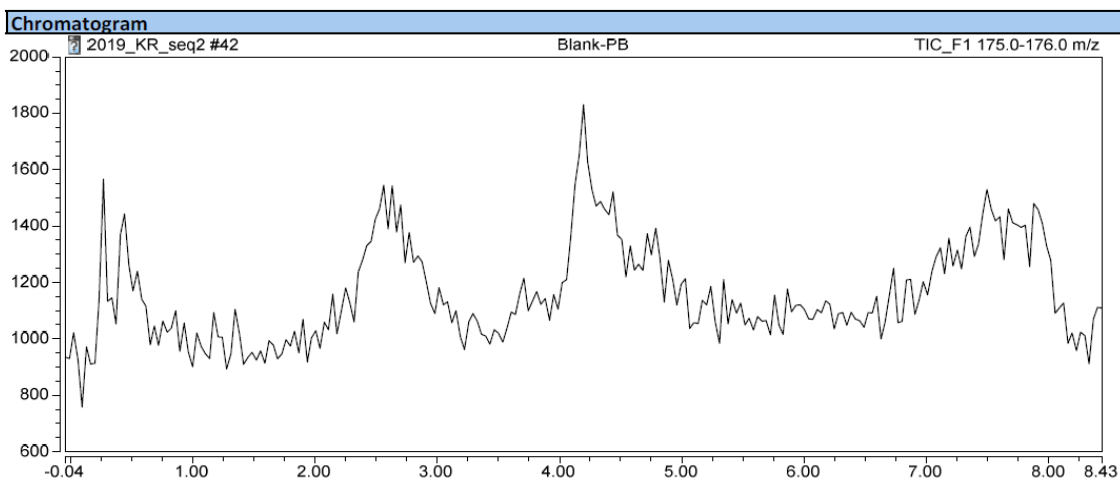
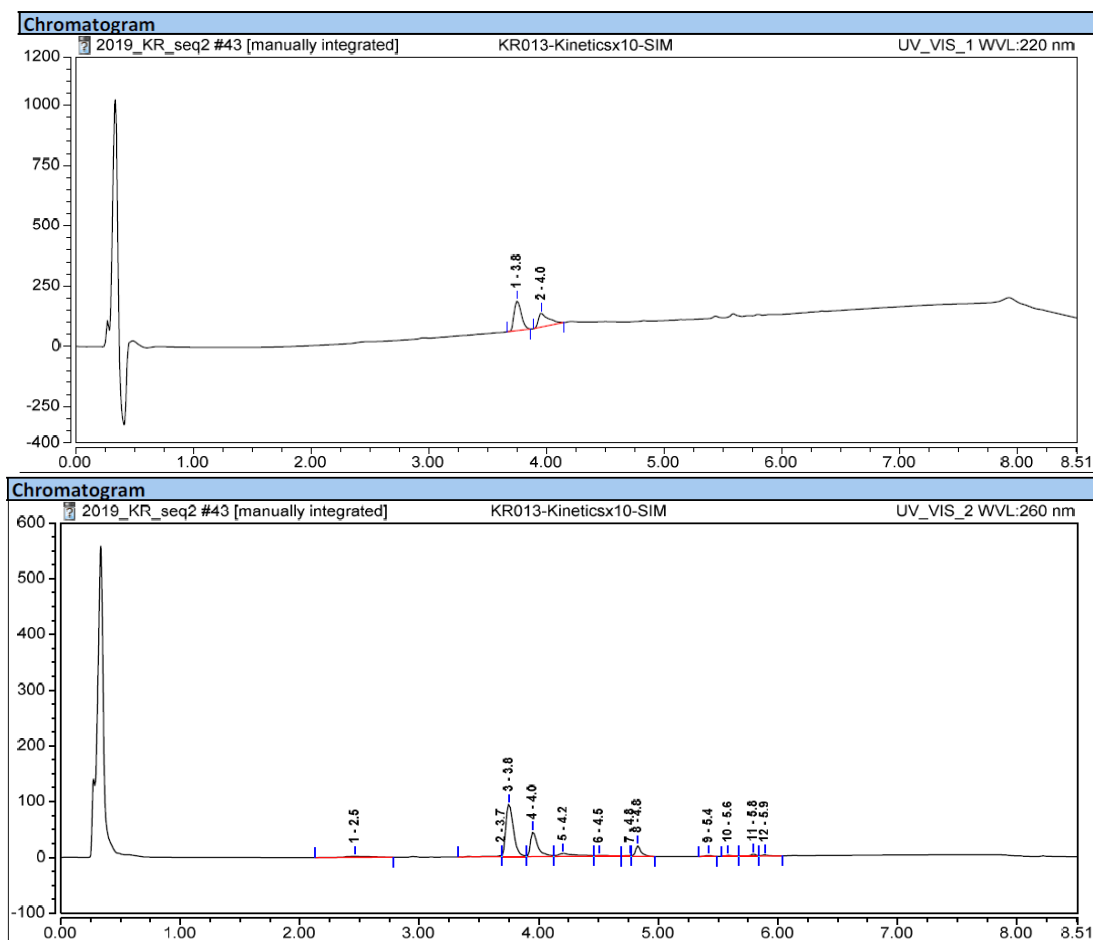


Fig. S39 RP-HPLC elution profiles (system B) of enzymatic reaction mixture of probe 10 with PGA (20 h of incubation in PB at 37 °C). UV detection at 220 nm; UV detection at 260 nm; visible detection at 470 nm; visible detection at 525 nm; ESI+ mass detection (SIM mode at $m/z = 175.5 \pm 0.5$) (top-down)



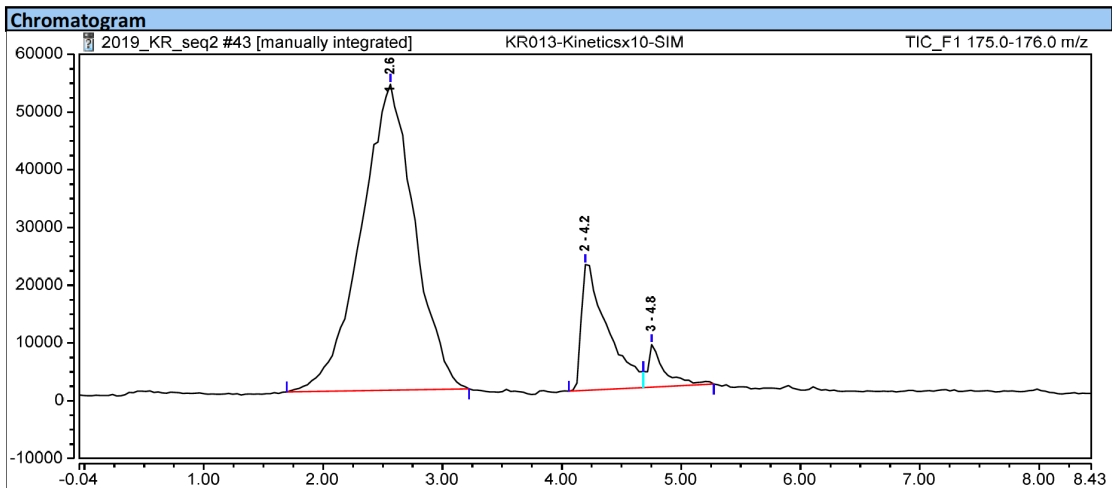
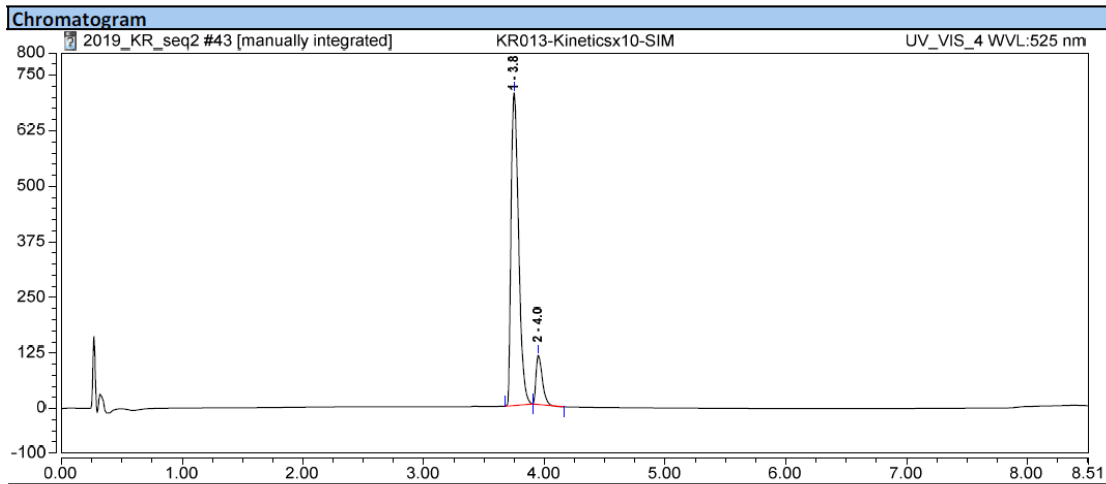
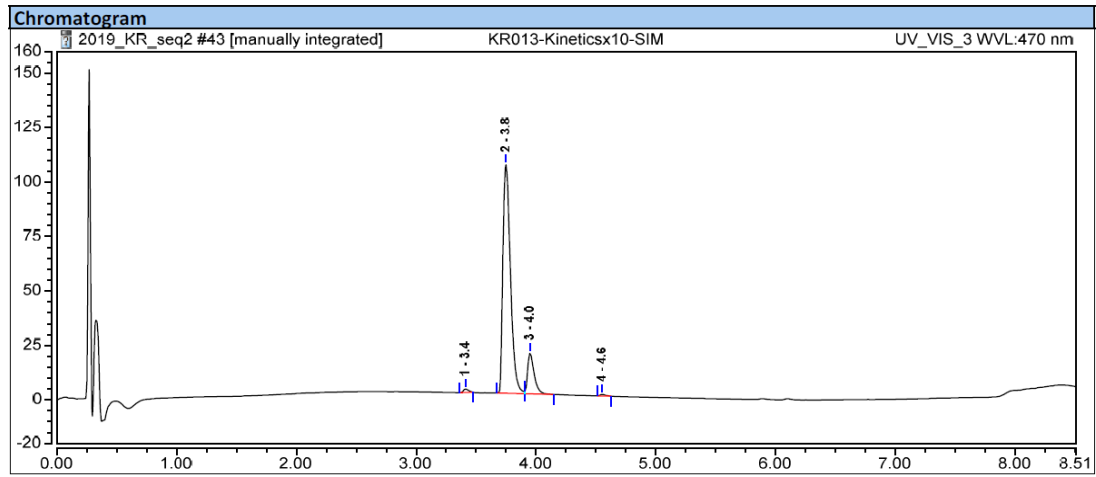
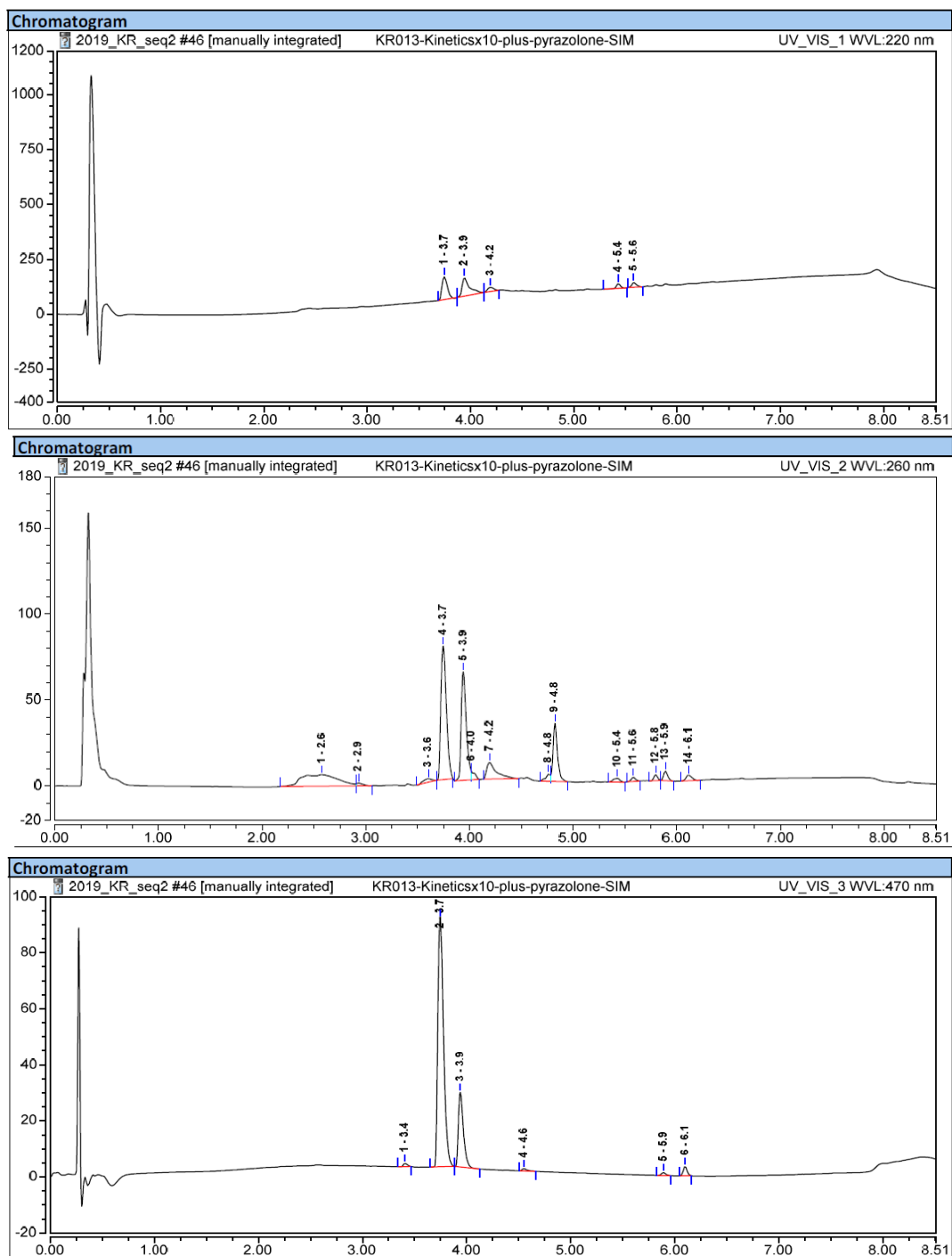


Fig. S40 RP-HPLC elution profiles (system B) of co-injection (enzymatic reaction mixture of probe 10 + edaravone). UV detection at 220 nm; UV detection at 260 nm; visible detection at 470 nm; visible detection at 525 nm; ESI+ mass detection (SIM mode at $m/z = 175.5 \pm 0.5$) (top-down)



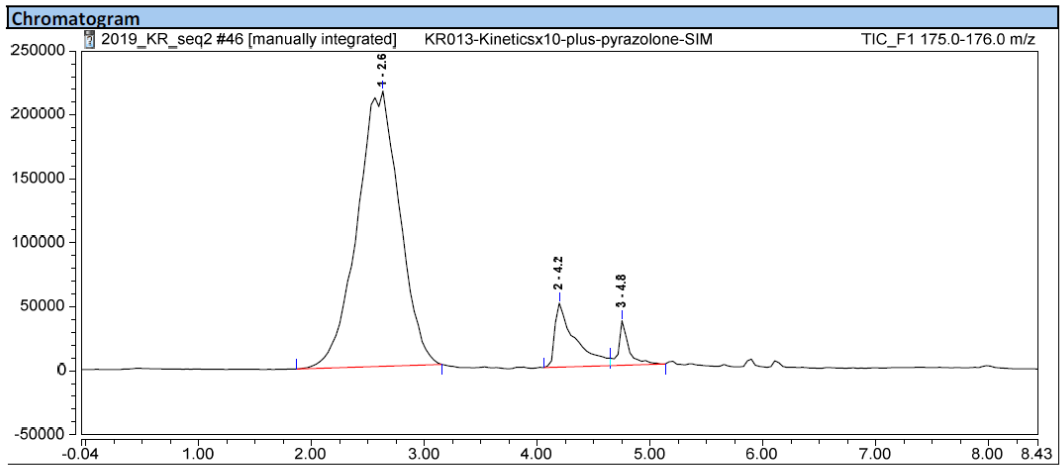
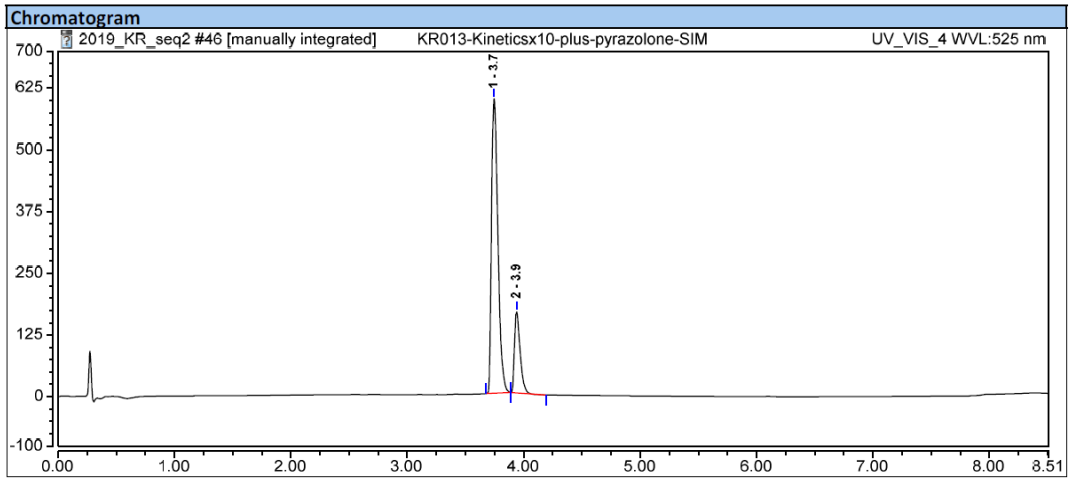


Fig. S41 RP-HPLC elution profiles (system B) of pure sample of edaravone. UV detection at 220 nm; UV detection at 260 nm; visible detection at 470 nm; visible detection at 525 nm; ESI+ mass detection (SIM mode at $m/z = 175.5 \pm 0.5$) (top-down)

